Mechanisms of tigecycline resistance in the Enterobacteriaceae and *Acinetobacter baumannii*

Thesis

Mechanisms of tigecycline resistance in the Enterobacteriaceae and *Acinetobacter baumannii*

Michael Andrew Hornsey, BSc (Hons), MSc

Life and Biomolecular Sciences

Submitted June 2011 and offered for the degree: Doctor of Philosophy

Health Protection Agency (affiliated research centre)

APPENDIX NOT COPIED

ON INSTRUCTION FROM

UNIVERSITY

Contents

Acknowledgements

I would like to take this opportunity to thank my supervision team, Dr Matthew Ellington, Prof David Livermore, Dr Neil Woodford and indeed all ARMRL staff, past and present, especially Dr Michel Doumith, for their guidance and support (both academic and pastoral!) throughout the duration of the studentship and beyond. In addition, I am also grateful to Dr David Wareham for his advice and for his understanding during the final stages of thesis preparation.

I do not have the words to express the depth of my gratitude to my family and friends, especially my fiancée, Katy Lake, whose love and unquestioning support even during my 'difficult' moments inspired me to carry on.

Finally, I thank the two people to whom I owe everything, my Mother and late Father, to whom this thesis is dedicated.

List of tables

List of figures

Abstract

Tigecycline is the first glycylcycline to enter clinical use and displays good *in vitro* activity against a broad range of Gram-positive and Gram-negative pathogens. It is often used as an agent of last resort for the treatment of infections caused by multidrug-resistant Gram-negative bacteria including some Enterobacteriaceae species and *Acinetobacter baumannii*. Therefore, the recent emergence of tigecycline resistance in some strains of these species is a serious public health concern. Efflux was investigated as a possible mechanism of tigecycline resistance using pre- and post-therapy pairs of clinical isolates and laboratory-selected, tigecycline-resistant mutants of *A. baumannii* and *Enterobacter cloacae* and a type strain, laboratory mutants, and a clinical isolate of *Serratia marcescens*. Minimum inhibitory concentrations (MICs) of tigecycline and other agents were determined by agar dilution. Pulsed-field gel electrophoresis was used to assign clones / determine isolate relatedness. Expression of efflux pump genes and genes thought to be implicated in their regulation was monitored by real-time reverse-transcriptase polymerase chain reaction and their role in tigecycline resistance was further investigated by knockout mutagenesis. There was an association between increased expression of specific resistance-nodulation-division (RND) efflux pump genes and elevated tigecycline MICs in all species studied. Insertional inactivation of RND efflux pump genes implicated the AdeABC, AcrAB and SdeXY-HasF systems of *A. baumannii*, *E. cloacae* and *S. marcescens*, respectively. The results of this study support the hypothesis that tigecycline resistance in clinical isolates of Gram-negative bacteria arises as a result of the up-regulated activity of intrinsic efflux systems of the RND family.

1. Introduction

1.1. The problem of antimicrobial resistance

Antimicrobial chemotherapy revolutionised 20th century healthcare and is one of the cornerstones of modern medicine. Antibiotics are used not just to treat acute bacterial infections but also as prophylactics, reducing the risks of infection for patients undergoing cancer chemotherapy, organ transplantation and other surgical procedures.

Antimicrobial resistance is a serious public health problem worldwide. The complete loss of the antimicrobial arsenal would result in a human catastrophe of global proportions. In such a scenario, medical intervention would be problematic and many procedures that are currently considered routine would carry severe risks of infection. Antimicrobial resistance also increases the cost of healthcare delivery because it can mean patients are ill for longer periods, lengthening the course of therapy and hospital stays and thus potentially putting individuals and public health institutions under increased financial pressure.

Fleming noted in 1929 that certain bacteria were innately resistant to penicillin whereas others were innately susceptible (85). He later recognised that organisms that were initially susceptible could develop resistance, especially when exposed to low doses of penicillin, and warned that careless use of the drug might promote resistance and compromise treatment. History has demonstrated that Fleming was right to be cautious as, since then, resistance has been reported to every class of antimicrobial compound to have entered clinical use. The real and unsettling prospect of a return to the pre-antibiotic era less than a century after the discovery of penicillin prompted the World Health Organisation (WHO) to declare antimicrobial resistance the subject of World Health Day 2011, highlighting it as one of most important issues adversely affecting human health (142).

Intense antibiotic selection pressure as a result of the widespread use of antibiotics in human and veterinary medicine has selected resistant organisms. This was evident in the 1950s when researchers reported a shift in the pattern of the type of organism causing serious nosocomial infection (between 1935 and 1957) after antibiotics were introduced into clinical practice from susceptible Gram-positive pathogens to penicillin-resistant Gram-negative species (83). Antibiotic pressure continues to select organisms that are resistant to newer agents, with multidrug resistant (MDR –i.e. resistant to three or more compound classes) Gram-negative species being of most concern in hospitals. Unfortunately, there are very few new drugs in the final stages of development which offer advantage over existing treatment options for MDR Gram-negative bacteria, such as the carbapenems (19).

Antibiotic resistance can arise as a result of mutation or can be acquired by bacteria via mobile genetic elements. Some acquired resistance determinants can spread between different strains or, in some instances, between different species and genera. Diverse mechanisms of antimicrobial resistance have been described, including enzymatic modification of the drug or drug target, membrane permeability changes and active drug efflux, which is the topic of this thesis.

1.2. Active efflux in Gram-negative bacteria

The ability to extrude compounds, in an energy-dependent fashion, from the intracellular to the extracellular environment is a core biological function that appears to be a prerequisite for survival. Active transport systems have been described across all three domains of life, namely the Prokarya, Eukarya and the Archaea.

In bacteria, efflux transporters can extrude toxins, including antimicrobial compounds, and have been classified into five families, namely, the major facilitator

superfamily (MFS), the small multidrug resistance (SMR) family, the multidrug and toxic compound extrusion (MATE) family, the ATP-binding cassette (ABC) superfamily and the resistance-nodulation-division (RND) superfamily. In Gram-negative bacteria these transporter proteins are associated with the cytoplasmic membrane although, as described below, some form part of multi-component complexes that span the entire cell envelope.

1.2.1. MFS pumps

The MFS represents the largest group of secondary transporters and are ubiquitous in nature (226). As opposed to primary transporters, which rely on the hydrolysis of ATP to provide the energy to extrude substrates against their concentration gradient, secondary transporters link to other physiological gradients and, in the cases of MFS systems, to the proton motive force. In bacteria, they mainly function as antiporters, where a molecule of substrate is exchanged for a hydrogen ion (Figure 1). Efflux pumps belonging to this family are α-helical cytoplasmic membrane proteins that contain 12 or 14 transmembrane segments (TMs). There are six MFS transporter families, though only the 12-TM drug/H^+ antiporter 1 (DHA-1) family and the 14-TM DHA-2 family frequently occur in bacteria (226). Much of the knowledge of this efflux pump family has been acquired through the study of the archetypal MFS transporter, MdfA of *Escherichia coli* (74) which seems to function as a monomer (235). MFS pumps are known to export a wide range of structurally unrelated compounds. In Gram-negative bacteria, MFS pumps are of clinical importance since some members are able to efflux antibiotics, notably the tetracyclines (section 1.2.2.1).

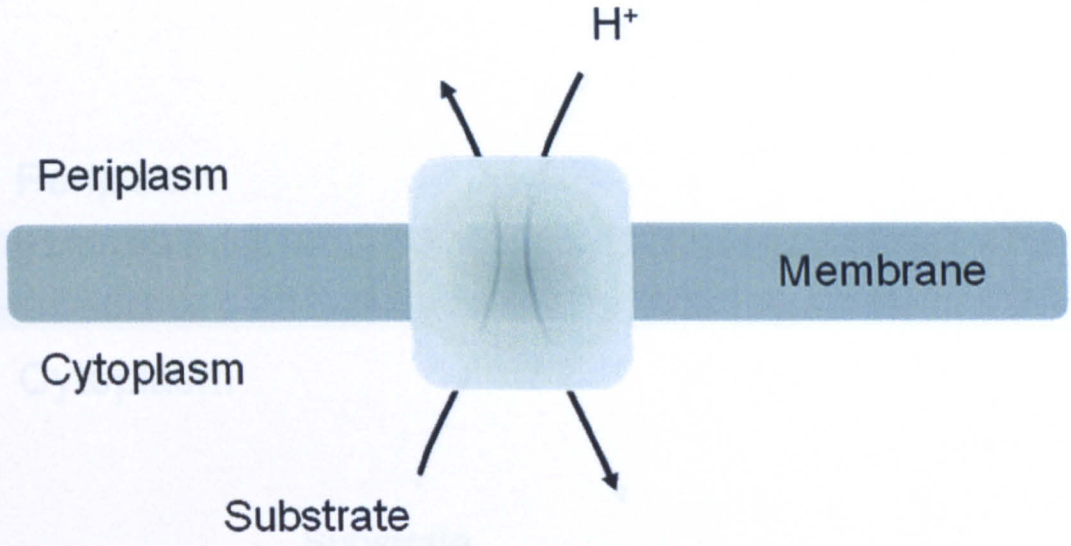

Figure 1. Principle of antiporter action.

1.2.2. SMR pumps

As suggested by the nomenclature, SMR efflux proteins are small molecules of approximately 110 amino acid residues. They too are cytoplasmic membrane proteins which contain just four TMs. They utilise the proton motive force and act as antiporters (Figure 2). Of all SMR-type pumps described in Gram-negative bacteria, EmrE of *E. coli* has been studied most extensively (229). EmrE extrudes a range of toxic cationic compounds, functions as a homodimer and displays an unusual anti-parallel (oppositely oriented) membrane topology (181). The substrate profiles of SMR transporters include dyes (e.g. ethidium bromide), antiseptics (e.g. acriflavine) and antimicrobials (147).

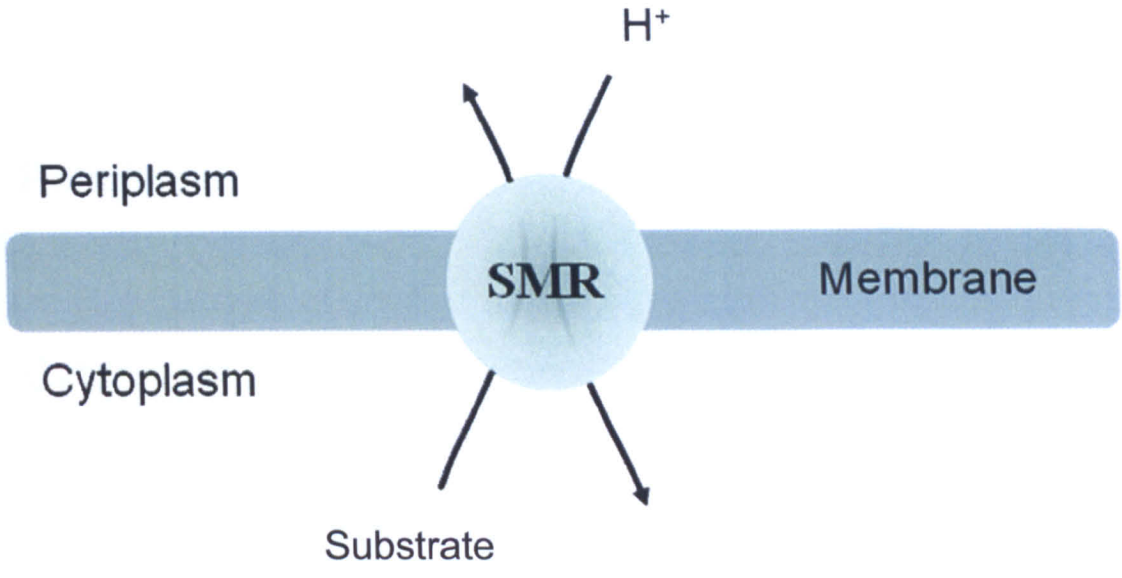

Figure 2. Schematic of a SMR transporter.

1.2.3. MATE pumps

MATE family efflux proteins have been identified in all domains of life and share membrane topology characteristics with MFS proteins as they too contain 12 TMs (though no sequence homology). In contrast with MFS transporters, MATE-type pumps primarily use the Na^+ gradient as an energy source (Figure 3). The archetypal pump of the MATE family is NorM which was initially described in *Vibrio parahaemolyticus* and was the first Na^+ / drug antiporter multidrug efflux system to be characterised (176). The substrate profile of NorM includes cationic dyes and certain antibiotics, including some fluoroquinolones (177).

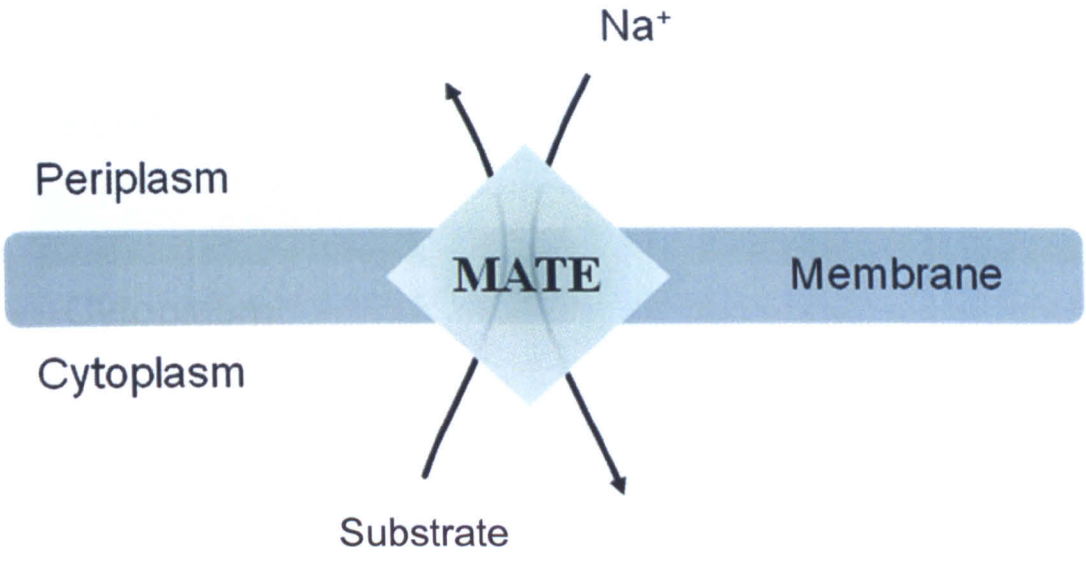

Figure 3. Schematic of a MATE transporter.

1.2.4. ABC pumps

Transporters of the ABC superfamily are multi-protein complexes that are driven by the hydrolysis of ATP and hence are primary transporters (Figure 4). ABC-type transporters of clinical importance in terms of multidrug resistance (MDR) have been described relatively rarely in Gram-negative bacteria; rather most prokaryotic efflux systems implicated in antibiotic extrusion are secondary transporters. Nevertheless, a few ABC-type pumps that efflux antibiotics have been described, of which the best studied is arguably the macrolide-specific transporter, MacB which has been identified in multiple species including *E. coli* and *Neisseria gonorrhoeae* (130;218). Studies in *E. coli* show that it functions in concert with the periplasmic adapter protein, MacA and the promiscuous outer membrane channel TolC (section 1.1.5), to form the functional complex MacAB-TolC (148;279).

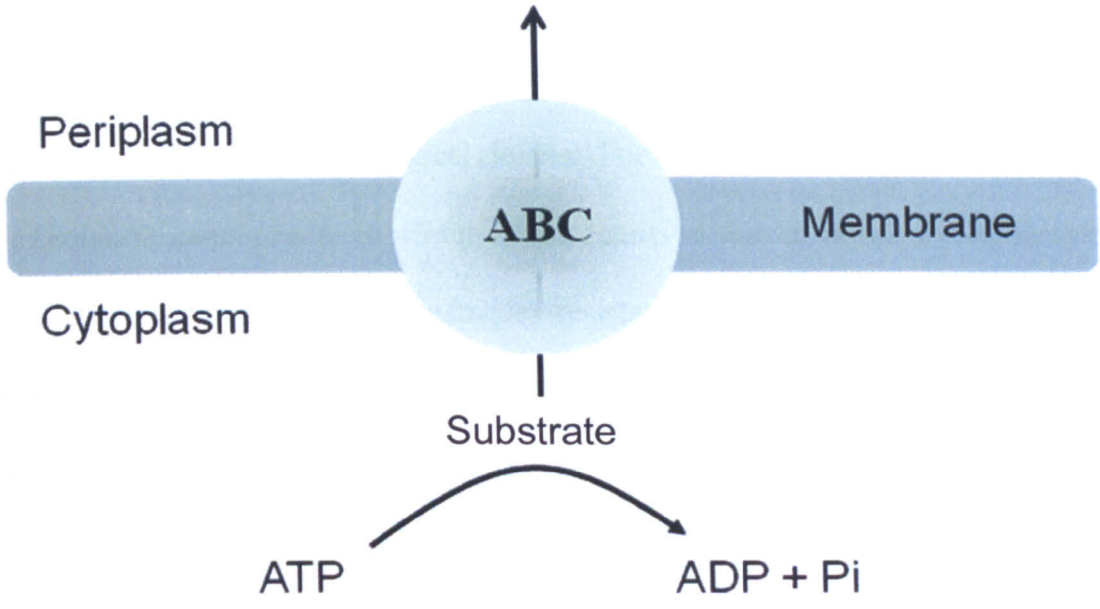

Figure 4. Schematic of an ABC transporter.

1.2.5. RND transporters

Efflux pumps of the resistance-nodulation-division (RND) family are ubiquitous in nature. In Gram-negative bacteria they are cytoplasmic membrane proteins that cooperate with a periplasmic adapter (otherwise known as membrane fusion) protein and an outer membrane channel. These tripartite complexes span the entire Gram-negative cell envelope and utilise the proton motive force to transport a broad range of structurally and chemically unrelated compounds to the extracellular environment, including bacterial derived products, dyes, detergents and antibiotics (Figure 5).

It is increasingly recognised that RND efflux systems contribute significantly to MDR in Gram-negative bacteria (145). They have been implicated in resistance to multiple classes of clinically important antimicrobial agents that have diverse structures and modes of action. Extrusion of the antibiotic substrate, which may be captured from the periplasm or the cytoplasm, lowers the concentration of drug in the cellular environment (meaning fewer molecules of the drug reach their target) to a

sub-inhibitory level thus negating its toxic effect(s). In some instances, innate resistance to certain antimicrobials is due to the action of RND transporters which are expressed at normal physiological levels. For example, the innate resistance of *Burkholderia cenocepacia* to a number of agents is due to efflux by RND systems (21). However, in certain circumstances resistance occurs only when these systems become up-regulated as a result of genetic changes (e.g. via mutations in genes or in the motifs involved in the regulation of expression of pump genes).

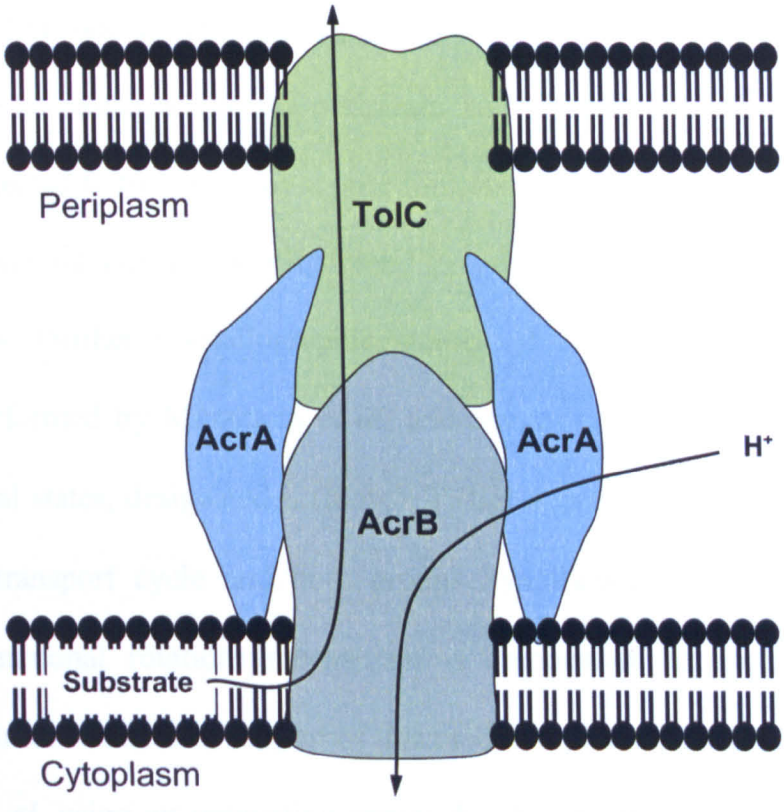

Figure 5. Schematic of the RND transporter AcrAB-TolC of *E. coli*.

1.2.5.1 Structure and function of RND transporters

To date, crystal structures of two of the most intensively studied RND pumps have been solved. These are the closely-related MexB (multiple efflux) and AcrB (acriflavin resistance) proteins of *Pseudomonas aeruginosa* and *E. coli*, respectively (179;232), which operate *in situ* as part of functional tripartite units in complex with the periplasmic adapter proteins MexA and AcrA and the outer membrane channels OprM and TolC, respectively, forming the functional MexAB-OprM and AcrAB-TolC transporters (88;146;159;202). Data from crystallographic studies indicate that both MexA and AcrB function as asymmetric homotrimers, with each subunit containing 12 TMs and a relatively large periplasmic domain that consists of a central cavity with three passages into the periplasm and a funnel-like structure at the top which is connected to the cavity by a pore formed of three α-helices (Figure 6). Each protomer (structural unit of the oligomeric protein) exists in one of three possible conformations. Further crystallographic studies of AcrB both with and without substrates performed by Murakami *et al.* and Seeger *et al.* indicated that the three conformational states, designated L (loose), T (tight), and O (open) represent distinct stages in a transport cycle and both groups hypothesise that a novel peristaltic pumping (functional rotation) mechanism is responsible for substrate extrusion (178;230). Direct evidence in support of this model of pump activity was presented by Takatsuka *et al.* using an innovative approach whereby three *acrB* sequences were linked together to form a 'giant gene' which allowed for inactivation of individual protomers in the trimeric structure (243). Upon inactivation of a single protomeric unit, the entire complex was inactivated (243). Further evidence of the functional rotation mechanism of AcrB activity described by Seeger *el al.* was provided by site-directed disulphide cross-linking of AcrB subdomains (231). It was demonstrated that

such cross-linking had an adverse affect on pump function (231). Subsequently, normal pump activity was restored upon exposure to a reducing agent to split these cross links (231).

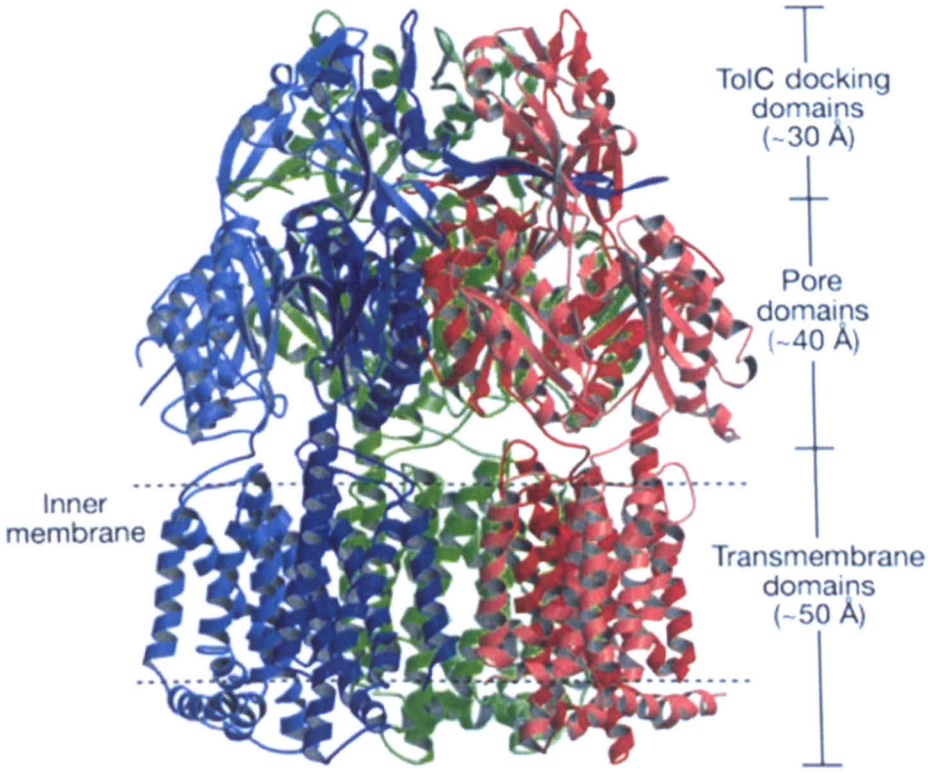

Figure 6. Ribbon representation (side view) of the structure of AcrB (Murakami *et al.* 2002).

The cytoplasmic membrane-associated RND proteins define the substrate specificity of the functional tripartite complex. The mechanics of substrate binding and substrate specificity of RND proteins have been studied intensively over the last decade. Most reports have focused on the archetypal RND proteins AcrB and MexB and a number of regions have been implicated within both the periplasmic and transmembrane domains.

In a study where hydroxylamine-mutagenized *mexB* was expressed in a Δ*mexB* strain, 19 single mutations were identified that adversely affected pump function (170). Most of these were located within the periplasmic loops between TMs 1 and 2 and between TMs 7 and 8 (170) and lay in regions that were predicted to be involved in the interaction of MexB with MexA (the periplasmic adapter protein) or MexB trimer formation (170). Crystallographic and site-directed mutagenesis studies of AcrB bound with structurally diverse substrates by Yu *et al.* implicated both periplasmic and transmembrane domains in substrate recognition (282;283). Bound substrate was observed not only in the central cavity but also within an external depression produced by the C-terminal periplasmic loop (282;283). In addition, a single point mutation that was selected during levofloxacin exposure resulted in a Val-610→Phe substitution in AcrB that had the effect of altering substrate specificity, thus providing further evidence of periplasmic domain involvement (28). In another study, chimeric constructs of AcrB and another *E. coli* RND protein, AcrD were produced in which portions of the periplasmic domain (specifically the loops between TMs 1 and 2 and between TMs 7 and 8) were replaced with those of the other protein (76). These constructs were expressed in a Δ*acrB* Δ*acrD* host strain and substrate specificity was investigated. It was observed that AcrB chimeras containing the AcrD periplasmic regions conferred resistance only to substrates of AcrD and vice versa, thus implicating the periplasmic loop domains in substrate specificity (76). Protomers of AcrB in the conformational state T (tight) were shown to form hydrophobic binding pockets that were rich in phenylalanine and other aromatic residues (230). It has been demonstrated that different substrates can interact with different residues within the binding pocket. For example, Murakami *et al.* reported that doxorubicin appeared to interact with Gln-176, Phe-615 and Phe-617 whereas minocycline seemed

to interact with Phe-78, Asn-274 and Phe-615 and hence proposed that the broad substrate profile of AcrB could perhaps be explained by the flexible nature of the interaction of different ligands primarily with hydrophobic and to a lesser extent polar residues within the binding pocket (178). A systematic site-directed mutagenesis study of phenylalanine residues within the binding pocket was carried out by Bohnert *et al* (29). They observed variable effects on the susceptibility to a number of substrates when different residues were mutated, but were able to identify Phe-610→Ala as the mutation that had the most dramatic impact in terms of lowering substrate (e.g. macrolides) minimum inhibitory concentrations (MICs) (29).

A number of crystallographic studies have shed light on the structure and function of the periplasmic adapter proteins, MexA of *P. aeruginosa* and AcrA of *E. coli* (4;105;171;242). It was established in the 1990s that these proteins are essential for transporter function (159;202). A detailed picture has since emerged of their functional role in stabilising the tripartite complex through interaction with both the RND and outer membrane components. It is clear that these proteins have four distinct subdomains: an α-helical hairpin, a lipoyl domain and a six-stranded β-barrel domain, which is linked via a β-ribbon to the recently modelled membrane proximal domain (242). The similarity of the β-barrel and the membrane proximal domains is intriguing and it has been postulated that the overall structure of the protein arose as a result of domain duplication (242). The N-terminal cysteine residue has a lipid tail which acts as an anchor by inserting into the cytoplasmic membrane (Figure 7). A significant degree of conformational flexibility has been observed in the structures of both MexA and AcrA. This is due to the hinged nature of the linkers between the lipoyl domain and the β-barrel and α-helical hairpin domains (171;263).

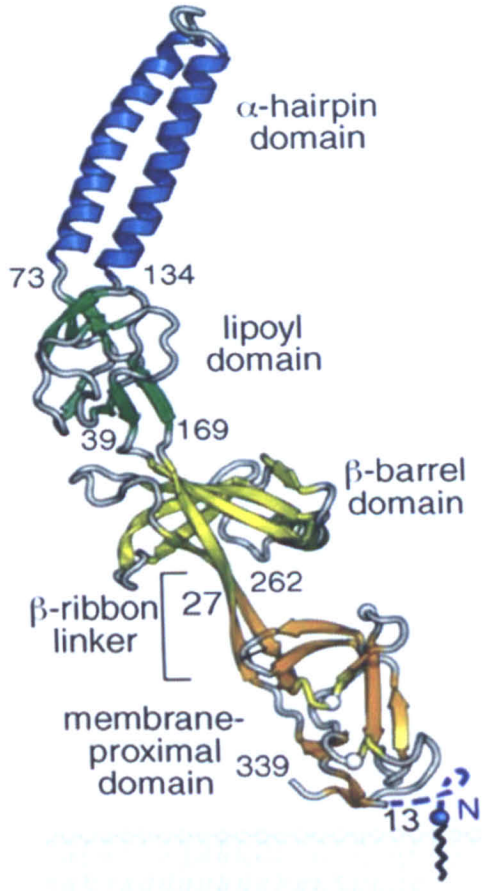

Figure 7. Complete structure of MexA (Akama *et al.* 2004).

The outer membrane channel proteins associate with both the RND proteins and the periplasmic adapter components to form the functional transporter and act as exit ducts for the substrates (Figure 5). X-ray crystallography has once again played a pivotal role in elucidating the structure and informing on the function of these important proteins. To date, the crystal structures of several of these proteins have been solved including TolC of *E. coli*, OprM of *P. aeruginosa*, and VceC of *V. cholerae* all of which have a similar structure even though their sequence identity is low (3;80;134;196). Of these, TolC has been the best studied and exists as a trimer, with each protomer consisting of a membrane-anchored β-barrel and a long α-helical domain containing 12 coiled coils which extend into the periplasmic space (134). The

trimeric complex forms an outer membrane pore and a periplasmic tunnel which is closed at the proximal end by coiled α-helices (Figure 8) (134). Until relatively recently, these helices were thought to relax from a tightly packed state, in a iris-like fashion, thus allowing for TolC opening (8). However, molecular dynamic simulations of TolC hint at a more complex mechanism whereby a peristaltic action of the periplasmic domain aids the transport of substrate through the tunnel (264). Site-specific crosslinking experiments suggested that the interaction of TolC with AcrA is most favourable when TolC is an open conformation (242). Binding of AcrA to AcrB facilitates TolC recruitment to the complex which in turn leads to TolC opening. The interaction of AcrB and TolC is stabilised by AcrA which prevents substrate leaking into the periplasmic space, thus allowing TolC to adopt a constitutively open conformation in the functional tripartite complex (242).

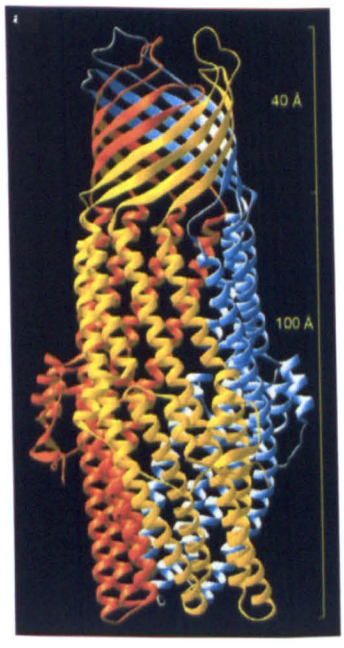

Figure 8. Ribbon representation (side view) of the structure of TolC (Koronakis *et al.* 2000).

There is also limited evidence of AcrB functioning in complex with another transmembrane protein, YajC which was reported to induce rotation of the periplasmic domain of AcrB (252). Data presented by the authors suggested that YajC binding was functionally significant, as a Δ*yajC* mutant *E. coli* strain displayed increased susceptibility to ampicillin (252).

The stoichiometry of RND apparatus has been investigated using the archetypal pumps of *E. coli* and *P. aeruginosa*. In the case of AcrAB-TolC, Symmons *et al.* proposed a stoichiometry of 3 : 3 : 3 (AcrA : AcrB : TolC) based upon modelling using the solved structures of all the components and crosslinking experiments performed at pH 7.5 (242). In contrast, a study of MexA / OprM interaction suggested a stoichiometry of 2 : 1 at pH 7.5 and 6 : 1 (MexA : OprM) at pH 5.5 (209). There are also descriptions in the literature of RND systems containing either two unique RND or periplasmic adapter proteins in which both are required for efflux activity (22;174).

1.2.5.2. Regulation of RND transporters

Since the degree to which RND transporters confer resistance to antimicrobial agents has been linked to their levels of expression there has been much interest in the mechanisms of transcriptional regulation of efflux pump genes. Much of the knowledge about RND efflux gene regulation has come from studies in *E. coli*. It has become clear that the regulation of RND transporter genes is complex, involving both local and global regulatory elements. The pump genes are chromosomally encoded with the periplasmic adapter and RND components most often co-transcribed as an operon whereas the outer membrane channel gene may either be part of the same

structural operon or may be located elsewhere on the chromosome, as is the case for the AcrAB-TolC system of *E. coli* (88;158).

Expression of *acrAB* in *E. coli* is modulated at the local level by the divergently transcribed repressor gene *acrR*, which encodes a helix-turn-helix (HTH) DNA-binding domain-containing protein of the TetR family (157). AcrR negatively regulates *acrAB* as well as its own expression through binding to the regulatory region located between *acrR* and *acrAB* (Figure 9); however AcrR is not involved in up-regulating the pump in response to environmental stress, as demonstrated by elevated *acrAB* expression under stressed conditions (e.g. 4 % ethanol, 0.5 M NaCl and entry into stationary phase) in the absence of functioning AcrR (157). This suggests that other regulatory elements are involved in *acrAB* induction under these conditions. It has been demonstrated that mutations in *acrR* can lead to increases in *acrAB* expression that are sufficient to contribute to fluoroquinolone resistance both in *E. coli* and *Salmonella enterica* serovar Typhimurium (190;269). AcrAB and AcrEF, another *E. coli* RND system, have similar substrate profiles and a high degree of sequence homology. The *acrS* gene which encodes another repressor of the TetR family, AcrS and is the local regulator found upstream of the *acrEF* operon has also been shown to repress the expression of *acrAB* (109).

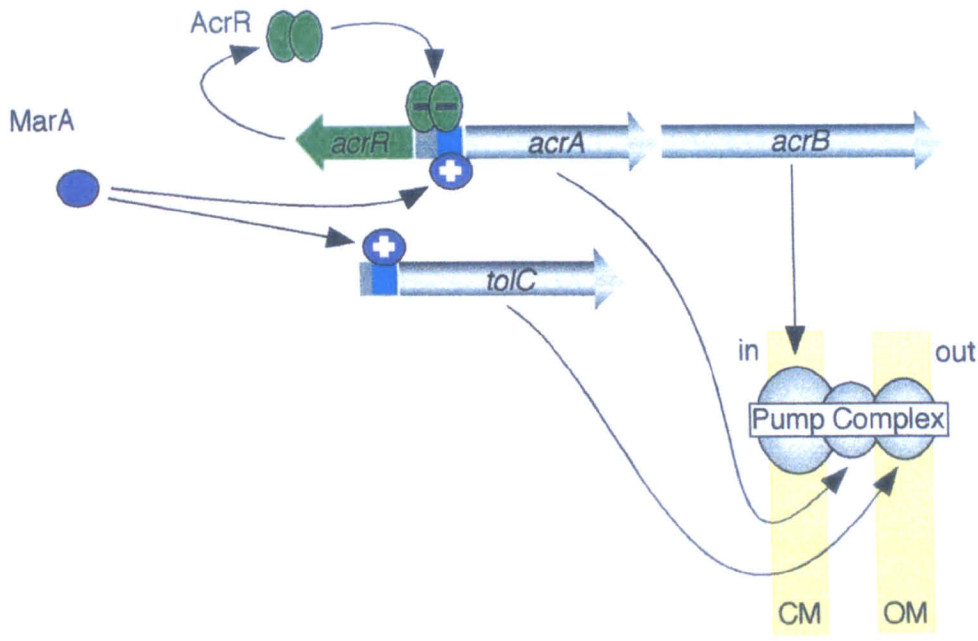

Figure 9. Regulation of *acrAB* and *tolC* by AcrR and MarA [adapted from Grkovic *et al.* 2002 (98)].

Bacteria are able to sense changes in environmental conditions and respond at the transcriptional level through the action of two-component signal transduction systems. These comprise of a sensor kinase and its cognate response regulator. When the membrane-associated sensor kinase protein binds a specific ligand it autophosphorylates at a conserved histidine residue. The phosphate group is then transferred to a conserved aspartic acid residue in the DNA-binding response regulator which then undergoes conformational change and modulates gene expression (38). A number of studies of *E. coli* have identified two-component systems that regulate the expression of RND transporters; these include the BaeSR and CpxAR regulatory systems which are activated by indole and which modulate transcription of the RND system *mdtABC* (18;108;187).

AcrAB of *E. coli* is also regulated by SdiA, which is a transcriptional regulator of the LuxR family that is involved in regulating cell division in a manner which is

dependent on cell density and hence quorum sensing (206). It was demonstrated that overexpression of *sdiA* resulted in increased fluoroquinolone MICs as a result of AcrAB activity and that a Δ*sdiA* mutant was more susceptible to fluoroquinolones and produced less AcrB than its wild-type parent (206). More recently, *sdiA* was found to be overexpressed in two mutants of *E. coli* selected *in vitro*; these were shown to have elevated levels of *acrB* and *tolC* transcript, and displayed decreased susceptibility to a number of antimicrobial agents (245).

Expression of RND-type efflux pump genes in the Enterobacteriaceae is also controlled by global transcriptional regulators of the AraC family including MarA, SoxS, Rob and RamA, of which MarA of *E. coli* is the best studied. The *mar* (multiple antibiotic resistance) regulatory region comprises the *marRAB* operon; *marC*, which is divergently transcribed, and the *marO* operator/promoter region which is located between *marRAB* and *marC* (6). MarA activates transcription of a large number of genes including *acrAB*, *tolC* and *marA* itself by forming complexes with RNA polymerase which then bind to 20-bp DNA sequences known as marboxes that are located adjacent to the promoter regions of genes that are part of the MarA regulon, including within *marO* (6;12;165). Both *marB* and *marC* encode proteins of unknown function though studies by McDermott *et al.* indicate that MarC is not involved in MDR since neither inactivation or overexpression of *marC* led to changes in susceptibility to a number of antimicrobial agents (168). MarR is the repressor that restricts expression of *marRAB* by binding to *marO* at two sites located downstream from the marbox; the first is located between the -35 and -10 regions of the *marRAB* promoter and the second is further downstream at the ribosome binding site (166).

Induction of the *mar* regulon occurs upon suppression of MarR activity. A number of compounds have been shown to induce *marRAB* expression through

interference with MarR / *marO* binding, including salicylate, plumbagin, menadione, 2,4-dinitrophenol and the bacterial metabolite 2,4-dihydroxybenzoate (7;47). Chloramphenicol and tetracycline have also been shown to induce the *mar* regulon (99). Hence, MarR is able to sense the presence of some toxic compounds and mediate derepression of *marRAB*, resulting in MarA-mediated activation of the *mar* regulon, which includes *acrAB* and *tolC*. More recent work suggested that, surprisingly, MarR may also interact with the unrelated bacterial proteins GyrA and TktA (transketolase A, involved in metabolism) and inhibit *marRAB* repression (70;71) highlighting the fact that global regulation of RND transporters is highly complex and much of the detail remains obscure.

1.2.5.2. Physiological role of RND transporters

Over the last two decades, a large body of work has provided much evidence in support of the hypothesis that RND transporters play important roles in the biology of Gram-negative pathogens. One prominent example, with particular relevance to human infections, is their role in virulence. RND efflux systems have been implicated in the virulence of a number of species including *P. aeruginosa*, *S. enterica*, *N. gonorrhoeae*, *Campylobacter jejuni*, *Francisella tularensis*, *Legionella pneumophila* *Borrelia burgdorferi*, and *Burkholderia pseudomallei* (27;36;37;39;81;107;123;149;188). Gene knockout studies in *S. enterica* serovar Typhimurium indicated that Δ*acrB* and Δ*tolC* mutants were unable to invade mouse monocyte macrophages (36) while a strain lacking all multidrug efflux systems was reported to be avirulent in orally-inoculated mice (188). The virulence of a mutant *F. tularensis* strain that lacked functional AcrB was attenuated in a murine infection

model (27). In *B. burgdorferi*, the outer membrane protein BesC, a TolC homologue, forms part of the RND system BesABC and was shown to be essential for establishing infection in mice (37). The BpeAB-OprB efflux transporter of *B. pseudomallei* was shown to be important for virulence, as demonstrated by the attenuation of invasion of human lung epithelial and human macrophage cells by Δ*bpeAB* mutants as well as strains overexpressing a repressor of the *bpeAB-oprB* operon (39). The causative agent of legionnaire's disease, *L. pneumophila*, which is an intracellular parasite of amoeba, displayed attenuated virulence towards both human monocyte macrophages and amoebae upon inactivation of TolC (81).

RND efflux systems contribute to bacterial virulence at least in part because they appear to aid in the survival of bacterial cells within the often hostile host environment through their ability to extrude toxic host-derived products, including fatty acids, bile salts, and steroid hormones (73;75;159). It has been reported that expression of RND efflux genes can be induced by bile and other agents present in the human digestive tract, thus facilitating *in vivo* survival (108;185;186). Perhaps unsurprisingly, there is evidence to suggest that *E. coli* AcrAB has greater affinity for bile acids than for antimicrobials, which hints at the core biological function of these efflux systems in *E. coli* (285). There is also evidence that some RND efflux pumps confer resistance to mammalian antimicrobial peptides, pointing to a possible role in evading innate defence mechanisms (233;272) although the *E. coli* AcrAB and *P. aeruginosa* MexAB pumps were not able to confer resistance to human antimicrobial peptides, even when overexpressed, suggesting this may not be a universal phenomenon (214).

An interesting study that investigated the global impact of *acrAB-tolC* interruption in *S. enterica* by Webber *et al.* showed differential expression of genes

and proteins involved in pathogenesis in mutants lacking individual components of the transporter (274). Genes involved in chemotaxis, motility and type III secretion were shown to be expressed at lower levels in efflux-deficient strains, thus explaining how such mutants are attenuated, and demonstrating the importance of this transporter to the core biology of Gram-negative bacteria (274).

In addition to promoting *in vivo* survival as described above, another important natural role of RND transporters appears to be cell-to-cell communication. As discussed in section 1.2.5.1, AcrAB of *E. coli* is positively regulated by the quorum sensing transcription factor SdiA (206). In further work it was demonstrated that Δ*acrB* and Δ*tolC* mutants grew to a higher cell density in stationary phase than wild-type strains despite having the same growth rate in exponential phase, whereas overexpression of *acrAB* had the effect of lowering cell density (280). The authors also present evidence that expression of *rpoS*, which encodes the stationary phase sigma factor, RpoS, is induced later in *acrAB* mutants and earlier in cells where *acrAB* was overexpressed (206;280). These results, combined with observations that some quorum sensing molecules bear structural similarities to the fluoroquinolones (known substrates of *E. coli* RND systems), suggest that these transporters may have a role in the extrusion of quorum sensing signals (206;280).

Taken together, the evidence described above suggests that RND transporters perform multiple biological functions. It seems unlikely that the primary role of such efflux systems is the extrusion of antibiotics used in modern medicine since, for example, RND systems appear critical for bacterial survival *in vivo*. However, antimicrobial selection pressure has undoubtedly shaped bacterial evolution and will continue to do so. The widespread use of antibiotics over the last 70 years has selected

for Gram-negative bacteria which are better adapted to use these intrinsic efflux transporters as a defence mechanism against the chemotherapeutic offensive.

1.2.5.3. Inhibitors of RND transporters

Given their established role in MDR, there has been much interest in developing strategies for the disruption of RND pump activity. An ability to inhibit efflux is useful in order both to study pump function and to investigate the potential of therapeutic combinations of antibiotics and efflux pump inhibitors (EPIs) to restore antimicrobial activity (161;192). Inhibition of RND transporter activity may be achieved using a number of approaches including blocking the outer membrane channel, inhibiting the assembly of the functional tripartite complex, collapsing proton motive force required for efflux activity, competing with the antimicrobial substrate or interfering with regulatory networks that control expression of pump genes.

To date, no EPIs have entered clinical use since the experimental molecules often have toxic effects on eukaryotic cells, although the drug company Mpex Pharmaceuticals has a number of compounds in preclinical development (191). However, a number of EPIs are available to study the function of RND transporters including the peptidomimetic compound MC-207,110, Phe-Arg-β-napthylamine (PAβN), which competes with the antimicrobial substrates (155;213). Another example of an EPI that is used to study RND systems is carbonyl cyanide *m*-chlorophenylhydrazone (CCCP) which acts an ionophore, collapsing the proton gradient; as such it disrupts active efflux by RND transporters (192). However, by their very nature, many of the effects of EPIs are non-specific and while they are a useful research tool the data obtained from them cannot be taken in isolation.

1.3. The tetracycline class of antimicrobials

Tetracyclines were discovered over 60 years ago during investigations of the antimicrobial properties of the fermentation products of actinomycetes. The naturally occurring, first-generation tetracyclines, oxytetracycline, chlortetracycline and 6-demethylchlortetracycline were the products of actinomycetes' secondary metabolism and entered clinical and agricultural use soon after their discovery. They were the first naturally occurring agents with broad spectrum antimicrobial activity that included both Gram-positive and Gram-negative pathogens (45). Second-generation tetracyclines such as doxycycline and minocycline were developed two decades later in response to the emergence of resistance to the first-generation compounds.

The pharmacophore of the tetracycline class includes a four-membered ring system, one of which is aromatic (Figure 10). Chemical modification of carbons 4, 5, 6 and 7 has resulted in the production of new molecules. These are semi-synthetic derivatives with improved spectrums of action and pharmacological profiles and include minocycline (45;249) (Figure 10).

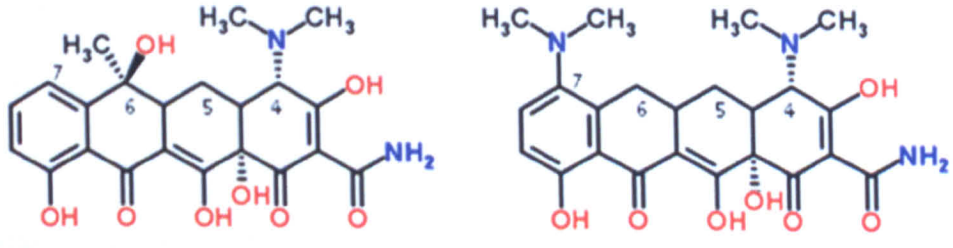

Figure 10. Chemical structures of tetracycline (left hand side) and minocycline (right hand side) (PubChem).

1.3.1. Mode of action

Antibiotics of the tetracycline class are bacteriostatic agents that exert their antimicrobial activity through binding to the 30S subunit of the prokaryotic ribosome and disrupting translation (5;10;34;228). Specifically, tetracycline molecules, in complex with $Mg,^{2+}$ bind in the aminoacyl-tRNA acceptor site region (A site). This binding sterically prevents aminoacyl-tRNAs from entering the A site, and protein synthesis is arrested (34). To gain access to the target site on the ribosome, tetracycline preferentially crosses the outer membrane of *E. coli* cells in its Mg^{2+}-chelated form via porin OmpF, as illustrated by a study that demonstrated a reduction in the intracellular accumulation of tetracycline in tetracycline-susceptible *E. coli* in the absence of this porin or when there was a low proportion of the Mg^{2+}-bound versus free drug (251). Tetracycline most probably enters the cytoplasm by passive diffusion in its unbound form across the inner membrane (15). Thus, the ability of tetracycline to bind divalent cations is essential both for drug entry and target binding.

1.3.2. Tetracycline resistance

The widespread use of tetracyclines in human and veterinary medicine and agriculture over the last 60 years has created intense selection pressure for resistance. Since the 1950s, resistance to this class of antimicrobials has rapidly increased in many species of both Gram-positive and Gram-negative bacteria, predominantly through horizontal transfer of tetracycline resistance (*tet*) and oxytetracycline resistance (*otr*) genes located on mobile genetic elements. Multiple mechanisms of tetracycline resistance have been described including active efflux, ribosomal protection, enzymatic inactivation and target modification/mutation. Of these mechanisms, active efflux and ribosomal protection are the most common (45). In 2001 a website was created in

order to collate information on acquired *tet* and *otr* genes (available at: http://faculty.washington.edu/marilynr/). It is updated biannually and is curated by Dr Marilyn Roberts. An attempt to standardise the nomenclature for tetracycline resistance determinants based upon letters of the alphabet was proposed at the end of the 1980s (144). Subsequently, as more determinants were identified, Levy *et al.* suggested that future determinants be designated with Arabic numerals (143).

1.3.2.1. Efflux

The efflux pumps that confer acquired resistance to tetracyclines are the most intensively studied Tet determinants. The vast majority are members of the MFS of efflux transporters (section 1.2.1) and were initially divided into six groups a decade ago based upon protein sequence identity, although this number was subsequently increased to accommodate the multiple resistance determinants since identified (45;216). Group 1 consists of members of the DHA-1 transporter family which are Tet(A), Tet(B), Tet(C), Tet(D), Tet(E), Tet(G), Tet(H), Tet(J), Tet(Y), Tet(Z), Tet(30), Tet(31), Tet(33), Tet(39), Tet(41) and Tet(42) (45;249). Most of the Tet determinants belonging to group 1 are found only in Gram-negative bacteria; exceptions are Tet(Z), which was identified in the soil organism *Corynebacterium glutamicum* (244) and Tet(42), which was identified in various uncharacterised Gram-positive and Gram-negative bacteria recovered from deep terrestrial sediment (35). Group 2 contains Tet(L) and Tet(K) which are found mostly in Gram-positive species. Those of *Streptomyces* origin, namely Otr(B) and Tcr(3), have similar topology to group 2 and are classified as group 3 (45). The sole member of group 4, TetA(P) was identified in *Clostridium perfringens* and lacks conserved motifs characteristic of the MSF (236). Group 5 also has only a single member, namely Tet(V), which was

identified in *Mycobacterium smegmatis* (60). There are two members of group 6, namely, Tet(35) and Otr(C) (216;247), and finally, Tet(38), which was identified in *Staphylococcus aureus*, and is most similar to Tet(K) (249;254) so should be assigned to Group 2.

The acquired *tet* genes that encode efflux transporters are common among Gram-negative bacteria, having been identified in 25 genera, and are generally found on transposons that have integrated into plasmids from diverse incompatibility groups (125;216). Most confer resistance to tetracycline but not minocycline, though *tet*(B) confers resistance to both agents (44). The *tet*(B) gene is associated with the transposon Tn*10*, has been found on conjugative plasmids, and is the most widely disseminated acquired efflux pump gene among Gram-negative species (45;216).

Along with *tet*(A), *tet*(B) it is also one of the most common *tet* determinants among clinical isolates of *Acinetobacter baumannii* and is the predominant *tet* determinant associated with the internationally-disseminated European clone II (section 1.5) (118;118). Mak *et al.* showed that 28 out of 32 *A. baumannii* isolates which were collected from multiple centres in Sydney, Australia were positive by PCR for *tet*(B) (162).

1.3.2.2. Ribosomal protection

Ribosomal protection proteins (RPPs) are cytoplasmic proteins of approximately 72.5 kDa that protect the bacterial ribosome from the action of first- and second-generation tetracyclines. They have homology to the elongation factors EF-Tu and EF-G GTPases (246). RPPs interact with the ribosome in a manner that allosterically disrupts the primary tetracycline binding sites, resulting in the release of tetracycline from the ribosome (50). It has been proposed that RPPs evolved through divergence

of an ancient GTPase independent of the presence of tetracyclines, implying that these proteins have biological function(s) other than antimicrobial resistance (131). They are currently divided into three groups based upon protein sequence identity. Group 1 consists of Tet(M), Tet(O), Tet(S), Tet(W), Tet(32) and Tet(36); group 2 contains TetB(P), Otr(A) and Tet; the two members of group 3 are Tet(Q) and Tet(T) (249). Tet(44), a novel RPP, has been recently described in the cattle pathogen *Campylobacter fetus* subsp. *fetus* associated with a transferable pathogenicity island and is most similar to Tet(O) and so should be assigned to group 1 (1).

RPP genes have been detected in 42 genera including both Gram-positive and Gram-negative organisms as well as some members of the Mycoplasmataceae (216). Of all *tet* genes, *tet*(M) is the most widely disseminated. This can perhaps be explained by it often being found on integrative and conjugative elements of the Tn*916*-Tn*1545* family which have a broad host range (48;216). Surveillance studies of ribosomal protection mechanisms have been complicated by the discovery of mosaic RPP genes in the ruminant commensal *Megasphaera elsdenii* (240). Nucleotide sequencing of what was initially thought to be *tet*(O) from two isolates revealed that the genes were actually two different mosaics which comprised of *tet*(O) and *tet*(W) sequences that presumably arose through recombination events (240). A study of human faecal samples taken from individuals across Europe found that 46 % of resistance genes amplified directly from the samples using *tet*(O) primers were mosaics that included fragments of *tet*(O), *tet*(W) and *tet*(32) sequences, suggesting that such mosaic genes may be widespread (195).

1.3.2.3. Enzymatic inactivation of tetracyclines

Enzymatic modification and inactivation of antimicrobial agents is a common mechanism of resistance to other compound classes such as the aminoglycosides and β-lactams, but less so for the tetracyclines. To date, just three genes that encode tetracycline-modifying enzymes have been described (66;189;238). The first to be characterised, Tet(X), was originally identified in *Bacteroides fragilis* where it was non-functional (239). However, when the *tet*(X) gene was cloned and expressed in aerobically-growing *E. coli* it was shown to modify tetracycline and destroy its antimicrobial activity (238). Further characterisation of Tet(X) activity has shown that it is a flavin-dependent monooxygenase that hydroxylates tetracyclines at carbon 11a (281). Another gene encoding an oxidoreductase enzyme with tetracycline-modifying activity was recovered from a cloned part of the human oral metagenome (encompassing all the genetic material present in the human mouth) and was designated *tet*(37) (66). Despite having similar properties, there is no homology between Tet(37) and Tet(X). The third gene encoding an enzyme that inactivates tetracycline, named *tet*(34), was identified in *Vibrio* sp. and is homologous to the xanthine–guanine phosphoribosyl transferase from *V. cholerae* (189).

1.3.2.4. Target modification

Modification of antimicrobial targets that arises through mutation is another common mechanism of drug resistance. Mutational changes to the bacterial ribosome that affect tetracycline activity have been documented in Gram-positive and Gram-negative species. The first report of tetracycline resistance mediated by this mechanism was that describing a G → C point mutation at position 1058 in 16S rRNA in clinical isolates of *Propionibacterium acnes* that were resistant to

tetracycline (217). When this mutation was engineered in *E. coli* by site-directed mutagenesis the resulting mutants were less susceptible to tetracycline than wild-type strains (217).

Mutations in 16S rRNA located within the primary tetracycline binding site have also been implicated in tetracycline resistance in *Helicobacter pylori* (54;96). Further work on this species showed that successive contiguous nucleotide substitutions have a cumulative effect on the level of tetracycline resistance with triple bp mutations conferring a higher level of resistance than single or double bp mutations (95).

1.4. Glycylcyclines and the development of tigecycline

During a programme in the early 1990s at the pharmaceutical company American Cyanamid (which later became Wyeth after American Home Products acquired the company in 1994) to discover novel antibiotics with activity against MDR bacteria, it was observed that molecules with certain chemical modifications to the tetracycline scaffold at carbon 9 displayed better *in vitro* activity against organisms that possessed Tet efflux determinants (205).

Further work led to the discovery of N,N-dimethylglycylamido (DMG) derivatives of minocycline (DMG-MINO) and 6-demethyl-6-deoxytetracycline (DMG-DMDOT). These compounds were the first semi-synthetic, third-generation tetracyclines, or so called glycylcyclines, that were shown to be active *in vitro* and *in vivo* versus Gram-positive and Gram-negative species that harboured *tet* genes encoding either efflux pumps or RPPs (248). However, concerns over the propensity for resistance to these novel agents to emerge through mutation of known *tet* genes

spurred the search for other glycylcyclines that had similarly potent or even greater activity but which did not possess such resistance liabilities (205).

Tigecycline (initially known in the literature as TBG-MINO and GAR-936), is the 9-*t*-butylglyclamido derivative of minocycline (Figure 11). This broad-spectrum compound was more active than DMG-MINO and DMG-DMDOT (201;241). An early study showed it to be active *in vitro* versus a range of aerobic and anaerobic Gram-positive and Gram-negative organisms, including those which possessed *tet* genes encoding efflux pumps and RPPs (201). In particular, it displayed good *in vitro* activity versus clinical isolates of methicillin-resistant *S. aureus* (MRSA), vancomycin-resistant enterococci (VRE) and penicillin-resistant streptococci, with MIC_{90s} (i.e. the MIC required to inhibit the growth of 90% of isolates) of ≤ 0.5 mg/L while it was as active or more active than minocycline versus most Gram-negative species tested (201). It was demonstrated that tigecycline was also efficacious *in vivo* (murine model) against infections caused by *E. coli* and *S. aureus* (including MRSA) that harboured *tet* genes (201).

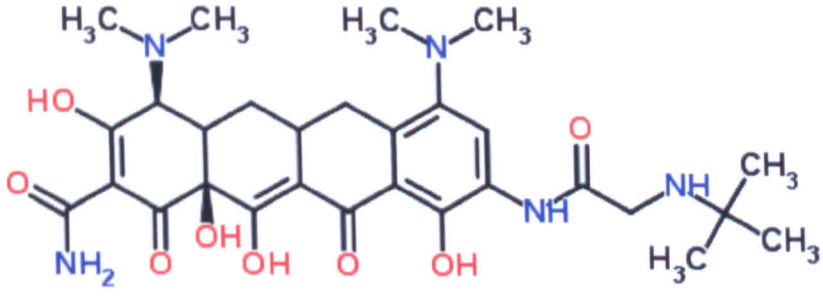

Figure 11. Chemical structure of tigecycline (PubChem).

Further *in vitro* studies confirmed the findings of the initial report with MIC_{90s} of ≤ 1 mg/L for all Gram-positive cocci and ≤ 2 mg/L for most Gram-negative species tested including *Acinetobacter* spp. (31;91;172;211). Notably, some studies showed minocycline to be more active than tigecycline versus *Acinetobacter* spp. (91;104). Tigecycline displayed only modest activity against *Pseudomonas* spp., *Proteus* spp., and *Morganella morganii* which generally had tigecycline MIC_{90s} of ≥ 4 mg/L (31;91;172). Wild-type tigecycline MIC distributions are shown in Table 1.

Table 1. Wild-type tigecycline MIC distributions for multiple species of Gram-negative and Gram-positive bacteria*

Organism	MIC (mg/L)																		
	0.002	**0.004**	**0.008**	**0.016**	**0.032**	**0.064**	**0.125**	**0.25**	**0.5**	**1**	**2**	**4**	**8**	**16**	**32**	**64**	**128**	**256**	**512**
Acinetobacter baumannii	0	0	0	0	2	24	34	51	63	62	51	12	0	0	0	0	0	0	0
Acinetobacter spp	0	0	0	0	2	19	99	83	29	23	8	3	2	0	1	0	0	0	0
Burkholderia cepacia	0	0	0	0	0	2	3	4	10	31	36	44	29	11	5	6	2	0	0
Citrobacter freundii	0	0	0	0	6	3	24	99	56	19	6	0	2	0	0	0	0	0	0
Enterobacter cloacae	0	0	0	0	0	0	3	98	465	241	51	19	15	2	0	0	0	0	0
Escherichia coli	0	0	0	0	0	88	1341	1970	659	145	22	8	3	1	0	1	0	0	0
Klebsiella pneumoniae	0	0	0	0	0	1	17	276	921	429	144	60	6	2	0	0	0	0	0
Morganella morganii	0	0	0	0	0	0	1	4	40	133	121	48	11	0	0	0	0	0	0
Proteus mirabilis	0	0	0	0	0	0	2	4	27	212	344	442	163	3	0	0	0	0	0
Pseudomonas aeruginosa	0	0	0	0	0	0	1	5	8	16	21	117	363	408	140	33	5	3	0
Salmonella typhimurium	0	0	0	0	0	0	7	94	100	56	12	0	0	0	0	0	0	0	0
Serratia marcescens	0	0	0	0	0	0	0	4	55	164	29	3	2	0	0	0	0	0	0
Enterococcus faecalis	0	0	0	3	112	512	356	161	6	0	0	0	0	0	0	0	0	0	0
Enterococcus faecium	0	0	0	5	159	445	164	24	1	1	0	0	0	0	0	0	0	0	0
Staphylococcus aureus (MRSA)	0	0	0	0	0	0	26	218	41	1	0	0	0	0	0	0	0	0	0
Staphylococcus aureus (MSSA)	0	0	0	0	0	1	172	261	8	1	2	0	0	0	0	0	0	0	0
Staphylococcus epidermidis	0	0	0	0	10	99	242	123	130	8	3	0	0	0	0	0	0	0	0
Streptococcus pneumoniae	0	2	31	96	630	2107	657	127	4	0	0	0	0	0	0	0	0	0	0
Streptococcus pyogenes	0	0	0	68	68	219	60	3	1	0	0	0	0	0	0	0	0	0	0

* European Committee on Antimicrobial Susceptibility Testing (EUCAST). Data from the EUCAST MIC distribution website that represent the pool of multiple studies and unpublished collections, last accessed 09/06/11. http://www.eucast.org

The safety and clinical efficacy of tigecycline in the treatment of complicated skin and skin structure infections (cSSSI) and complicated intra-abdominal infections (cIAI) was assessed in a number of double-blind, phase III, multicentre clinical trials using a 100 mg loading dose followed by 50 mg intravenously every 12 hours for a duration of between 5 and 14 days (33;77;87;225). These studies concluded that tigecycline monotherapy was efficacious in the treatment of cSSSI and cIAI as demonstrated by noninferiority to that of vancomycin plus aztreonam in the case of the former (33;77;225) and noninferiority to that of imipenem plus cilastatin in the case of the latter (87). In all studies, reports of adverse events were similar in the two groups with nausea and vomiting the most frequently reported events in the tigecycline group (33;77;87;225).

Further phase III trials evaluated the efficacy of tigecycline in the treatment of hospitalised patients with community-acquired pneumonia (CAP) (24;57) and hospital-acquired pneumonia (HAP) (89). The CAP studies both concluded that tigecycline was safe and efficacious (noninferior to levofloxacin). However, data from the HAP trial demonstrated that tigecycline was inferior to imipenem in the ventilator-associated pneumonia (VAP) patient group (89).

Tigecycline has only limited oral bioavailability and therefore is only available as an intravenous formulation. Pharmacokinetic analysis of phase I trial data on healthy volunteers indicated that tigecycline has a long terminal elimination half-life ($t_{1/2}$) of approximately 40 hours and a large steady-state volume of distribution (V_{ss}) of approximately 7 - 10 L/kg, displaying widespread tissue penetration (169). While tigecycline rapidly and extensively penetrates body tissue, it displays relatively low maximum plasma concentrations (C_{max}), which for multiple-dose regimens is approximately 0.6 – 1.1 mg/L (169). Tigecycline is not extensively metabolised and

the primary route of elimination is through biliary / faecal excretion as unchanged drug (169).

Tigecycline was licensed under the brand name Tygacil® for the treatment of cSSSI and cIAI in adults by the Food and Drug Administration (FDA) in the United States (US) in 2005 and in Europe by the European Medicines Agency (EMA) in 2006. In 2009, tigecycline was also approved by the FDA in the US for the treatment of CAP in adult patients.

1.4.1. Mode of action

Early studies showed that the glycylcyclines, DMG-MINO and DMG-DMDOT are bacteriostatic agents and that their mode of action is like that of the tetracyclines in that they bind to the bacterial ribosome and inhibit protein synthesis by preventing aminoacyl-tRNAs from entering the A site although more effectively than tetracycline or minocycline, suggesting a mechanism of evasion of RPP-mediated resistance (25;208). Further work investigating the antibacterial activity of tigecycline found that, like tetracycline, tigecycline bound in the A site of the 30S subunit in complex with Mg^{2+} but in a manner that allowed tigecycline to escape ribosomal protection mechanisms (20).

1.5. Gram-negative species studied

Rates of tigecycline non-susceptibility among the Enterobacteriaceae (MIC, > 1 mg/L; EUCAST) remain low in the UK with the highest rates seen among *Klebsiella* spp. and *Enterobacter* spp. (17.7% and 6.8%, respectively; UK tigecycline survey, 2007 data) (111). Despite *Klebsiella* spp. displaying the highest non-susceptibility rate, isolates of this genus were not studied here. This was because, unlike *E. cloacae*

and *A. baumannii*, no pre- and post-therapy pairs of *Klebsiella* spp. were available in the Antibiotic Resistance Monitoring and Reference Laboratory's (ARMRL's) isolate collection. More importantly, other researchers have previously published a number of manuscripts on tigecycline resistance mechanisms in *K. pneumoniae* both before and during the studentship (102;220;224). *S. marcescens* was selected for study because there were no reports describing the mechanisms of tigecycline resistance in the species.

1.5.1. *A. baumannii*

Over the past three decades the Gram-negative organism, *A. baumannii* has emerged as a major nosocomial pathogen (253). It poses a particular problem in intensive care units (ICUs) and other departments caring for debilitated patients who are vulnerable to infections (124). There have also been reports (although rarely in the UK) of severe community-acquired *A. baumannii* infections, including meningitis (156). The most common manifestations of hospital-acquired infection are: VAP; bacteraemia; and to a lesser extent, skin and soft tissue infection; wound infection (124). There are reports of high mortality rates in patients with *A. baumannii* VAP and secondary bacteraemia (79;215). There is debate over the real clinical impact of *A. baumannii* infection, since this organism mostly affects individuals with severe underlying illness. It is therefore argued that the high mortality rates are actually due to the underlying disease rather than attributable directly to *A. baumannii* infection (68). Whatever the truth, this organism is certainly a serious public health concern, owing to its capacity to cause outbreaks of disruptive cross-infection in ICUs.

A. baumannii is a highly adaptable organism. Both sporadic and outbreak strains persist in the nosocomial environment, at least in part, due to an ability to

survive desiccation (121). *A. baumannii* is intrinsically resistant to certain antibiotics but it also has the capacity to acquire resistance determinants via mobile genetic elements. Isolates of this species are commonly resistant to multiple antibiotic classes, thus compromising the clinician's ability to treat patients. Diverse mechanisms of resistance have been reported in *A. baumannii* (30;78). These include antibiotic-modifying enzymes from AmpC-type cephalosporinases and other β-lactamases including serine (OXA) and metallo-enzymes (IMP, VIM, SIM and NDM), to aminoglycoside-modifying enzymes (acetylating, nucleotidylating, and phosphorylating) (30;78;126). Antibiotic target modifications are also important mechanisms of resistance including *gyrA* and *parC* mutations that mediate quinolone resistance, and 16S rRNA methylases which confer aminoglycoside resistance (20;59). Other mechanisms include alterations in membrane permeability through porin loss or down-regulation and active efflux (section 1.5.2) (30;78;126). Carbapenems are important agents for the treatment of *A. baumannii* infection (84). Therefore, the emergence and spread of carbapenem-resistant strains around the world is alarming (270;278;284). These mostly have OXA carbapenemases but a few have metallo types, including NDM-1.

Molecular typing data on European isolates strongly indicate that *A. baumannii* is a clonal organism. Three distinct clusters have been identified which have caused wide-scale, nosocomial epidemics; these are designated European clones I, II and III (67;265). More recent work looking at a large global collection of isolates identified eight so called world-wide (WW) clonal lineages, of which, WW1, WW2 and WW3 contain representatives of European clones I, II, and III, respectively (106).

In the UK, a number of PFGE-defined clones belonging to European clone II are of particular concern. One prominent example is the OXA-23 clone 1 lineage (49),

with over 60 centres affected to date, clustered mainly in London and the South East of England. Treatment options are severely limited since representatives of this clone are resistant to multiple antibiotic classes, including to carbapenems (due to production of OXA-23 carbapenemase). Indeed, OXA-23 clone 1 isolates are typically susceptible only to the polymyxins and tigecycline (49).

Another widespread and problematic clone in the UK is known as the South East (SE) clone (259). First appearing in 2000, it has been detected in over 40 centres, again, particularly in London and South East England. Similarly to OXA-23 clone 1, the SE clone is MDR, although it displays variable resistance to the carbapenems (259). In the SE clone this resistance, where present, typically was mediated by up-regulation of the *bla*$_{\text{OXA-51}}$-like gene by the insertion sequence, IS*Aba*1 (260), though an increasing proportion of isolates now also carry OXA-23 (257).

There are currently no EUCAST species-specific MIC breakpoints for *A. baumannii* due to insufficient clinical evidence. Despite this, tigecycline is one of the few agents generally to remain active *in vitro* versus MDR lineages, although there is some variation in modal tigecycline MIC between distinct clones. For instance, OXA-23 clone 1 is intrinsically more susceptible to tigecycline than the SE clone; modal MICs are 0.5 and 2 mg/L, respectively (49;259). This variation in modal tigecycline MIC between distinct clones is further exemplified by the ACB20 clone which has caused a multicity outbreak in the United States since 2005; it has OXA-40 carbapenemase and a higher modal tigecycline MIC of 4 mg/L (154). The reasons for these differences in modal MIC are explored in this thesis.

1.5.1.1. Characterised RND transporters of *A. baumannii*

The first RND system to be described in *Acinetobacter* spp. was AdeABC (*Acinetobacter* drug efflux) in 2001 (160). The authors used degenerate oligonucleotide primers with complementarity to conserved motifs of the RND protein family to PCR-amplify the *adeB* gene from the DNA of an isolate recovered from a patient with a urinary tract infection (160). The genes encoding the structural proteins *adeA* (periplasmic adapter), *adeB* (RND pump) and *adeC* (outer membrane channel) are co-transcribed as an operon that is regulated by a divergently co-transcribed two-component regulatory system, AdeRS (Figure 12) (164). This comprises of a sensor kinase, AdeS and its cognate response regulator, AdeR. AdeABC is stringently controlled by AdeRS and is therefore expressed at low levels in wild-type *A. baumannii*. Specific amino acid substitutions in both AdeS (Thr153 → Met; Gly30 → Asp) and AdeR (Pro116 → Leu) have been linked with constitutive expression of this efflux system (51;164). There is evidence that AdeABC contributes to antimicrobial resistance and its known antibiotic substrates include fluoroquinolones, aminoglycosides, chloramphenicol, trimethoprim, macrolides, β-lactams (predominantly cephalosporins), and tetracyclines (32;160). Some studies suggest a role for AdeABC in carbapenem resistance by demonstrating associations between increased MICs and *adeABC* overexpression (116;139). Wong *et al.* reported that insertional inactivation of *adeB* in three clinical isolates resulted in four-fold decreases in meropenem MICs compared with the parent strains, whereas MICs of imipenem were unchanged (276).

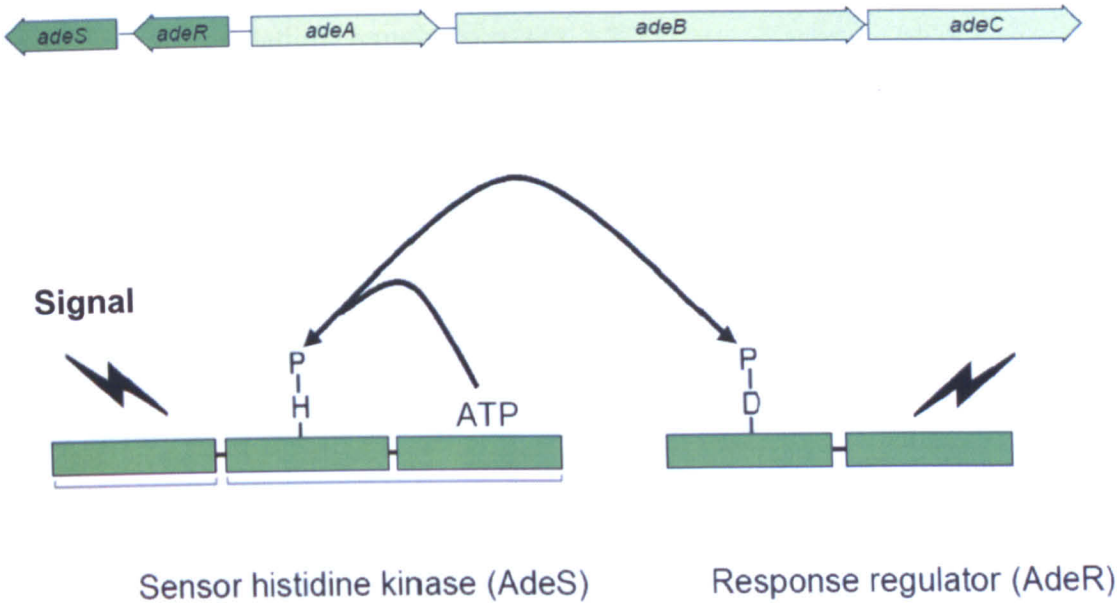

Figure 12. Genetic organisation of the structural and regulatory operons and regulation of *adeABC* expression by AdeRS. AdeS autophosphorylates at a conserved histidine residue upon ligand binding. The phosphate group is then transferred to AdeR that then drives *adeABC* expression.

It has been suggested that *adeB* sequence typing could be used to investigate the epidemiology of clinical *A. baumannii* strains (117). Since then, this approach has been used, in combination with other typing methods, for that purpose (110). However, studies have shown that a minority of isolates (approximately 30%) lack the *adeB* gene, which appears to be mostly associated with MDR strains (46;117;118).

The next RND transporter to be described in *A. baumannii* was the AdeIJK system (56). AdeIJK was first identified in the same clinical isolate as AdeABC and, similarly, the structural genes are co-transcribed as an operon, which comprises of the periplasmic adapter gene, *adeI*, the RND protein gene, *adeJ* and the gene encoding the outer membrane component, *adeK* (56). However, unlike with *adeABC*, no

regulatory genes have been found adjacent to *adeIJK* and so the mechanism(s) of transcriptional regulation remain obscure (56). The substrate profile of AdeIJK includes β-lactams (cephalosporins and carboxypenicillins), chloramphenicol, tetracyclines, lincosamides and fluoroquinolones (56). The *adeJ* gene has a similar distribution to *adeB*, being present in the majority of MDR isolates (150).

Recently, a third RND transporter, AdeFGH was described in the species (52). It was identified in laboratory-selected MDR mutants of a Δ*adeABC* Δ*adeIJK* strain by comparative microarray analysis (51;52). Again, the pump genes are co-transcribed, and the authors present evidence that *adeFGH* expression is controlled by the divergently-transcribed LysR-type transcriptional regulator, *adeL* (52). The laboratory-selected mutants displayed overexpression of *adeFGH* and MICs of chloramphenicol, fluoroquinolones, tetracyclines, trimethoprim and clindamycin were elevated compared with their parent (52). The *adeG* gene was identified by PCR in 40 out of 44 clinical isolates of *A. baumannii* (52).

1.5.2. *E. cloacae*

E. cloacae is a member of the Enterobacteriaceae family, is the most clinically important pathogen in the genus *Enterobacter* and is an important cause of nosocomial infection. Common sites of infection include the urinary and respiratory tracts, wounds, and the bloodstream. Like *A. baumannii*, *E. cloacae* bacteraemia is associated with high mortality rates in patients that have severe underlying disease (151).

Increasing levels of antibiotic resistance in this species are of serious concern to the clinician because it compromises empiric regimens and, as such, contributes increased morbidity and mortality. Antibiotic- and target-modifying resistance

mechanisms have been described in *E. cloacae*. For example, a chromosomally-encoded AmpC β-lactamase which, hyperproduced owing to mutation, confers resistance to penicillins, monobactams, and expanded-spectrum cephalosporins except cefepime and cefpirome (120). In addition, some isolates are extended-spectrum β-lactamase (ESBL) producers, with TEM, SHV and CTX-M-type enzymes (163). Resistance to the aminoglycoside class of antimicrobials in this species, although rare, can be mediated by aminoglycoside-modifying enzymes, many of which have been detected (266) and by the 16S rRNA methylases (43;193). Mutations in *gyrA* and *parC* contribute to fluoroquinolone resistance (62). Resistance to the carbapenems can arise as a result of membrane permeability changes combined with AmpC or an ESBL (72), or via acquisition of IMP (234), VIM (122) and NDM (137) metallo-β-lactamases or KPC enzyme production (114), and is worrying since these antibiotics are considered the treatment of choice for serious infections caused by MDR isolates of Enterobacteriaceae (194).

1.5.2.1. Characterised RND transporters of *E. cloacae*

An RND efflux system with a high level of similarity to the AcrAB-TolC transporter of *E. coli* and the closely-related species *E. aerogenes* was identified in a MDR clinical isolate of *E. cloacae* that was recovered from a patient admitted to an ICU (200). AcrAB-TolC of *E. cloacae* is the only characterised RND pump described to date in the species. The genetic organisation of the structural genes resembles that of *E. coli* and the authors also identified a divergently-transcribed *acrR*-like gene (200). The substrate profile includes aminoglycosides, tetracyclines, fluoroquinolones, clindamycin and linezolid (200). The authors also report that *acrA* was present in six other unrelated *E. cloacae* isolates (200).

1.5.3. *S. marcescens*

S. marcescens also belongs to the Enterobacteriaceae, and is an opportunistic pathogen that can cause serious problems for immunocompromised patients and those with underlying morbidities. It is especially associated with outbreaks in neonatal units (65;100).

The infections that it causes can be difficult to treat owing to the intrinsic and acquired resistance of *S. marcescens* to many antimicrobial agents. A variety of resistance mechanisms and determinants have been identified in this organism. Antibiotic-modifying enzymes including TEM and CTX-M-type ESBLs, carbapenemases, IMP, VIM and KPC, and chromosomally-encoded SME carbapenem-hydrolyzing enzymes also have been described (115;138;180;255). *S. marcescens* also possesses an inducible, chromosomal AmpC β-lactamase, which can be derepressed by mutation conferring cefotaxime resistance. Target modifications, mediated by both enzymatic and mutational mechanisms contribute to resistance to aminoglycosides and fluoroquinolones (69;129). Other mechanisms of resistance include membrane permeability changes and active efflux (section 1.5.3.1) (219).

1.5.3.1. Characterised RND transporters of *S. marcescens*

Three RND transporters have been described to date in *S. marcescens* (22;42;135). The first to be characterised was the SdeXY system (*Serratia* drug efflux) which was identified through screening of a genomic library prepared from DNA obtained from a clinical isolate (42). The genetic organisation of the pump genes, *sdeX* (periplasmic adapter) and *sdeY* (RND) was typical of this type of transporter and suggested they are co-transcribed (42). Antibiotic substrates of SdeXY include tetracycline, erythromycin and norfloxacin (42).

The two other RND systems, SdeAB and SdeCDE were identified again through screening of a *S. marcescens* genomic library (135). The *sdeAB* locus consists of the periplasmic adapter gene, *sdeA* and the RND component gene, *sdeB* while the *sdeCDE* locus consists of the periplasmic adapter gene, *sdeC* and, unusually, two genes encoding RND proteins, *sdeD* and *sdeE*, both of which are required for activity (135). The SdeAB pump has been shown to function with the outer membrane channel, HasF, a TolC homologue, to form a functioning tripartite complex (23;136). The substrate profile of SdeAB-HasF includes ciprofloxacin and other fluoroquinolones, whereas SdeCDE appears to have only limited substrate specificity (22).

1.6. Tigecycline resistance

Currently, the EUCAST defines tigecycline MIC breakpoints as follows: enterococci, > 0.5 mg/L resistant and ≤ 0.25 mg/L susceptible; staphylococci, > 0.5 mg/L resistant and ≤ 0.5 mg/L susceptible; Enterobacteriaceae, > 2 mg/L resistant and ≤ 1 mg/L susceptible; *Acinetobacter* spp., no MIC breakpoints (www.eucast.org/fileadmin/src/media/PDFs/EUCAST_files/Disk_test_documents/EUCAST_breakpoints_v1.3_pdf.pdf. last accessed 11/04/11). The US FDA defines tigecycline MIC breakpoints for the Enterobacteriaceae as, ≥ 8 mg/L resistant and ≤ 2 mg/L susceptible, with other values identical to those of EUCAST and, again, with no values for *Acinetobacter* spp. The EUCAST Enterobacteriaceae breakpoints shall be used to define resistance when discussing all species, including *A. baumannii*.

Tigecycline is not generally affected by the 'classical' tetracycline resistance determinants including MSF efflux pumps and RPPs (86). Indeed, tigecycline resistance rates remain low in the UK (0.8% resistant for all species excluding

Proteus spp. and *P. aeruginosa* and 1.4% intermediate; UK tigecycline survey) (111), as elsewhere although rates are lower in countries using FDA breakpoints. Despite this, there have been reports of clinical resistance (MIC, > 2 mg/L) emerging in a number of different species of Gram-negative bacteria, especially *A. baumannii* where there are reports of isolates with high-level resistance (MIC, > 256 mg/L) (119;182) and instances of resistance emerging during tigecycline therapy (11;199). Tigecycline resistance is very rare in Gram-positive organisms and, to date, there have only been two reports of resistance emerging in clinical isolates of *E. faecalis* and *E. faecium* where the mechanisms have been investigated (113;275).

1.6.1. Mechanisms of tigecycline resistance in Gram-positive bacteria

1.6.1.1. Efflux

Reduced susceptibility and resistance to tigecycline in Gram-positive organisms has been described only very rarely. McAleese *et al.* investigated the mechanisms of tigecycline resistance in *S. aureus* by exposing two tigecycline-susceptible clinical isolates of MRSA to tigecycline *in vitro* (167). Tigecycline MICs for the resulting final laboratory-selected mutants were 16- and 32-fold higher (4 and 16 mg/L, respectively) than those for their susceptible parents. Transcriptional profiling experiments revealed overexpression of a MATE-type efflux pump gene designated *mepA*. However, when this gene was overexpressed in the susceptible parent strains, only four-fold increases in tigecycline MICs were observed, suggesting that the 16- and 32-fold MIC rises for the laboratory mutants were the result of a combination of *mepA* overexpression and alterations in other unknown elements (167).

The first report of tigecycline resistance in a Gram-positive species where the mechanisms were investigated was that of a clinical isolate of *Enterococcus feacalis*

with a tigecycline MIC of 2 mg/L (defined as resistant by current EUCAST criteria) that was isolated in Germany from the urine of a patient with a complicated clinical history who had received, among other antibiotics, a two week course of tigecycline to treat MDR *S. maltophilia* (275). The molecular basis of resistance was not established although the authors did not detect; *tet*(X) by PCR; mutations in 16S rDNA; potentiation by efflux pump inhibitors (275). Recently, the emergence of tigecycline resistance during tigecycline therapy in a vancomycin- and linezolid-resistant clinical isolate of *E. faecium* was described (tigecycline MIC, 8 mg/L) that was recovered from the bloodstream of a post-second liver transplant patient (113). Up-regulation of a MepA-like MATE efflux pump was observed in the resistant isolate compared with two tigecycline-susceptible, pre-therapy *E. faecium* isolates recovered from the same patient (113).

1.6.2. Mechanisms of tigecycline resistance in Gram-negative bacteria

1.6.2.1. Enzymatic modification

There is evidence that tigecycline is a substrate for the tetracycline modification enzyme, Tet(X) (175). Tet(X) hydroxylates tigecycline at carbon 11a and the product, 11a-hydroxytigecycline is inherently unstable at physiological pH and thus antibiotic activity is abolished (175). To date, there have been no reports of clinical isolates that are resistant to tigecycline that harbour *tet*(X). A recent description of the crystal structure suggested that overcoming Tet(X)-mediated resistance by chemical modification would be problematic (268). These results, together with the finding that *tet*(X) has been found on transposons Tn*4351* and Tn*4400* (237) highlight the need to remain vigilant.

1.6.2.2. Tet(A)-mediated efflux

Tuckman *et al.* (256) identified two veterinary isolates of *Salmonella* with reduced susceptibility to tigecycline (MIC, 2 mg/L) which were found to harbour a variant of the *tet*(A) gene, the sequence of which differed from that of the corresponding gene on transposon Tn*1721* (273) by four nucleotides. Two of these were synonymous mutations while the two others led to a double frameshift of codons 201-203 that resulted in changes to the amino acid sequence in the interdomain loop (between TMs 6 and 7) of the efflux pump protein from Ser-Phe-Val to Ala-Ser-Phe (256). When the *tet*(A) genes from both isolates were expressed in a laboratory strain of *E. coli*, tigecycline MICs were increased four- to eight-fold. The authors concluded that the double frameshift was responsible for the increases in tigecycline MIC. In one isolate, *tet*(A) was located on the chromosome, but it was plasmid-associated in the other. The authors expressed their concern that since this *tet*(A) variant was transposon-associated, it might quickly and easily move into organisms pathogenic to humans (256).

More recently, a clinical isolate of *S. enterica* serovar Hadar with a tigecycline MIC of 16 mg/L was found with a Tn*1721*-associated *tet*(A) variant that contained the same double frameshift mutation described above as well as RamA-mediated AcrAB up-regulation (101). When this *tet*(A) gene alone was expressed in a laboratory strain of *E. coli*, a four-fold increase in tigecycline MIC was observed (101).

1.6.2.3. RND transporter-mediated resistance

There is evidence that tigecycline is a substrate for some members of the RND family of efflux transporters.

1.6.2.3.1. Enterobacteriaceae

RND efflux systems have been implicated in reduced susceptibility and resistance to tigecycline in a number of Enterobacteriaceae species (127;128;222;224;267).

Isolates of *E. coli* are usually susceptible to tigecycline and, with a modal MIC of 0.25 mg/L, it is the most susceptible Enterobacteriaceae species (EUCAST). However, two clinical isolates with reduced susceptibility to tigecycline (MIC, 2 mg/L) were isolated from a single patient who had received the drug during Phase III clinical trials (128). Transcriptional profiling and real-time RT-PCR revealed overexpression of the RND efflux operon *acrAB*, its outer membrane component gene, *tolC* and transcriptional regulator, *marA* in these isolates compared with tigecycline-susceptible isolates recovered from the same patient (128). The involvement of AcrAB and MarA in reduced susceptibility to tigecycline in these isolates was confirmed by transposon mutagenesis (128).

Transposon mutagenesis studies of a tigecycline-resistant clinical isolate of *E. cloacae* (MIC, 8 mg/L) yielded two tigecycline-susceptible mutant isolates with the transposon insertion mapped to *acrA* in one isolate and *acrB* in the other (127). When these isolates were trans-complemented with a plasmid carrying *acrAB*, tigecycline resistance was restored (127). Real-time RT-PCR and Northern blot analyses identified overexpression of *acrAB* and the transcriptional regulator gene *ramA* though not *marA*, suggesting the tigecycline-resistant phenotype was the result of RamA-mediated AcrAB up-regulation (127). More recently, an isolate of *E. hormaechei* (belonging to the *E. cloacae* complex) resistant to tigecycline that was recovered from a patient who had received the drug (among other antibiotics) was shown to overexpress *acrAB* compared with a susceptible isolate recovered from the same patient (58).

The majority of *K. pneumoniae* isolates are susceptible to tigecycline (modal tigecycline MIC, 0.5 mg/L; EUCAST) although in the UK 17.7% (111) are non-susceptible. Tigecycline resistance in this species has been associated with AcrAB up-regulation (102;103;224). In one study a clinical isolate with a tigecycline MIC of 4 mg/L was subjected to transposon mutagenesis and a tigecycline-susceptible mutant was obtained where the transposon insertion mapped to *ramA* (224). The resistant phenotype was restored upon trans-complementation with a plasmid carrying *ramA* and the *ramA* gene and *acrAB* were shown to be overexpressed in the resistant isolate by Northern blot analysis compared with tigecycline-susceptible strains confirming the role of RamA and AcrAB in tigecycline resistance (224). In another more recent study, Hentschke *et al.* sequenced the *ramR* gene, the putative local repressor of *ramA*, in five *K. pneumoniae* isolates, each with a tigecycline MIC of 2 mg/L, and found various genetic lesions that were not present in 12 tigecycline-susceptible isolates (102). Trans-complementation of two of the mutants with wild-type *ramR* restored tigecycline susceptibility and repressed overexpression of both *ramA* and *acrAB* suggesting that non-functional RamR was responsible for RamA-mediated AcrAB up-regulation (102).

Some members of the Enterobacteriaceae are intrinsically resistant or less susceptible to tigecycline as well as to other tetracyclines; these include *P. mirabilis* and *M. morganii* (modal MICs, 4 and 1 mg/L, respectively; EUCAST). Studies investigating tigecycline resistance mechanisms in clinical isolates of these two species also implicated the RND transporter, AcrAB (222;267)

1.6.2.3.2. Non-fermenters

Efflux by RND transporters has also been described as a mechanism of tigecycline resistance in non-fermenting species (61;197;207;221;223).

Despite evidence of upward tigecycline MIC creep globally in recent years (271), the majority of *A. baumannii* isolates remain susceptible (modal MIC, 0.5 mg/L; EUCAST). However, resistance has been described and in each case has been associated with efflux systems (197;199;221;223). There is laboratory evidence that tigecycline is a substrate of the three characterised RND transporters of *A. baumannii* described to date, namely AdeABC, AdeIJK and AdeFGH (52;56;197;223). However, where studies have focused on investigating resistance in clinical isolates, only the AdeABC transporter has been implicated (197;221;223). Ruzin *et al.* reported that *adeABC* was overexpressed in two clinical isolates of the *A. calcoaceticus-A. baumannii* complex recovered from the same patient which had tigecycline MICs of 4 mg/L compared with susceptible isolates which were also recovered from the same patient (223). When the *adeB* gene of the resistant isolates was disrupted by a suicide plasmid, tigecycline MICs were reduced 8-fold (223). It was also demonstrated that the sensor kinase gene, *adeS* was disrupted by the insertion sequence, IS*Aba*1 in both resistant isolates which may have resulted in *adeABC* overexpression (223). In a separate study, two clinical isolates recovered from different patients who had both received tigecycline therapy were tigecycline non-susceptible (MIC, 2 mg/L) (197). Real-time RT-PCR revealed that *adeABC* was overexpressed in these isolates compared with another clinical isolate recovered from a different patient which was tigecycline-susceptible (197). *In vitro* exposure of this susceptible isolate to tigecycline selected for a tigecycline-resistant mutant which overexpressed *adeABC* in comparison with the susceptible parent (197). When the regulatory operon *adeRS* was

sequenced, no differences were found between the susceptible clinical isolate and it's *in vitro*-selected tigecycline-resistant mutant (197).

P. aeruginosa is intrinsically resistant to tigecycline, (modal MIC, 16 mg/L; EUCAST). The mechanism of resistance was investigated using mutant derivatives of *P. aeruginosa* PA01 that lacked functional MexAB or MexXY (61). The strain lacking MexXY was susceptible to tigecycline with an MIC of 0.5 mg/L whereas the tigecycline MIC of its parent and the strain lacking MexAB was 8 mg/L thus implicating MexXY (61).

There is limited evidence that efflux transporters may also contribute to tigecycline resistance in clinical isolates of the *B. cepacia* complex (207). It was demonstrated by checkerboard titration that tigecycline MICs decreased with increasing concentrations of the EPI PAβN (207), although further work will be required to positively identify the efflux system(s) responsible.

1.7. Aims

Over the past five to six years the ARMRL at the HPA has received isolates of *A. baumannii* and of Enterobacteriaceae (mostly *E. cloacae* and *K. pneumoniae* but also a single isolate of *S. marcescens*) displaying reduced susceptibility (MIC, 2 mg/L) or resistance (MIC, > 2 mg/L) to tigecycline, including pre- and post-treatment pairs of particular strains where resistance had emerged during therapy.

In this work, these isolates were characterised, and the role of the RND efflux systems was investigated. Specific pumps investigated were AcrAB and AdeABC in the emergence of tigecycline resistance in pre- and post-therapy isolates of *E. cloacae* and *A. baumannii*, respectively. In addition, expression of *adeABC* was investigated in multiple isolates of three epidemic clones of *A. baumannii* in an attempt to explain observed differences in their modal tigecycline MICs. For *S. marcescens*, efflux by RND transporters was analysed as a possible mechanism of tigecycline resistance in a clinical isolate.

2. Materials and Methods

2.1. Reagents and consumables

All reagents and consumables were obtained from Sigma-Aldrich, Poole, UK and all restriction enzymes from Roche, Burgess Hill, UK, unless otherwise stated.

2.2. Bacterial isolates and growth conditions

All organisms were type strains, clinical isolates, laboratory-selected mutants or gene knockout mutants of *A. baumannii*, *E. cloacae*, or *S. marcescens* (Table 2) with the exception of the following strains that were used for cloning only: α-select *E. coli* (Bioline, London, UK) and *pir*$^{+}$ *E. coli* (Cambio, Cambridge, UK). Isolates were propagated in Luria–Bertani (LB) or Iso-Sensitest (Thermo Fisher, Basingstoke, UK) media at 37°C unless otherwise stated.

Table 2. Organisms used in this study

Isolate/clone	Species	Origin	Notes
OXA-23 clone 1 (n=9)	*A. baumannii*	clinical isolates (UK)	
SE (n=8)	*A. baumannii*	clinical isolates (UK)	
ACB20 (n=5)	*A. baumannii*	clinical isolates (USA)	
AB210	*A. baumannii*	pre-therapy clinical isolate (UK)	clinical pair, see Results for clinical information
AB211	*A. baumannii*	post-therapy clinical isolate (UK)	
AB210-6	*A. baumannii*	final tigecycline-selected lab mutant	
AB211Δ*adeB*	*A. baumannii*	*adeB* knockout derivative	
W6976	*A. baumannii*	pre-therapy clinical isolate (UK)	clinical pair, see Results for clinical information
W7282	*A. baumannii*	post-therapy clinical isolate (UK)	
TGC-S	*E. cloacae*	pre-therapy clinical isolate (UK)	clinical pair, see Results for clinical information
TGC-R	*E. cloacae*	post-therapy clinical isolate (UK)	
TGC-S7	*E. cloacae*	final tigecycline-selected lab mutant	
TGC-RΔ*acrB*	*E. cloacae*	*acrB* knockout derivative	
EC390	*E. cloacae*	pre-therapy clinical isolate (UK)	clinical pair, see Results for clinical information
EC391	*E. cloacae*	post-therapy clinical isolate (UK)	
SM346	*S. marcescens*	clinical isolate (UK)	
NCTC 10211	*S. marcescens*	type strain	
10211-6	*S. marcescens*	intermediate tigecycline-selected lab mutant	
10211-10	*S. marcescens*	final tigecycline lab mutant	
10211-10Δ*sdeY*	*S. marcescens*	*sdeY* knockout derivative	
10211-10Δ*hasF*	*S. marcescens*	*hasF* knockout derivative	
10211-TC7	*S. marcescens*	final tetracycline-selected lab mutant	

2.3. Identification of bacteria

2.3.1. Enterobacteriaceae

Isolates were identified to species level by API20E (bioMérieux, Marcy l'Etoile, France).

2.3.2. *A. baumannii*

Isolates were identified to genus level by API20NE (bioMérieux) and by *A. baumannii*-specific PCR for the $bla_{\text{OXA-51-like}}$ gene (261;277). This PCR was undertaken as outlined in section 2.11.1 using primers OXA-51-likeF and OXA-51-likeR (Table 8), an annealing temperature of 60°C and an extension time of 30 seconds, to amplify a 353-bp product. Single colonies from an overnight culture were suspended in 50 µl molecular biology grade water and incubated at 95°C for five minutes, cooled on ice and centrifuged at 12000 g for 30 seconds; 5 µl of the resulting supernatant (crude DNA extract) was used as template. A clinical isolate known to be positive for the $bla_{\text{OXA-51-like}}$ gene was used as a positive control.

2.4. Molecular typing of bacteria

2.4.1. Pulsed-field gel electrophoresis (PFGE)

Clinical isolates, laboratory-selected mutants and gene knockout mutants were profiled by PFGE in order to assign clones and/or determine isolate relatedness.

After overnight culture on LB agar plates at 37°C, the organisms were suspended in SE buffer (75 mM NaCl, 25 mM EDTA, pH 7.5) to a turbidity of between 2.3 and 2.7 McFarland. This suspension was mixed with an equal volume of 2% MacroSieve LM agarose (Flowgen Bioscience, Nottingham, UK) in SE buffer at 56°C and dispensed into a plug mould, which was then kept at 4°C until set.

The plugs were transferred into bijoux bottles and 3 ml of FL buffer (6 mM Tris, 100 mM EDTA, 1 M NaCl, 0.5% w/v Brij 58, 0.2% w/v sodium deoxycholate, 0.5% N-lauroyl sarcosine, 1 mM $MgCl_2$, pH 7.5) containing 0.5 mg/ml lysozyme was added. The bottles were then incubated with shaking (150 rpm) overnight at 37°C. After this incubation, the FL buffer was replaced with 3 ml of AL buffer (1% w/v N-lauroyl sarcosine, 0.5 M EDTA, pH 9.5) containing 60 µg/ml proteinase K (Invitrogen, Paisley, UK) and the bottles were then incubated with shaking (150 rpm) overnight at 56°C.

Buffer AL was removed, and the plugs were washed three times with 4 ml TE buffer (10 mM Tris, 10 mM EDTA, pH 7.5), each time for 30 minutes at 4°C. The plugs were cut to give a portion of the appropriate size (i.e. to fit in the wells of the running gel) which was washed in ApaI (*A. baumannii*) or XbaI (Enterobacteriaceae) reaction buffer for 30 minutes at 4°C. The buffer was then replaced with fresh buffer and 20 U of ApaI or XbaI and incubated overnight at 30°C or 37°C, respectively. For *A. baumannii*, a second incubation was then performed as above using fresh buffer and enzyme for a further 5 h.

PFGE was performed using the CHEF-DR II system (Bio-Rad, Hemel Hempstead, UK). The running buffer was 0.5X TBE (44.5 mM Tris, 44.5 mM boric acid, 1 mM EDTA). Plugs and a phage λ ladder marker (New England Biolabs, Hitchin, UK) were loaded into a 1.2% molecular grade agarose (Bio-Rad) gel and the wells were sealed with molten agarose at 56°C. The CHEF parameters were as follows: 6 V/cm, 5 seconds initial and 35 seconds final switching time for 30 h at 12°C. The gel was stained with 1 mg/L ethidium bromide for one hour and destained for one hour with distilled water. Bands were visualised and gels photographed using

a UV transilluminator and the GeneSnap image acquisition system version 6.03 (Syngene, Cambridge, UK).

2.5. Antimicrobial susceptibility testing

MICs were determined by agar dilution on Iso-Sensitest agar and an inoculum of 10^4 CFU according to BSAC guidelines (see Table 3 for control organisms) or by Etest (AB Biodisk, Solna, Sweden) on Iso-Sensitest agar. The concentrations of inhibitors used were as follows: clavulanic acid, 4 mg/L; cloxacillin, 100 mg/L; EDTA, 320 mg/L. For the Etest methodology, several colonies from overnight cultures were suspended in 4 ml of Iso-Sensitest broth to the opacity of a 0.5 McFarland standard. This suspension was spread evenly on to Iso-Sensitest agar plates and allowed to dry. The Etest strip was then applied to the plate, which was incubated overnight at 37°C. The MIC was read after between 16 and 20 h incubation. MICs were interpreted using BSAC/EUCAST breakpoints (9).

Table 3. MIC control organisms

Organism	Strain	Purpose
E. cloacae	E684-con	AmpC control
E. coli	NCTC 10418	susceptible control
E. coli	NCTC 11560	clavulanic acid control
E. coli	ATCC 25922	susceptible control
E. coli	ATCC 35218	clavulanic acid control
P. aeruginosa	ATCC 27853	susceptible control
P. aeruginosa	PS 10586	VIM control
P. aeruginosa	M2297	AmpC control
K. pneumoniae	ATCC 700603	ESBL control

2.6. Plasmid extraction

Plasmids were isolated from all strains of *E. coli* using the PureYield Plasmid Miniprep System (Promega, Southampton, UK) and the manufacturer's protocol which is outlined below:

The required volume of culture (to a maximum of 3 ml) was centrifuged at 18000 x *g* for 30 seconds. The supernatant was discarded and the pellet re-suspended in 600 µl TE buffer (pH 8.0). Cell Lysis Buffer was added (100 µl) and mixed by inverting the tube. After mixing, 350 µl of cold (4°C) Neutralization Solution was added, mixed as above and then centrifuged at 18000 x *g* for three minutes. The supernatant was then transferred to a PureYield Minicolumn, which was centrifuged at 18000 x *g* for 30 seconds; the flow-through was discarded.

The column was then washed by the addition of 200 µl of Endotoxin Removal Wash and centrifuged at 18000 x *g* for 15 seconds followed by the addition of 400 µl of Column Wash Solution and further centrifugation at 18000 x *g* for 30 seconds. The flow-through was discarded and the column transferred to a clean microcentrifuge tube. Plasmid DNA was then eluted by the addition of 30 µl Elution Buffer and centrifugation at 18000 x *g* for 15 seconds.

2.7. Genomic DNA purification

Genomic DNA was purified from all organisms using the Wizard Genomic DNA Purification Kit (Promega) and the manufacturer's protocol, which is outlined below:

Up to 1 ml of overnight culture was centrifuged at 18000 x *g* for two minutes and the supernatant discarded. The pellet was re-suspended in 600 µl of Nuclei Lysis Solution, incubated at 80°C for five minutes and cooled to room temperature. After

cooling, 3 µl of RNase Solution was added, mixed by inversion and incubated at 37°C for 1 h.

The lysate was cooled to room temperature and 200 µl of Protein Precipitation Solution was added, mixed by vortexing and incubated on ice for five minutes. The precipitated protein was pelleted by centrifugation at 18000 x *g* for three minutes.

The supernatant was transferred to a clean microcentrifuge tube containing 600 µl of isopropanol, mixed by inversion and centrifuged at 18000 x *g* for two minutes. The supernatant was discarded and the pellet was washed by the addition of 600 µl of 70% ethanol followed by centrifugation at 18000 x *g* for two minutes. The ethanol was aspirated and the pellet air-dried for 15 minutes. The DNA was rehydrated by the addition of 100 µl of Rehydration Solution and incubation for one hour at 65°C.

2.8. RNA extraction

Total RNA was extracted using the RNeasy Mini Kit (Qiagen, Crawley, UK) and the manufacturer's protocols which are outlined below:

Isolates were grown overnight with shaking (225 rpm) in 10 ml of LB or Iso-Sensitest broth at 37°C. Those of *A. baumannii* and *E. cloacae* were used directly, whereas isolates of *S. marcescens* were sub-cultured to fresh LB broth and incubated at 37°C with shaking (225 rpm) until mid-log (OD_{600} = 0.5) phase before RNA extractions were performed. Two volumes (1 ml) of RNAprotect Bacteria Reagent (Qiagen) were added to one volume (500 µl) of culture in a microcentrifuge tube, mixed by vortexing and incubated for five minutes at room temperature. The mixture was centrifuged for 10 minutes at 5000 x *g*, the supernatant was discarded and the pellet was re-suspended in 100 µl TE buffer (pH 8.0) containing 1 mg/ml lysozyme

and incubated with shaking (150 rpm) for five minutes at room temperature. After incubation, 350 µl of buffer RLT containing 10 µl/ml β-mercaptoethanol was added and mixed by vortexing. If particulate material was visible, it was pelleted by centrifugation and then the supernatant was transferred to another tube containing 250 µl of 100% ethanol and mixed by pipetting.

The lysate was transferred to an RNeasy Mini spin column and centrifuged at 8000 x *g* for 15 seconds. The flow-through was discarded and the column washed with 350 µl of buffer RW1 (8000 x *g* for 15 seconds). On-column DNase digestion was then performed using the RNase-free DNase Set (Qiagen) by adding 70 µl of buffer RDD to 10 µl of DNase and incubating the reaction mixture on-column for 15 minutes at room temperature. The column was washed with 350 µl of buffer RW1 (8000 x *g* for 15 seconds) and the flow-through and collection tube were discarded. Two further washes were performed with 500 µl buffer RPE, the first at 8000 x *g* for 15 seconds and the second at 8000 x *g* for two minutes. The column was transferred to an RNase-free microcentrifuge tube and RNA was then eluted by the addition of 50 µl RNase-free water and centrifugation at 8000 x *g* for one minute.

2.9. Quantification of nucleic acids

Nucleic acids were quantified spectrophotometrically at 260 nm using a Nanodrop ND-1000 spectrophotometer (Thermo Scientific, Basingstoke, UK).

2.10. DNA transformations

Clinical isolates and laboratory-selected mutants were transformed by electroporation as outlined below unless otherwise stated.

2.10.1. Preparation of electrocompetent cells

Isolates of all species except α-select *E. coli* and *pir*$^{+}$ *E. coli*, were made electrocompetent as follows: 10 ml of modified LB broth (without NaCl) was seeded with 100 µl of an overnight LB broth culture of the relevant organism and incubated with shaking (225 rpm) at 37°C to mid-log phase (OD_{600} = 0.5). The culture was then centrifuged at 4°C at 4000 x *g* for 10 minutes, the supernatant removed and the pellet re-suspended in 40 ml of cold sterile water and re-centrifuged as before. The final pellet was suspended in 90 µl of 15% sterile glycerol. If necessary, competent cells were stored at -70°C for later use.

2.10.2. Electroporation

Competent cells (40 µl) were mixed with the DNA (in a maximum volume of 5 µl) by gentle pipetting and incubated on ice for one minute. Electroporation was performed with the Gene Pulser system (Bio-Rad) using cold 0.1 cm cuvettes (Bio-Rad) and the following conditions: 1.8 kV, 25 µF, 200 Ω. Cell suspensions were made up to 1 ml with SOC medium (0.5% yeast extract, 2 % tryptone, 10 mM NaCl, 2.5 mM KCl, 10 mM $MgCl_2$, 10 mM $MgS0_4$, 20 mM glucose) and incubated at 37°C with shaking (225 rpm) for one hour before being plated on to appropriate selective agar plates.

2.11. PCR

PCR was performed in 0.2-ml PCR tubes with the following reaction components and cycling conditions unless otherwise stated. Master mixes (n+2) were prepared if multiple samples were to be analysed.

2.11.1. *Taq* DNA polymerase (Invitrogen)

The components of a typical 50 µl reaction were as follows:

Table 4. Components of a typical PCR reaction using *Taq* DNA polymerase

Component	Final concentration/volume
Taq DNA polymerase	2.5 U
10X PCR Buffer	5 µl
$MgCl_2$	1.5 mM
Primers	0.5 µM each
dNTP mix (Invitrogen)	250 µM of each
Template DNA (crude, genomic or plasmid extract)	variable
Molecular biology grade water (Invitrogen)	up to 50 µl

Thermocycling was performed using an Eppendorf Mastercycler (Eppendorf, Cambridge, UK) and the following conditions: initial denaturation at 94°C for three minutes, followed by 30 cycles of 94°C for 30 seconds, primer annealing at 50°C-60°C for 30 seconds, extension at 72°C for between 30 seconds and four minutes, and a final elongation step at 72°C for 10 minutes. Specific annealing temperatures and extension times are detailed subsequently.

2.11.2. Expand High Fidelity (HiFi) Plus PCR System (Roche)

The components of a typical 50 µl reaction were as follows:

Table 5. Components of a typical PCR reaction using the Expand HiFi Plus PCR System

Component	Final concentration/volume
Expand HiFi Plus Enzyme Blend	2.5 U
5X Expand HiFi Plus Reaction Buffer with $MgCl_2$	10 µl
Primers	0.5 µM each
dNTP mix	200 µM of each
Template DNA (crude, genomic or plasmid extract)	variable
Molecular biology grade water	up to 50 µl

Thermocycling was performed using an Eppendorf Mastercycler and the following conditions: initial denaturation at 94°C for two minutes, followed by 30 cycles of 94°C for 30 seconds, primer annealing at 50°C-60°C for 30 seconds, extension at 72°C for between 30 seconds and four minutes, and a final elongation step at 72°C for 7 minutes.

2.11.3. *Pfu* DNA polymerase (Promega)

The components of a typical 50 µl reaction were as follows:

Table 6. Components of a typical PCR reaction using *Pfu* DNA polymerase

Component	Final concentration/volume
Pfu DNA polymerase	1.25 U
10X *Pfu* DNA polymerase Buffer with $MgSO_4$	5 µl
Primers	0.5 µM each
dNTP mix	200 µM of each
Template DNA (crude, genomic or plasmid extract)	variable
Molecular biology grade water	up to 50 µl

Thermocycling was performed using an Eppendorf Mastercycler and the following conditions: initial denaturation at 95°C for two minutes, followed by 30 cycles of 95°C for 30 seconds, primer annealing at 50°C-60°C for 30 seconds, extension at 72°C for between two and four minutes, and a final elongation step at 72°C for 5 minutes.

2.11.4. Visualisation of PCR products and estimation of amplicon size

PCR products were separated using agarose gel electrophoresis (0.7 to 2%) and were visualised and photographed using a UV transilluminator and the GeneSnap image acquisition system version 6.03 after ethidium bromide staining (1 mg/L). Amplicon

size was estimated by comparison to either the 1 Kb DNA ladder (Invitrogen) or the 123 bp DNA ladder (Invitrogen).

2.12. Screening clinical isolates for the presence of *tet*(X) by PCR

Tigecycline-resistant clinical isolates were screened for the presence of the *tet*(X) gene by PCR as outlined in section 2.11.1 using an annealing temperature of 58°C, an extension time of 30 seconds, primers tetXf and tetXr (Table 7) and 5 µl of a crude DNA extract (section 2.3.2) to amplify a 468 bp product. *E. coli* strain Em24 pBSJ was used a positive control (275).

Table 7. Generic oligonucleotide primers used in this study

Primer name	Sequence (5' to 3')	Tm	Source
M13 F	GTAAAACGACGGCCAGT	59	this study
M13 R	CAGGAAACAGCTATGAC	51	this study
MOD5 ori F	CGATGAATTTTCTCGGGTGT	64	this study
MOD5 ori R	CCTGAAGCTCTTGTTGGCTA	62	this study
tetXf	CAATAATTGGTGGTGGACCC	64	(184)
tetXr	TTCTTACCTTGGACATCCCG	64	(184)

2.13. Purification of DNA from enzymatic reactions and agarose gels

DNA was purified from enzymatic reactions and agarose gels using the Geneclean Turbo Kit (MP Biomedicals, Strasbourg, France) as described in the manufacturer's instructions which are outlined below:

The appropriate band(s) was located under UV illumination and excised from the gel, placed into a microcentrifuge tube containing the appropriate volume of Salt Solution (100 µl per 100 mg gel), incubated at 55°C for five minutes and mixed by inversion. For purification of DNA from enzymatic reactions in solution, five volumes of the Salt Solution were added to the sample and mixed by inversion.

No more than 600 µl of the DNA/Salt Solution was transferred to the Geneclean Turbo column and pulsed in a microcentrifuge for five seconds. The supernatant was discarded and 500 µl of Wash Solution was added to the column, which was then centrifuged as above. The column was then centrifuged for a further four minutes at 12000 x *g*, the supernatant discarded, and the DNA eluted into a clean Catch Tube with 30 µl Elution Solution by centrifugation for one minute at 12000 x *g*.

2.14. Nucleotide sequencing

Sequencing was performed using the GenomeLab DTCS Quick Start Kit (Beckman Coulter, High Wycombe, UK) and the CEQ 8000 Genetic Analysis System automatic sequencer (Beckman Coulter). Samples were prepared as described in the manufacturer's instructions which are outlined below:

2.14.1. Preparation of template DNA

Template DNA was either a PCR product or a plasmid, both of which were purified as described in sections 2.11.3 and 2.6, respectively. The sequencing reaction was prepared by mixing the following components: 2 µl of primer (1.6 µM), 8 µl of DTCS Quick Start Master Mix, template DNA (between 50 and 100 ng), and molecular biology grade water to a final volume of 20 µl. The cycling conditions were as follows: 30 cycles of 96°C for 20 seconds, 50°C for 20 seconds, and 60°C for four minutes.

2.14.2. Ethanol precipitation and sample loading

The reaction mixture was transferred to clean 0.5 ml microcentrifuge tube containing 5 µl of freshly prepared Stop Solution/Glycogen mixture [2 µl of 3 M sodium acetate,

pH 5.2; 2 µl of 100 mM EDTA, pH 8.0; 1 µl of 20 mg/ml glycogen (Beckman Coulter)] and mixed by pipetting. Cold (-20°C) 95% ethanol was added (60 µl), mixed by vortexing and centrifuged at 18000 x *g* for 15 minutes. The supernatant was removed and the pellet washed by the addition of 200 µl of cold (-20°C) 70% ethanol and centrifugation at 18000 x *g* for three minutes. The supernatant was aspirated and the pellet air-dried for 30 minutes at 37°C, then re-suspended in 40 µl of Sample Loading Solution, transferred to the sample plate and overlaid with a single drop of mineral oil. The sample plate was then loaded on to the instrument and sequence was determined using dye-terminator chemistry.

2.15. Gene expression studies

Gene expression was monitored by real-time reverse transcriptase (RT)-PCR, performed on a LightCycler 2.0 Real-Time PCR System (Roche) using the QuantiFast SYBR Green RT-PCR Kit (Qiagen) and the manufacturer's protocols which are summarised below.

2.15.1. Post-elution DNase treatment

A post-elution DNase treatment step using molecular biology grade DNase I (Invitrogen) was performed on all RNA extracts (section 2.8) prior to RT-PCR. Up to 1 µg of RNA in a maximum volume of 8 µl was transferred to a 0.2 ml PCR tube to which 1 U of DNase I and 1 µl of Reaction Buffer were added and mixed by inversion. The reaction mixture was centrifuged briefly and incubated at room temperature for 15 minutes before the addition of 1 µl of 25 mM EDTA, pH 8.0 (Invitrogen). After mixing as above, the reaction was incubated for a further 10 minutes at 65°C and cooled on ice.

2.15.2. Reaction setup and cycling conditions

Reactions components were assembled on ice and consisted of the following: 10 µl of 2X QuantiFast SYBR Green RT-PCR Master Mix, primer mix (final concentration of each primer = 1 µM), 0.2 µl of QuantiFast RT Mix, 10 ng of template RNA, and RNase-free water to a final volume of 20 µl. Master mixes (n+2) were prepared if multiple samples were to be analysed. Template-free negative controls were included for each target. RT-negative controls were included for each sample/target combination. Each isolate was assayed in triplicate using template from separate RNA extractions.

All reactions were performed using the following parameters: RT step at 50°C for 10 minutes, followed by an initial activation step at 95°C for five minutes and then 35 cycles of denaturation at 95°C for 10 seconds and combined annealing/extension at 60°C for 30 seconds. Fluorescence data acquisition was performed during the combined annealing/extension step.

2.15.3. Data analysis

RT-PCR data were analysed on the 530 nm channel. Threshold cycles (C_T) were calculated using the LightCycler software version 4. Normalized expression of the target gene was then calculated relative to a housekeeping gene (*rpoB*) using the $2^{-\Delta\Delta CT}$ method (152), where $\Delta\Delta C_T$ = C_T of the target gene - C_T of the housekeeping gene.

2.16. Cloning into pCR2.1 (Invitrogen) and pCR-Blunt (Invitrogen)

PCR products were cloned into the TA cloning vector pCR2.1 or pCR-Blunt according to the manufacturer's guidelines (with some modifications), which are outlined below:

The amplicon to be cloned into pCR2.1 was prepared using *Taq* polymerase, whereas that to be cloned into pCR-Blunt was prepared by *Pfu* polymerase (see individual sections for details of reaction conditions and components). PCR products were then analysed by agarose gel electrophoresis, cleaned (section 2.13) and quantified (section 2.9).

The ligation reaction mixture was prepared on ice in 0.2-ml PCR tubes as follows: 1 µl of 10X Ligation Buffer, 2 µl of pCR2.1 vector (50 ng) or 1 µl of pCR-Blunt vector (25 ng), 1 µl of T4 DNA Ligase, PCR product to give a 1:1 (pCR2.1) or 1:10 (pCR-Blunt) molar ratio of vector: insert and molecular biology grade water to a final volume of 10 µl. The components were mixed by inversion and centrifuged briefly before being incubated overnight at 14°C (pCR2.1) or for one hour at 16°C (pCR-Blunt). After incubation, reactions were stopped by incubation for 10 minutes at 70°C then returned to ice before transformation into α-select *E. coli* by electroporation (section 2.10.2). Transformants were selected on LB agar plates containing 100 mg/L ampicillin (pCR2.1) or 50 mg/L kanamycin (pCR-Blunt), 0.1 mM isopropyl-β-D-thiogalactopyranoside (IPTG) and 40 mg/L 5-bromo-4-chloro-3-indolyl-β-D-galactopyranoside (X-Gal).

2.17. Ligation of DNA fragments using T4 DNA ligase (Promega)

After digestion with the appropriate restriction enzyme, vector DNA was dephosphorylated using 1U shrimp alkaline phosphatase (SAP) (Promega) and the

appropriate volume of 10X Dephosphorylation Buffer followed by incubation at 37°C for 10 minutes (cohesive ends) or one hour (blunt ends). Dephosphorylated vector DNA was then purified as described in section 2.13 and combined with the relevant insert DNA using either a 1:3 (cohesive-end cloning) or 1:10 (blunt-end cloning) molar ratio of vector: insert. The ligation reaction components were assembled on ice in 0.2 ml PCR tubes as follows: insert and vector DNA, 1 µl of Ligase Buffer, 1 U T4 DNA ligase and molecular biology grade water to a final volume of 10 µl. After mixing by inversion, the components were centrifuged briefly before incubation at room temperature for 3 h (cohesive-end cloning) or at 15°C overnight (blunt-end cloning). The ligase enzyme was then inactivated by incubation at 70°C for 10 minutes before the ligation mix was transformed into the appropriate strain of electrocompetent *E. coli* (section 2.10).

2.18. Laboratory-selection of tigecycline-resistant mutants

An overnight Iso-Sensitest broth culture of the parent strain was subjected to serial exposure to tigecycline or tetracycline, beginning at half the MIC and then doubling this concentration every 24 h until there was no further growth. MICs were monitored daily by Etest (section 2.5). PFGE was used to confirm parentage (section 2.4.1).

2.19. *A. baumannii*-specific methods

2.19.1. Sequencing of the *adeR* and *adeS* genes

DNA fragments containing the *adeR* (1342 bp) and *adeS* (1641 bp) genes were amplified by PCR with *Pfu* DNA polymerase from *A. baumannii* genomic DNA (~10 ng) using primers *adeS* seq1 R and ade reg seq1 F, and *adeS* TR and *adeR* seq F (Table 8), an annealing temperature of 55°C and an extension time of 100 seconds.

Nucleotide sequences of the resulting fragments were then determined (section 2.14) using primers *adeR* seq1 R, *adeR*r, *adeR*f, *adeS* seq3, *adeS* seq1 F, *adeS* KO F, *adeS*f and *adeS*r (Table 8) in addition to the above.

Table 8. Oligonucleotide primers used in this study with *A. baumannii*

Primer name	Sequence (5' to 3')	Tm	Source
ade reg seq1 F	CCGATTGCGGTTGAATGCTT	69	this study
adeB CR	GAAAGAATGAGTCCACGAGA	59	this study
adeB KO LF	GATGTGGAAATGGCTCAGGT	64	this study
adeB(quan)f	AACGGACGACCATCTTTGAGTATT	66	(197)
adeB(quan)r	CAGTTGTTCCATTTCACGCATT	66	(197)
adeR LC f	AGCCAACCCATCGATTTAAT	62	this study
adeR LC r	TGATCACGGGAGTCTGAGCT	65	this study
adeR seq F	GATACCGACACTCATAGCGT	59	this study
adeR seq1 r	ATCTTGATCTAGCGCCGTCA	65	this study
*adeR*f	ATGTTTGATCATTCTTTTTCTTTTG	61	(197)
*adeR*r	TTAATTAACATTTGAAATATG	49	(197)
adeS KO F	CGATTGAAAAAGGCTGGATT	63	this study
adeS KO R	ATCGTCTTGGAACTCGGTTG	64	this study
adeS seq1 f	TTGCAACCGAGTTCCAAGAC	65	this study
adeS seq1 r	GCTGCTTCGGCTAAGAAGTT	63	this study
adeS seq3	TTAGTCACGGCGACCTCTCT	64	this study
adeS TR	AGCGTCTCCCGATTTACCAA	66	this study
*adeS*f	ATGAAAAGTAAGTTAGGAATTAGTAAG	56	(197)
*adeS*r	TTAGTTATTCATAGAAATTTTTATG	53	(197)
OXA-51-likeF	TAATGCTTTGATCGGCCTTG	65	(277)
OXA-51-likeR	TGGATTGCACTTCATCTTGG	64	(277)
rpoB Acin F	GAGTCTAATGGCGGTGGTTC	63	this study
rpoB Acin R	ATTGCTTCATCTGCTGGTTG	63	this study
S-am	TTCAACAAGAAGATTGGACC	59	(164)
S-av	CTTGCTCAATACGACGG	58	(164)

2.19.2. Gene expression analysis in *A. baumannii*

Expression of the *adeABC* and *adeRS* operons was investigated using real-time RT-PCR as outlined in section 15 using primers *adeB*(quan)f and *adeB*(quan)r; *adeR* LC f and *adeR* LC r (Table 8), to amplify products of 84 bp and 102 bp, respectively. In both cases, expression was quantified relative to the RNA polymerase β subunit gene,

rpoB, which was assayed using primers *rpoB* Acin F and *rpoB* Acin R (Table 8) to amplify a 109 bp product.

2.19.3. Insertional inactivation of *A. baumannii* genes

2.19.3.1. Insertional inactivation of *adeB* in clinical isolate AB211

The *adeB* gene was disrupted by the insertion of the suicide plasmid pBK-5 as follows:

2.19.3.1.1. Construction of suicide plasmid pBK-5

An internal 2219-bp fragment of *adeB* was PCR-amplified from genomic DNA (~10 ng) of *A baumannii* isolate AB211 using primers *adeB* KO LF and *adeB*(quan)r (Table 8) as outlined in section 11.2, with an annealing temperature of 60°C and an extension time of 150 seconds. The resulting PCR product was cloned into pCR2.1 as described in section 16. Single white colonies were grown overnight with shaking (225 rpm) in LB broth containing 100 mg/L ampicillin. Plasmid extractions were then performed (section 2.6) and the resulting preparations were analysed for the presence of the *adeB* fragment by agarose gel electrophoresis after digestion with 5 U of *Eco*RI for 4 h at 37°C. The plasmid containing the desired fragment was designated pBK-5 (Figure 13).

Figure 13. Map of pBK-5.

Legend:

adeB: internal fragment of *adeB*
P: *lac* promoter/operator
lacZ: *lacZ*α gene
F1 *ori*: origin of replication
Kan^R: kanamycin resistance gene
Amp^R: ampicillin resistance gene
pUC *ori*: origin of replication

2.19.3.1.2. Interruption of *adeB* with pBK-5

Cells of isolate AB211 were made electrocompetent (section 2.10.1) and the suicide plasmid pBK-5 was introduced by electroporation (section 2.10.2). Transformants were selected on Iso-Sensitest agar containing 50 mg/L kanamycin. Chromosomal integration of pBK-5 was confirmed by PCR (section 2.11.1) using primers M13 F and *adeB* CR (Tables 7 and 8), an annealing temperature of 55°C, an extension time of four minutes, and 5 µl of a crude DNA extract (section 2.3.2) to amplify a 3040-bp product. The identity of this fragment was confirmed by nucleotide sequencing (section 2.14).

2.19.3.2. Insertional inactivation of *adeS* in clinical isolate AB211

The *adeS* gene was disrupted by the insertion of suicide plasmids pSK-1 and pSK-2 as follows:

2.19.3.2.1. Construction of suicide plasmids pSK-1 and pSK-2

Two internal fragments of *adeS* were PCR-amplified (section 2.11.2) from AB211 genomic DNA (~10 ng). The first, a 794-bp fragment, was amplified using primers *adeS* KO F and *adeS* KO R (Table 8), an annealing temperature of 60°C and an extension time of one minute. The second, a 620-bp fragment, was amplified using primers S-am and S-av (Table 8), an annealing temperature of 55°C and the same extension time. Both fragments were cloned separately into pCR2.1 as outlined in section 2.16. Individual white colonies were examined by PCR for the presence of insert DNA of the correct size, as described in section 2.11.1, using primers M13 F and M13 R (Table 7), an annealing temperature of 50°C and an extension time of one minute. The template was 5 µl of a crude DNA extract, prepared as in section 2.3.2. Single colonies that were positive for the correct insert DNA were grown overnight with shaking (225 rpm) in LB broth containing 100 mg/L ampicillin, after which plasmid extractions were performed as outlined in section 2.6. The resulting plasmids were designated pSK-1, containing the 794 bp fragment of *adeS* and pSK-2, containing the 620 bp fragment (Figures 14a and 14b).

Figure 14a. Map of pSK-1.

Figure 14b. Map of pSK-2.

Legend:

adeS: internal fragment of *adeS*
P: *lac* promoter/operator
lacZ: *lacZ*α gene
F1 *ori*: F1 origin of replication
Kan^R: kanamycin resistance gene
Amp^R: ampicillin resistance gene
pUC *ori*: origin of replication

2.19.3.2.2. Interruption of *adeS* with pSK-1 and pSK-2

Plasmids pSK-1 and pSK-2 were introduced separately into electrocompetent AB211 cells (section 2.10). Transformants were selected on Iso-Sensitest agar plates containing 50 mg/L kanamycin. Chromosomal integration of pSK-1 and pSK-2 was confirmed by PCR (section 2.11.1) using primers M13 R and *adeS* TR (Tables 7 and 8), an annealing temperature of 50°C, an extension time of two minutes and 5 µl of a crude DNA extract (section 2.3.2) to amplify products of 1292 bp and 1118 bp, respectively. The nucleotide sequences of these fragments were then determined (section 2.14).

2.20. *E. cloacae*-specific methods

2.20.1. Gene expression analysis in *E. cloacae*

Expression of *ramA* and the *acrAB* operon was investigated using real-time RT-PCR as outlined in section 2.15, using primers *ramA* seqLC F and *ramA* seqLC R; *acrB* Fex and *acrB* Rex (Table 9) to amplify products of 185 bp and 92 bp, respectively. In both cases, expression was quantified relative to the RNA polymerase β subunit gene, *rpoB*, using primers *rpoB* Fex and *rpoB* Rex (Table 9) to amplify a 147-bp product.

Table 9. Oligonucleotide primers used in this study with *E. cloacae*

Primer name	Sequence (5' to 3')	Tm	Source
acrB Fex	CGATAACCTGATGTACATGTCC	61	(72)
acrB KOF	AGTGAAAGGCCAGCAGCTTA	64	this study
acrB KOR	CATCCAGCACTTTCTGCGTA	64	this study
acrB KOT R	GAGAAACGAAGGCGATACCA	64	this study
acrB Rex	CCGACAACCATCAGGAAGCT	66	(72)
EBGH3	GGGAAGCTTATTATCGTGAGGATGCGTCA	74	(41)
EBGNHe-5	CCCGCTAGCGAAAAGATGTTTCGTGAAGC	77	(41)
Full *ramA* F	CTGGCAAAACACACCTGGAA	66	this study
Gm F	TGGCGGCGTTGTGACAATTTAC	71	this study
Gm R	TGGACGCACACCGTGGAAACGG	78	this study
Km2.1 F	GCTTACATGGCGATAGCTAGACT	63	this study
Km2.1 R	AGTTCGATGTAACCCACTCGTGC	68	this study
pBADseq F1	TCAGACATTGCCGTCACTGCG	72	this study
pBADseq R1	TCAGACCGCTTCTGCGTTCTG	70	this study
pBADseq R2	TCGACGGCGCTATTCAGATCCT	71	this study
ramA CDS R	TCAGTGCGTCCGACTATGGTTTTC	70	this study
ramA CDS RH	TGAAGCTTTCAGTGCGTCCGACTATGGTTTTC	77	this study
ramA seqCDS F	ATGACGATTTCCGCTCAGGTC	68	this study
ramA seqLC F	CCGTTACGCATCGAAGAGAT	64	this study
ramA seqLC R	CCCAGACTTTCGCCTTTGTA	64	this study
rpoB Fex	AAGGCGAATCCAGCTTGTTCAGC	71	(72)
rpoB Rex	TGACGTTGCATGTTCGCACCCATCA	79	(72)

2.20.2. Insertional inactivation of *E. cloacae* genes

2.20.2.1. Disruption of *acrB* in the clinical isolate *E. cloacae* TGC-R

The *acrB* gene was inactivated by the insertion of a linear DNA fragment containing a gentamicin resistance cassette as outlined below, using methods described previously by Pérez *et al.* (200) with some modifications:

2.20.2.1.1. Preparation of electrocompetent cells of isolate *E. cloacae* TGC-R harbouring pKOBEG

The helper plasmid pKOBEG (41) (Figure 15) was introduced into electrocompetent TGC-R cells by electroporation (section 2.10), and transformants were selected on LB agar plates containing 100 mg/L chloramphenicol during overnight incubation at 30°C. Individual colonies were analysed by PCR for the presence of pKOBEG as outlined in section 2.11.1, using primers EBGNhe-5 and EBGh3 (Table 9), an annealing temperature of 60°C and an extension time of two minutes to amplify a 1960-bp product. Plasmid DNA was used as a positive control, while 5 µl of a crude DNA extract (section 2.3.2) was used as template.

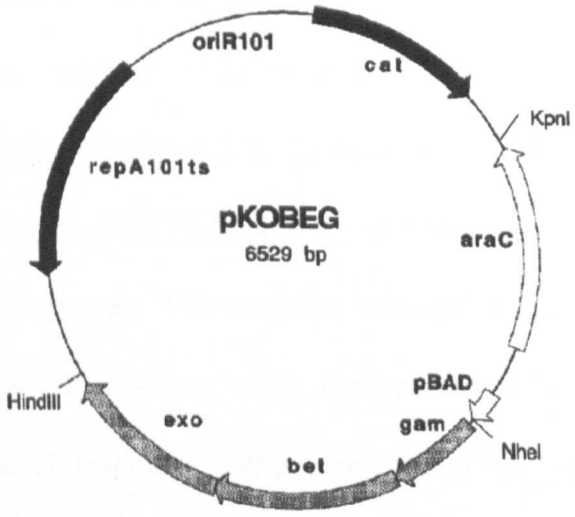

Figure 15. Map of pKOBEG [adapted from Chaveroche *et al.* (41)].

Legend:

cat:	chloramphenicol resistance gene
araC:	regulatory gene (*ara*BAD promoter)
pBAD:	*ara*BAD promoter region
gam, *bet*, *exo*:	phage λ Red functions
repA101ts:	temperature-sensitive replication
*ori*R101:	origin of replication

A single transformant was made electrocompetent as follows: 20 ml of modified LB broth (without NaCl) containing 100 mg/L chloramphenicol was seeded with 200 µl of an overnight culture of TGC-R harbouring pKOBEG and incubated at 30°C with shaking (225 rpm). When the OD_{600} reached 0.2, the phage λ Red genes encoded by pKOBEG were induced by the addition of L-arabinose to a final concentration of 0.2% w/v. When the OD_{600} reached 1.0 the culture was centrifuged at 4000 x *g* at 4°C for 10 minutes, the supernatant removed and the pellet re-suspended in 40 ml of cold sterile water and re-centrifuged as before. The final pellet was suspended in 90 µl of 15% sterile glycerol.

2.20.2.1.2. Construction of pCRBK-2

An internal 1558-bp fragment of the *acrB* gene was amplified by the Expand High Fidelity Plus PCR system (section 2.11.2) from TGC-R genomic DNA (~10 ng) using primers *acrB* Fex and *acrB* KOR (Table 9), an annealing temperature of 55°C and an extension time of 95 seconds. The resulting fragment was cloned into pCR2.1 (section 2.16). Individual white colonies were analysed by PCR (section 2.11.1) for the presence of the *acrB* fragment using primers M13 F and M13 R (Table 7), an annealing temperature of 50°C, an extension time of 100 seconds, and 5 µl of a crude DNA extract (section 2.3.2). A single colony that was PCR-positive for the *acrB* fragment was grown overnight with shaking (225 rpm) at 37°C in LB broth containing 100 mg/L ampicillin. Plasmid extractions were then performed as described in section 2.6. The resulting plasmid was designated pCRBK-1 (Figure 16a).

The gentamicin resistance cassette from cloning vector pBBR1MCS-5 was amplified by PCR using *Pfu* DNA polymerase (section 2.11.3), primers Gm F and Gm R (Table 9), an annealing temperature of 60°C and an extension time of two minutes.

The resulting 854-bp fragment was cloned into *Nru*I-digested pCRBK-1 (within the *acrB* fragment) to generate pCRBK-2 (Figure 16b). Briefly, pCRBK-1 was digested with 5 U of *Nru*I for 4 h at 37°C, treated with SAP for one hour at 37°C and ligated overnight at 15°C with the above fragment using T4 DNA ligase and a 1:10 molar ratio of vector: insert DNA (section 2.17). The ligation was introduced into electrocompetent α-select *E. coli* (section 2.10.2) and transformants were selected on LB agar plates containing 10 mg/L gentamicin. Individual colonies were grown overnight with shaking (225 rpm) in LB broth containing 10 mg/L gentamicin. Plasmid extractions were then performed (section 2.6) and the plasmid preparations were examined for the presence of the gentamicin resistance cassette by agarose gel electrophoresis after digestion with *Eco*RI (5 U for 4 h at 37°C).

2.20.2.1.3. Inactivation of *acrB* with a linear DNA fragment

The 2412-bp linear DNA fragment employed to interrupt *acrB* was amplified from pCRBK-2 using the internal *acrB* fragment primers detailed above, the Expand High Fidelity Plus PCR system (section 2.10.2), an annealing temperature of 55°C and an extension time of 150 seconds. The resulting PCR product was introduced into electrocompetent TGC-R::pKOBEG cells (section 2.10) and transformants were selected on LB agar plates containing 10 mg/L gentamicin. Chromosomal integration of the gentamicin resistance cassette was confirmed by PCR (section 2.11.1) using primers Gm F and *acrB* KOT R (Table 9), an annealing temperature of 60°C, an extension time of 120 seconds and 5 µl of a crude DNA extract (section 2.3.2) to amplify a 1405-bp product, the nucleotide sequence of which was then determined (section 2.14).

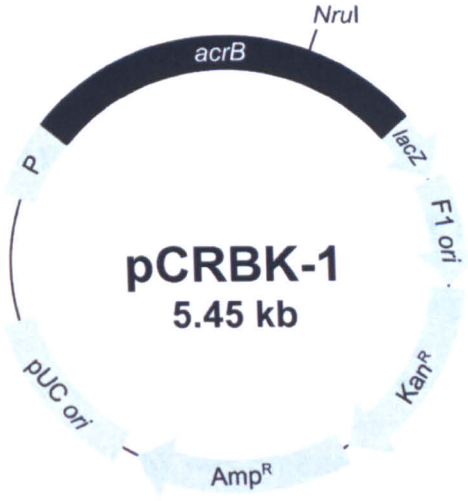

Figure 16a. Map of pCRBK-1.

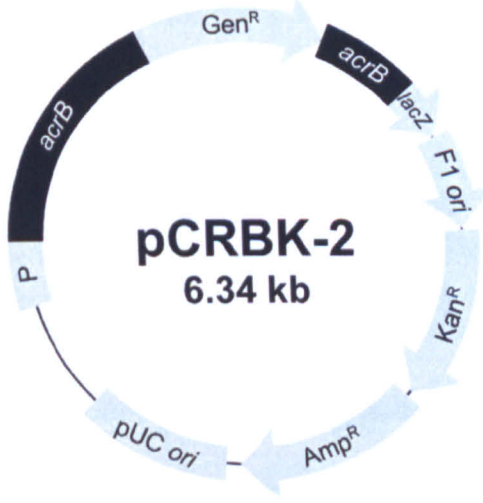

Figure 16b. Map of pCRBK-2.

Legend:

acrB: internal fragment of *acrB*
P: *lac* promoter/operator
lacZ: *lacZ*α gene
F1 *ori*: F1 origin of replication
Kan^R: kanamycin resistance gene
Amp^R: ampicillin resistance gene
pUC *ori*: origin of replication
Gen^R: gentamicin resistance gene

2.20.2.2. Disruption of *acrB* in clinical isolate *E. cloacae* EC391

The *acrB* gene was inactivated by the insertion of the suicide plasmid, pRSACRB.

2.20.2.2.1. Construction of pRSACRB

An internal 1102-bp fragment of *acrB* was amplified from EC391 genomic DNA (~10 ng) by PCR with *Pfu* DNA polymerase (section 2.11.3) using primers *acrB* KOF and *acrB* KOR (Table 9), an annealing temperature of 60°C and an extension time of 70 seconds. Plasmid pSMY-2 (Figure 19b) was digested for 4 h at 37°C with *Xba*I to yield two fragments, which were separated by agarose gel electrophoresis. The 2263-bp fragment was gel-purified (section 2.13) and end filled to create a blunt fragment by treatment with *Pfu* DNA polymerase for 10 minutes at 72°C. The fragment was then dephosphorylated by SAP treatment for 1 h and then ligated with the *acrB* fragment using T4 DNA ligase at 15°C overnight and a 1:10 molar ratio of vector: insert DNA (section 2.17). The ligation was introduced into electrocompetent pir^+ *E. coli* as described in section 2.10.2. Transformants were selected on LB agar plates containing 50 mg/L kanamycin. Individual colonies were examined for the presence of the *acrB* fragment by PCR (section 2.11.1) using primers M13 F and *acrB* KOR (Tables 7 and 9), an annealing temperature of 55°C, an extension time of 80 seconds, and 5 µl of a crude DNA extract (section 2.3.2). A single colony that was positive for the *acrB* fragment by PCR was grown overnight with shaking (225 rpm) in LB broth containing 50 mg/L kanamycin at 37°C. Plasmid extraction was performed as described in section 2.6. The resulting plasmid was designated pRSACRB (Figure 17).

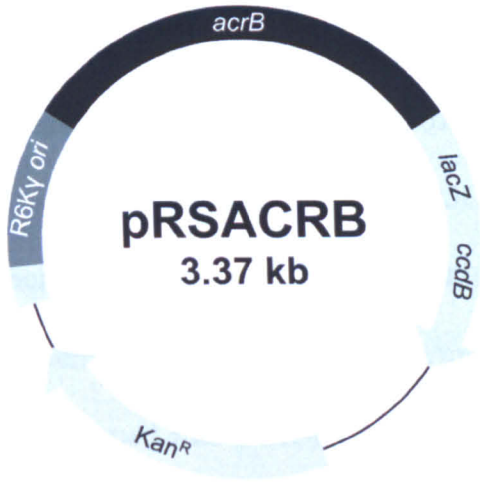

Figure 17. Map of pRSACRB.

Legend:

acrB:	internal fragment of *acrB*
lacZ:	*lacZ*α gene
*ccd*B:	lethal gene
Kan^R:	kanamycin resistance gene
R6Kγ *ori*:	origin of replication

2.20.2.2.2. Interruption of *acrB* with pRSACRB

The suicide plasmid pRSACRB was introduced into electrocompetent *E. cloacae* EC391 cells (section 2.10) and transformants were selected on LB agar plates containing 25 mg/L kanamycin. Chromosomal integration of pRSACRB was confirmed by PCR (section 2.11.1) using primers MOD5 ori R and *acrB* KOT R (Tables 7 and 9), an annealing temperature of 58°C, an extension time of 90 seconds, and 5 µl of a crude DNA extract (section 2.3.2) to amplify a 1540-bp product, the identity of which was confirmed by nucleotide sequencing (section 2.14).

2.20.3. Overexpression of *ramA* in clinical isolate *E. cloacae* TGC-S

2.20.3.1. Cloning and sequencing of *ramA* and GenBank accession numbers

A DNA fragment containing the *ramA* gene was amplified by PCR with *Pfu* DNA polymerase (section 2.11.3) from *E. cloacae* TGC-S, TGC-R and TGC-S7 genomic DNA (~10 ng) using primers Full *ramA* F and *ramA* CDS R (Table 9), an annealing temperature of 60°C and extension time of one minute to amplify a 517-bp product. The resulting products were cloned into pCR-Blunt (section 2.16). Individual white colonies were analysed for the presence of insert DNA by PCR (section 2.11.1) using primers M13 F and M13 R (Table 7), an annealing temperature of 50°C, an extension time of 45 seconds and 5 µl of a crude DNA extract (section 2.3.2). Single colonies that were positive for insert DNA of the correct size by PCR were grown overnight with shaking (225 rpm) in LB broth containing 50 mg/L at 37°C. Plasmid extractions were then performed (section 2.6) and the nucleotide sequences of the inserts were determined using the above primers and plasmid DNA as template (section 2.14). The nucleotide sequence data were deposited with GenBank with accession numbers GU180677 (TGC-S) and GU180678 (TGC-R).

2.20.3.2. Construction of pBADKM and pBADKM-R

The kanamycin resistance cassette from pCR2.1 was amplified by PCR with *Pfu* DNA polymerase (section 2.11.3) using primers Km2.1 F and Km2.1 R (Table 9), an annealing temperature of 60°C and an extension time of 150 seconds. The resulting 1138-bp product was cloned into a modified version of the expression vector, pBAD (Invitrogen), in which the unique *Nco*I restriction site had been replaced with a unique *Sma*I site, yielding plasmid pBADS (Figure 18a). Plasmid pBADS was digested with 5 U of *Eco*RV for 4 h at 37°C followed by SAP treatment for 1 h at 37°C. Ligation

with the above PCR product was then performed using T4 DNA ligase overnight at 15°C and a 1:10 molar ratio of vector: insert DNA (section 2.17). The ligation was introduced into electrocompetent α-select *E. coli* (section 2.10) and transformants were selected on LB agar plates containing 50 mg/L kanamycin. Individual colonies were grown overnight with shaking (225 rpm) in LB broth at 37°C. Plasmid extractions were performed (section 2.6) and preparations were analysed for the presence of insert DNA by agarose gel electrophoresis after digestion with *Sma*I (5 U) for 4 h at 25°C. The resulting plasmid was designated pBADKM (Figure 18b).

The *ramA* gene was amplified by PCR from TGC-R genomic DNA (~10 ng) with *Pfu* DNA polymerase (section 2.11.3) using primers *ramA* seqCDS F and *ramA* CDS RH (Table 9), an annealing temperature of 60°C and an extension time of one minute. The resulting 350 bp product was digested with *Hin*dIII for 4 h at 37°C then purified as described in section 2.13. Plasmid pBADKM was also digested with *Hin*dIII as above, followed by a further digestion with *Sma*I for 4 h at 25°C. The above *Hin*dIII-digested PCR product was then directionally cloned into *Hin*dIII/*Sma*I-digested pBADKM. Ligation was performed using T4 DNA ligase for 3 h at room temperature and a 1:3 molar ratio of vector: insert DNA (section 2.17). The ligation was introduced into α-select *E. coli*, and transformants were selected on LB agar plates containing 50 mg/L kanamycin. Individual colonies were screened by PCR (section 2.11.1) for the presence of the *ramA* insert using primers *ramA* seqCDS F and pBADseq R2 (Table 9), an annealing temperature of 60°C, an extension time of 30 seconds and 5 µl of a crude DNA extract (section 2.3.2). A single colony that was positive for the *ramA* insert was grown overnight in LB broth containing 50 mg/L kanamycin. Plasmid extraction was then performed as outlined in section 2.6. The resulting plasmid, pBADKM-R (Figure 18c), was used to overexpress *ramA* in

clinical isolate *E. cloacae* TGC-S (section 2.20.3.3); vector pBADKM was used as a negative control.

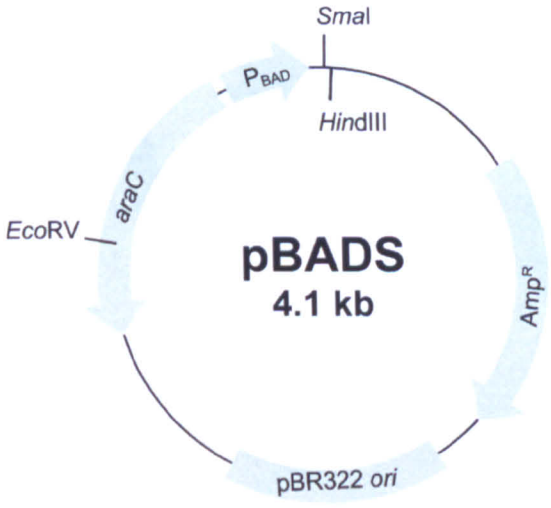

Figure 18a. Map of pBADS.

Figure 18b. Map of pBADKM.

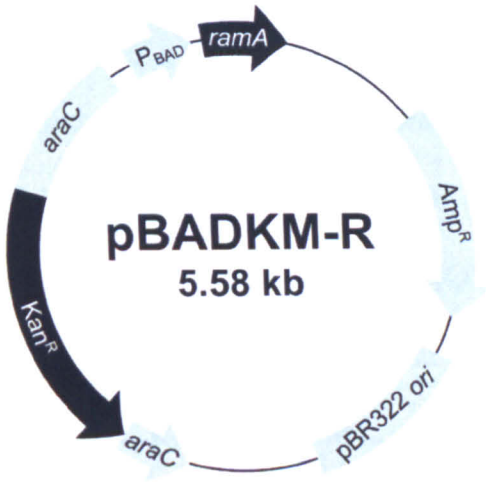

Figure 18c. Map of pBADKM-R.

Legend:

ramA:	global regulatory gene
Amp^R:	ampicillin resistance gene
pBR322 *ori*:	origin of replication
araC:	regulatory gene (*ara*BAD promoter)
Kan^R:	kanamycin resistance gene
P_{BAD}:	*ara*BAD promoter region

2.20.3.3. Overexpression of *ramA* in TGC-S using pBADKM-R

Plasmids pBADKM and pBADKM-R were introduced separately into electrocompetent *E. cloacae* TGC-S cells, as outlined in section 2.10.2. Transformants were selected on LB agar plates containing 50 mg/L kanamycin. Individual colonies were screened for the presence of pBADKM or pBADKM-R, as appropriate, by PCR (section 2.11.1) using primers pBADseq F1 and pBADseq R1 (Table 9), an annealing temperature of 60°C, an extension time of one minute and 5 µl of a crude DNA extract (section 2.3.2) to amplify products of 486 bp and 833 bp, respectively. Single colonies that were positive for either pBADKM or pBADKM-R

were grown overnight with shaking (225 rpm) in LB broth containing 50 mg/L kanamycin.

LB broth (10 ml) containing 50 mg/L kanamycin was then seeded with 100 µl of the overnight culture of TGC-S harbouring either pBADKM or pBADKM-R and incubated with shaking (225 rpm) at 37°C to mid-log phase (OD_{600} = 0.5). Expression of *ramA* was induced for 4 h by the addition of L-arabinose to final concentrations of 0.2, 0.02, 2 x 10^{-3}, and 2 x 10^{-4} % w/v. RNA extractions were then performed (section 2.8) and expression of *acrAB* was monitored by real-time RT-PCR (section 2.19.1).

2.21. *S. marcescens*-specific methods

2.21.1. Gene expression analysis in *S. marcescens*

Expression of the *sdeAB*, *sdeCDE*, and *sdeXY* efflux pump-encoding operons was monitored by real-time RT-PCR (section 2.15) using primers *sdeB* LC F and *sdeB* LC R; *sdeD* LC F and *sdeD* LC R; *sdeY* LC F and *sdeY* LC R (Table 10) to amplify products of 158 bp, 153 bp, 168 bp and 137 bp, respectively. Expression was quantified relative to the RNA polymerase β subunit gene, *rpoB*, using primers Sma *rpoB* F and Sma *rpoB* R (Table 10) to amplify a 137 bp fragment.

Table 10. Oligonucleotide primers used in this study with *S. marcescens*

Primer name	Sequence (5' to 3')	Tm	Source
hasF check F	GCAATGAGCCAGGCAGAGAA	68	this study
hasF KOF	CATGTCGAAATGGCGCCAAC	71	this study
hasF KOR	TTGTAGGCGTTGATGCTGCT	66	this study
sdeB LC F	AGATGGCCGATAAGCTGTTG	64	this study
sdeB LC R	CAGCGTCCAGCTTTCATACA	64	this study
sdeD LC F	AGCTTCATTCATCCGGTCAC	64	this study
sdeD LC R	CATGATGGCGTTCTTCTTCA	64	this study
sdeY KOR	CTGGTTACGCGCTTCGGTCAG	70	this study
sdeY LC F	TCCATCAACGAAGTGGTGAA	64	this study
sdeY LC R	GTTTATCGAGAAGCCGAACG	64	this study
Sma *rpoB* F	CTAACGAGTATGGCTTCCTG	59	this study
Sma *rpoB* R	CTTCTTCATCCAGGTTGGAG	61	this study
XY CDS R	TCACTGAGCGATCAGTGG	61	this study

2.21.2. Insertional inactivation of *S. marcescens* genes

2.21.2.1. Disruption of *sdeY* in the laboratory mutant 10211-10

The *sdeY* gene was inactivated by the insertion of the suicide plasmid, pSMY2 as detailed below:

2.21.2.1.1. Construction of the suicide plasmid pSMY2

An internal 1095-bp fragment of *sdeY* was amplified by PCR with *Pfu* DNA polymerase (section 2.11.3) from mutant 10211-10 genomic DNA (~10 ng) using primers *sdeY* LC F and *sdeY* KOR, an annealing temperature of 60°C and an extension time of 120 seconds. The resulting fragment was cloned into pCR-Blunt (section 2.16). Individual white colonies were analysed by PCR (section 2.11.1) for the presence of insert DNA, using primers M13 F and M13 R (Table 7), an annealing temperature of 50°C, an extension time of 70 seconds and 5 µl of a crude DNA extract (section 2.3.2). A single colony that was positive for insert DNA by PCR was grown overnight with shaking (225 rpm) at 37°C in LB broth containing 50 mg/L

kanamycin. Plasmid extraction was then performed as outlined in section 2.6. The new plasmid was designated pSMY1 (Figure 19a).

A 388-bp DNA fragment containing the R6Kγ origin of replication and multiple cloning site (containing a unique *Xba*I site) from plasmid pMOD-5 (Cambio) was amplified by PCR with *Pfu* DNA polymerase (section 2.11.3), primers MOD5 ori F and MOD5 ori R (Table 7), an annealing temperature of 58°C, an extension time of one minute and ~10 ng of extracted plasmid DNA. Plasmid pSMY-1 was sequentially digested (5 U for 4 h) with *Sma*I (25°C) and *Sac*I (37°C). The 3124-bp fragment resulting from *Sma*I/*Sac*I digestion of pSMY1 (containing the *sdeY* fragment and the kanamycin resistance cassette from pCR-Blunt, but not the pUC origin) was isolated by agarose gel electrophoresis and purified as described in section 2.13. This DNA fragment was then treated with *Pfu* DNA polymerase (section 2.20.2.2.1) to yield a blunt-ended fragment and ligated to the above PCR product using T4 DNA ligase; overnight incubation at 15°C and a 1:10 molar ratio of vector: insert DNA (section 2.17). The ligation was introduced into electrocompetent *pir*$^+$ *E. coli* (section 2.10.2) and transformants were selected on LB agar plates containing 50 mg/L kanamycin. Individual colonies were screened for the correct orientation of the R6Kγ origin of replication / multiple cloning site by PCR (section 2.11.1) using primers M13 F and MOD5 ori R (Table 7), an annealing temperature of 55°C, an extension time of 90 seconds and 5 µl of a crude DNA extract (section 2.3.2). A single colony with the correct R6Kγ*ori* orientation was grown overnight at 37°C in LB broth containing 50 mg/L kanamycin. The new plasmid, pSMY2 (Figure 19b) was extracted as described in section 2.6.

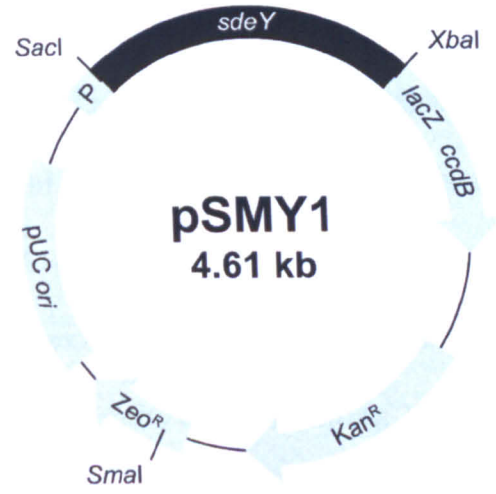

Figure 19a. Map of pSMY1.

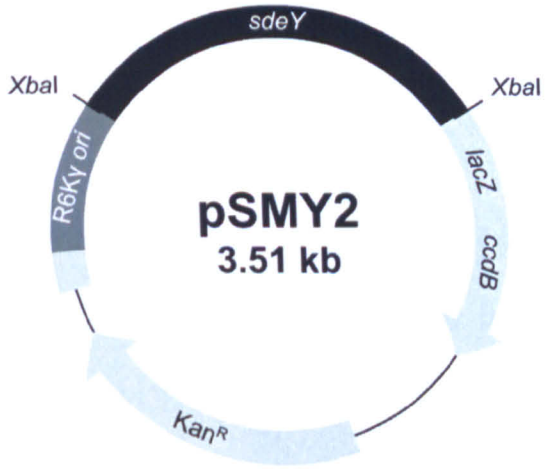

Figure 19b. Map of pSMY2.

Legend:

sdeY:	internal fragment of *sdeY*
lacZ:	*lacZ*α gene
*ccd*B:	lethal gene
Kan^R:	kanamycin resistance gene
R6Kγ *ori*:	origin of replication

2.21.2.1.2. Interruption of *sdeY* with pSMY2

The suicide plasmid pSMY2 was introduced into electrocompetent 10211-10 (section 2.10) and transformants were selected on LB agar plates containing 25 mg/L kanamycin. Chromosomal integration of pSMY2 was confirmed by PCR (section 2.11.1) using primers M13 F and XY CDS R (Tables 6 and 9), an annealing temperature of 55°C, an extension time of 140 seconds and 5 µl of a crude DNA extract (section 2.3.2). The identity of the resulting 2260 bp product was confirmed by nucleotide sequencing (section 2.14).

2.21.2.2. Disruption of *hasF* in the laboratory mutant *S. marcescens* 10211-10

The *hasF* gene was interrupted by a suicide plasmid pHASF.

2.21.2.2.1. Construction of the suicide plasmid pHASF

An internal 803-bp fragment of *hasF* was amplified from *S. marcescens* 10211-10 genomic DNA (~10 ng) by PCR with *Pfu* DNA polymerase (section 2.11.3), using primers *hasF* KOF and *hasF* KOR (Table 10), an annealing temperature of 60°C and an extension time of two minutes. The *sdeY* fragment of plasmid pSMY-2 (Figure 19b) was then replaced with the fragment of *hasF*, as described in section 2.19.2.2.1. Individual colonies were screened by PCR (section 2.11.1) for the presence of *hasF* using primers *hasF* KOF and MOD5 ori R (Tables 10 and 7), an annealing temperature of 58°C, an extension time of 70 seconds and 5 µl of a crude DNA extract (section 2.3.2). A single colony that was positive by PCR for the *hasF* insert was grown overnight with shaking (225 rpm) at 37°C in LB broth containing 50 mg/L

kanamycin. Plasmid pHASF (Figure 20) was then extracted as described in section 2.6.

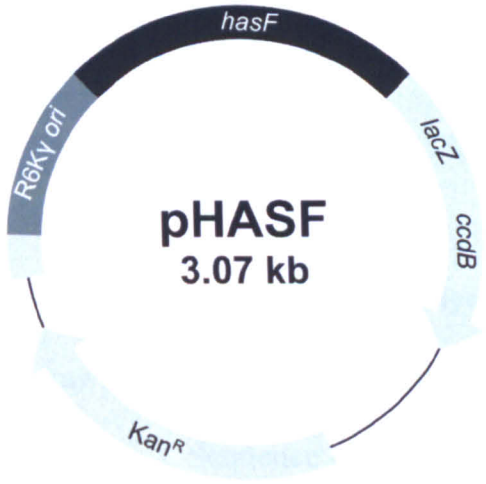

Figure 20. Map of pHASF.

Legend:

hasF:	internal fragment of *hasF*
lacZ:	*lacZ*α gene
*ccd*B:	lethal gene
Kan^R:	kanamycin resistance gene
R6Kγ *ori*:	origin of replication

2.21.2.2.2. Interruption of *hasF* with pHASF

The suicide plasmid pHASF was introduced into electrocompetent *S. marcescens* 10211-10 cells (section 2.10) and transformants were selected on LB agar plates containing 25 mg/L kanamycin. Chromosomal integration of pHASF was confirmed by PCR (section 2.11.1) using primers *hasF* check F and MOD5 ori R (Tables 10 and 7), an annealing temperature of 58°C, an extension time of 80 seconds and 5 µl of a crude DNA extract (section 2.3.2). The identity of the resulting 1372-bp product was confirmed by nucleotide sequencing (section 2.14).

2.22. Software packages used to analyse data and prepare figures

2.22.1. Analysis of DNA and protein sequence data

DNA and protein sequence data were analysed using BioEdit version 7.0.5.3 (http://www.mbio.ncsu.edu/BioEdit/page2.html). In some instances, primers were designed using Primer3 version 0.4.0 (http://frodo.wi.mit.edu/primer3/).

2.22.2. Figure preparation and statistical analysis

Plasmid maps and other drawings were prepared using Carbon Outlines version 1.1 (Go Figure Solutions, Bootle, UK). Sequence alignment figures were prepared using GeneDoc version 2.7.0 (http://www.nrbsc.org/gfx/genedoc/). All graphs were prepared and statistical analyses performed using GraphPad Prism version 5.0 (GraphPad Software, La Jolla, Ca., USA).

3. Results

3.1. *A. baumannii*

Clinical isolates of *A. baumannii* displaying reduced susceptibility or resistance to tigecycline were being referred to the HPA's ARMRL as early as 2004, two years before a marketing authorisation was granted by the EMA in 2006.

Many of the *A. baumannii* clinical isolates in ARMRL's collection are members of two prevalent European clone II lineages, namely OXA-23 clone 1 (49) and the SE clone (259). In the United States, a carbapenem-resistant *A. baumannii* clone, ACB20 has caused a multicity outbreak since 2005 largely in the state of Illinois (154). These clones were of particular interest for two reasons. Firstly, apart from polymyxins, tigecycline is usually one of the only therapeutic options available for treating infections caused by carbapenem-resistant *A. baumannii*. Secondly, although the three clones differ in their modal tigecycline MICs; the molecular basis of this variation was unclear. In order to study this latter observation, multiple representatives of the two UK clones, referred from numerous centres between 2004 and 2008, were selected from ARMRL's collection (these were selected as having the typical [modal] MICs for the clones) and representatives of the ACB20 clone were provided by Dr John Quinn (Table 2).

The mechanisms of tigecycline resistance also were investigated in two instances where resistance emerged during tigecycline therapy in representatives of OXA-23 clone 1. The emergence of tigecycline resistance in this lineage during therapy was, and indeed remains, an issue of considerable public health importance that justifies further investigation. Details of the two clinical cases are outlined below.

3.1.1. Clinical case reports

3.1.1.1. Case 1

MDR *A. baumannii* (MDRAB; designated AB210), susceptible (by the hospital's own testing and confirmed by ARMRL) only to colistin and tigecycline, was isolated from abdominal drain fluid from a patient admitted to a London hospital ICU in 2005. The patient had a complicated stay, having developed an intra-abdominal infection following a cholecystectomy, requiring several courses of antibiotics, based on microbiology and clinical status. Tigecycline-susceptible MDRAB was repeatedly isolated from abdominal fluid so, when the patient became septic again, tigecycline was commenced at the standard regimen; a loading dose of 100 mg, followed by 50 mg twice daily. As intra-abdominal infection this constituted on-label use. After one week of therapy, a tigecycline-resistant *A. baumannii* isolate (designated AB211) was recovered from the same site. Despite the microbiological failure of tigecycline therapy, the patient subsequently went on to make a full recovery.

3.1.1.2. Case 2

A patient presented to a London hospital with an infected femoral haematoma. Tissue samples grew mixed 'coliforms' and anaerobes and the patient was treated empirically with amoxicillin / clavulanic acid. Three weeks following admission the patient developed profound sepsis and multi-organ failure; antibiotics were changed to meropenem. Following a period of apparent recovery, the patient then developed acute necrotic pancreatitis and a further episode of severe sepsis. Despite receiving five days of intravenous vancomycin, ciprofloxacin and amikacin an intra-abdominal collection developed and tigecycline-susceptible MDRAB (designated W6976) was isolated from a line tip. The patient was treated with amikacin (W6976 was resistant

to this agent) and tigecycline (50 mg twice daily following a loading dose of 100 mg) and pus drained from the collection yielded a pure growth of MDRAB. This and a further isolate (designated W7282) obtained six days later at a second drainage procedure were tigecycline-resistant. Tigecycline was replaced with intravenous colistin and therapy was continued for a further two weeks. The patient made a slow recovery and was eventually discharged home four months after initial admission.

3.1.2. Isolate characterisation and antibiotic susceptibilities

All isolates were identified as the *A. calcoaceticus-A. baumannii* complex by API20NE and were positive by PCR for the $bla_{\text{OXA-51-like}}$ gene, confirming them as *A. baumannii* (261). Isolates were identified as representatives of either the SE clone, OXA-23 clone 1 or the USA clone ACB20 by PFGE, which was also used to confirm the parentage of mutants selected *in vitro* (Figure 21).

3.1.2.1. OXA-23 clone 1, SE clone and ACB20 clone representatives

Tigecycline MICs for nine representative isolates of OXA-23 clone 1 and eight of the SE clone were 0.25 and 1 mg/L, respectively, representing the mode (± 1 two-fold dilution) for these lineages (49;259); those for five representatives of the USA clone ACB20 were 2 mg/L (three isolates) or 4 mg/L (two isolates) (Table 11).

3.1.2.2. Case study isolates

Laboratory mutants with elevated tigecycline MICs were selected for by exposing susceptible isolates to tigecycline *in vitro*, in a step-wise fashion, until no further growth was observed (Materials and Methods section 2.18). This then allowed for

comparative investigations of efflux resistance mechanisms in the laboratory-selected and wild-type tigecycline-resistant mutants.

The post-therapy clinical isolate from case 1, AB211 (tigecycline MIC, 16 mg/L) and the final laboratory mutant AB210-6 (tigecycline MIC, 64 mg/L) showed 32- and 128-fold increases in tigecycline MIC, respectively, compared with the pre-therapy parent isolate AB210 (MIC, 0.5 mg/L). Similarly, there was a 16-fold increase in MIC for the post-therapy isolate W7282, from case 2 (MIC, 8 mg/L) compared with the pre-therapy isolate W6976 (MIC, 0.5 mg/L; Table 11) from the same patient. PFGE profiles were consistent within each of the two clinical series (Figure 21a and 21b), as were the profiles of the laboratory mutant, AB210-6 and its parent clinical isolate, AB210 (Figure 21c).

a.

b.

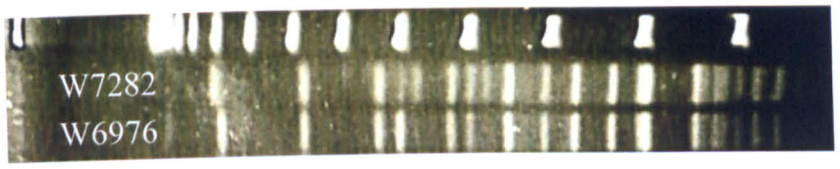

c.

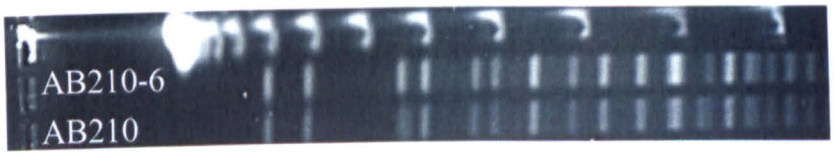

Figure 21. PFGE profiles of *A. baumannii* clinical isolates and mutants: (a) clinical isolates AB210 and AB211; (b) clinical isolates W7282 and W6976; (c) AB210 and mutant AB210-6.

Interestingly, AB211 (though not the laboratory mutant, AB210-6) displayed a $\geq$ 16-fold reduction in the MICs of tobramycin and amikacin and at least a four-fold reduction in the MIC of gentamicin compared with AB210 (Table 11). Further characterisation of this clinical pair by ARMRL and the Laboratory of HealthCare Associated Infection (LHCAI) revealed that isolate AB211 was negative by PCR for two distinct aminoglycoside resistance determinants, both of which were present in isolate AB210 (Turton, J. and Woodford, N., personal communication). The first of these, an aminoglycoside acetyltransferase gene, *aacA4*, which is located on a class 1 integron associated with the OXA-23 clone 1 lineage, is known to confer resistance to amikacin and tobramycin (258). The second, a 16S rRNA methylase gene, *armA*,

confers high-level resistance to all three tested aminoglycosides, as well as all other 4,6-disubstituted deoxystreptamines (92). These observations probably explain the differences in aminoglycoside resistance phenotypes of the two isolates.

There were also reductions of at least eight–fold in carbapenem MICs and a four-fold reduction in ceftazidime MIC for mutant AB210-6 compared with AB210 (Table 11). Both the mutant and parent were positive for *bla*$_{OXA-23}$ by PCR (Turton, J., personal communication) and the reasons for the difference in their MICs warrant further investigation; there were no similar MIC reductions within the two clinical pairs.

Table 11. Antibiotic susceptibilities of *A. baumannii* isolates and laboratory mutant

Isolate/clone	MIC (mg/L)															
	AMP	AUG	AZT	CAR	CLAV	CLOX	**CLAX**	CTX	CTXC	**CAZ**	CAZC	CPR	CPRC	FOX	PIP	PTZ
OXA-23 clone 1 (n=9)	>64	>64	≥64	>512	>4	>100	128->256	≥256	>32	64-256	>32	≥64	>32	>64	>64	>64
SE (n=8)	>64	>64	≥64	>512	>4	>100	32->256	≥256	>32	128->256	>32	≥64	≥32	>64	>64	>64
ACB20 (n=5)	>64	>64	≥64	>512	>4	>100	32-256	64->256	>32	16-256	16->32	64	>32	>64	>64	>64
AB210	>64	>64	64	>512	>4	>100	**256**	>256	>32	**64**	>32	>64	>32	>64	>64	>64
AB211	>64	>64	64	>512	>4	>100	256	>256	>32	64	>32	>64	>32	>64	>64	>64
AB210-6	>64	>64	32	>512	>4	>100	**64**	256	>32	**16**	32	>64	>32	>64	>64	>64
W6976	>64	>64	32	>512	>4	>100	>256	>256	>32	128	>32	>64	>32	>64	>64	>64
W7282	>64	>64	32	>512	>4	>100	256	256	>32	64	>32	>64	>32	>64	>64	>64

AMP, ampicillin; AUG, co-amoxiclav; AZT, aztreonam; CAR, carbenicillin; CLAV, clavulanic acid; CLOX, cloxacillin; CLAX, cloxacillin plus cefotaxime; CTX, cefotaxime; CTXC, cefotaxime plus clavulanic acid; CAZ, ceftazidime; CAZC, ceftazidime plus clavulanic acid; CPR, cefpirome, CPRC, cefpirome plus clavulanic acid, FOX, cefoxitin, PIP, piperacillin; PTZ, piperacillin plus tazobactam.

Table 11 cont. Antibiotic susceptibilities of *A. baumannii* isolates and laboratory mutant

Isolate/clone	MIC (mg/L)														
	EDTA	**IME**	**IM**	**MEM**	ERP	CIP	**TOB**	**AMK**	**GEN**	TET	**MIN**	**TGC**	SUB	COL	CHL
OXA-23 clone 1 (n=9)	NA	NA	16->32	16->32	>16	>8.0	0.25->32	≤0.5->64	0.5->32	NT	2-16	**0.25**	8-32	1	NT
SE (n=8)	NA	NA	4-32	16->32	≥16	>8.0	1->32	1->64	≥32	NT	2-8	**1**	≥32	≤0.5-1	NT
ACB20 (n=5)	NA	NA	>32	>32	>16	>8.0	16->32	8->64	>32	NT	0.5-1	**2-4**	8-16	≤0.5-1	NT
AB210	>320	**>16**	**>32**	**>32**	>16	>8.0	**>32**	**>64**	**>32**	NT	**2**	**0.5**	32	≤0.5	NT
AB211	>320	>16	>32	>32	>16	>8.0	**2**	**4**	**8**	NT	**16**	**16**	32	≤0.5	NT
AB210-6	>320	**8**	**8**	**4**	>16	>8.0	>32	>64	>32	NT	16	**64**	16	≤0.5	NT
W6976	>320	8	>32	>32	>16	>8.0	>32	>64	>32	NT	8	**0.5**	>32	1	NT
W7282	>320	8	32	32	>16	>8.0	>32	>64	>32	NT	8	**8**	>32	1	NT

EDTA, ethylenediaminetetraacetic acid; IME, imipenem plus EDTA; IPM, imipenem; MEM, meropenem; ETP, ertapenem; CIP, ciprofloxacin; TOB, tobramycin; AMK, amikacin; GEN, gentamicin, TET, tetracycline; MIN, minocycline; TGC, tigecycline; SUB, sulbactam; COL, colistin; CHL, chloramphenicol.

3.1.3. Analysis of expression of the efflux pump-encoding operon *adeABC* and the regulatory operon *adeRS* using real-time RT-PCR

Reduced susceptibility and resistance to tigecycline in *A. baumannii* clinical isolates has to date been associated with up-regulation of the chromosomally-encoded RND-type efflux system AdeABC (197;223), which is regulated by the two-component signal transduction system AdeRS (164).

3.1.3.1. Analysis of *adeABC* expression in OXA-23 clone 1, SE clone and ACB20 clone representatives

To investigate whether differential expression of the RND-type efflux pump-encoding operon *adeABC* correlated with differences in the modal tigecycline MICs for the three *A. baumannii* clones, expression of this operon was monitored in multiple representatives of each lineage. Real-time RT-PCR (Materials and Methods sections 2.15 and 2.19.2) identified a mean six-fold higher level of *adeABC* expression in isolates of the SE clone than those belonging to OXA-23 clone 1 (Figure 22; $p = <0.001$). Comparison to the ACB20 clone was more complicated owing to differences in tigecycline MIC among individual isolates; however, when the isolates were analysed separately, there was an association between a higher MIC and elevated *adeABC* expression (Figure 23).

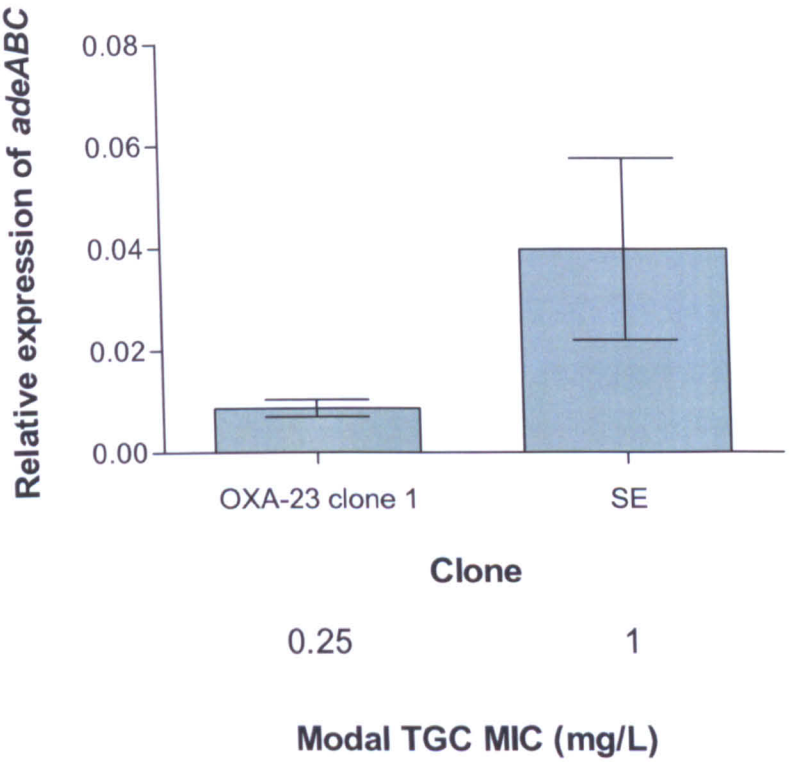

Figure 22. Expression of *adeABC* relative to that of *rpoB* (means ± standard deviations) in multiple isolates of two epidemic clones. OXA-23 clone 1: nine isolates; range = 0.006 – 0.012. SE clone: eight isolates; range = 0.015 – 0.082. Modal tigecycline (TGC) MICs are shown. Mann-Whitney test; $p = <0.001$.

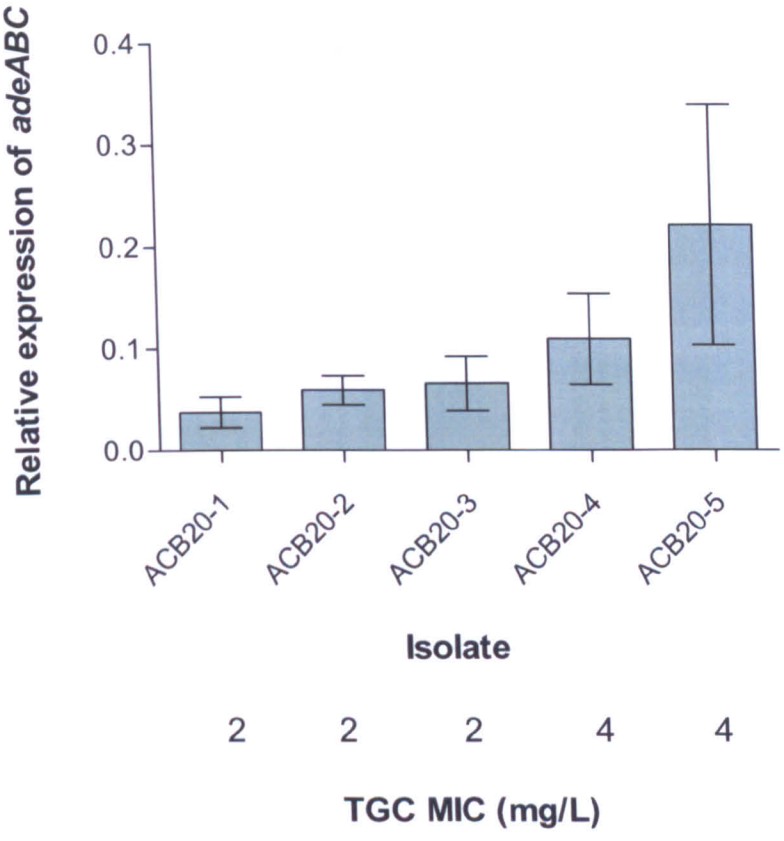

Figure 23. Expression of *adeABC* relative to that of *rpoB* (means ± standard deviations) in five isolates of the ACB20 clone. Tigecycline (TGC) MICs are shown.

3.1.3.2. Analysis of *adeABC* expression in mutants selected *in vivo* and *in vitro*

Overexpression of *adeABC* was also evident in both post-therapy isolates, and in the laboratory mutant compared with the pre-therapy isolates. There were mean 50- and 407-fold increases in AB211 and AB210-6, respectively, compared with AB210 (Figure 24), and a mean nine-fold increase in W7282 compared with W6976 (Figure 25). No difference in expression of the regulatory operon, *adeRS* was seen between AB210 and AB211 (Figure 26).

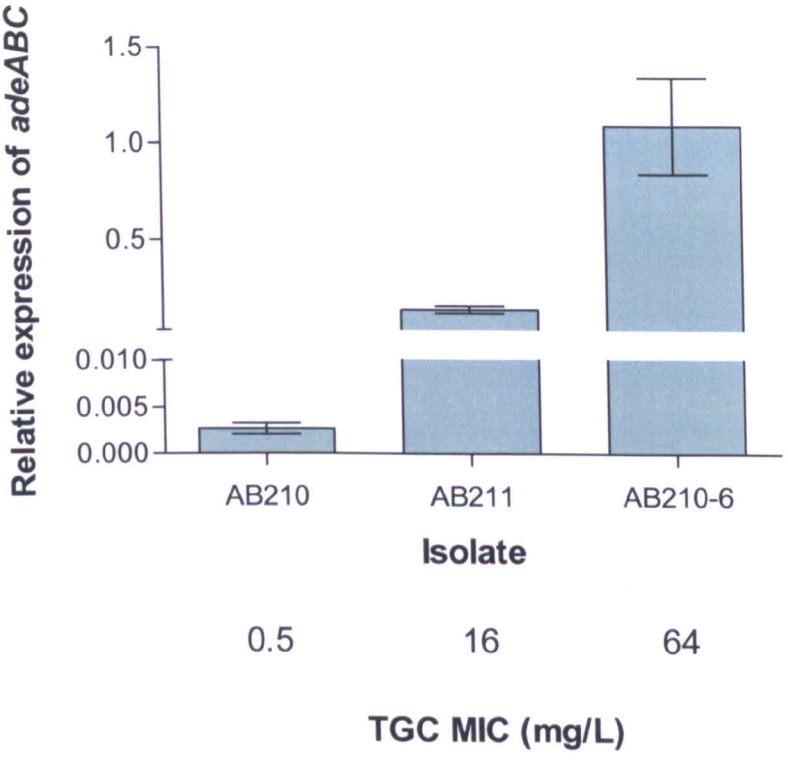

Figure 24. Expression of *adeABC* relative to that of *rpoB* (means ± standard deviations) in the pre- and post-therapy clinical isolates AB210 and AB211, the laboratory-selected mutant AB210-6. Tigecycline (TGC) MICs are shown.

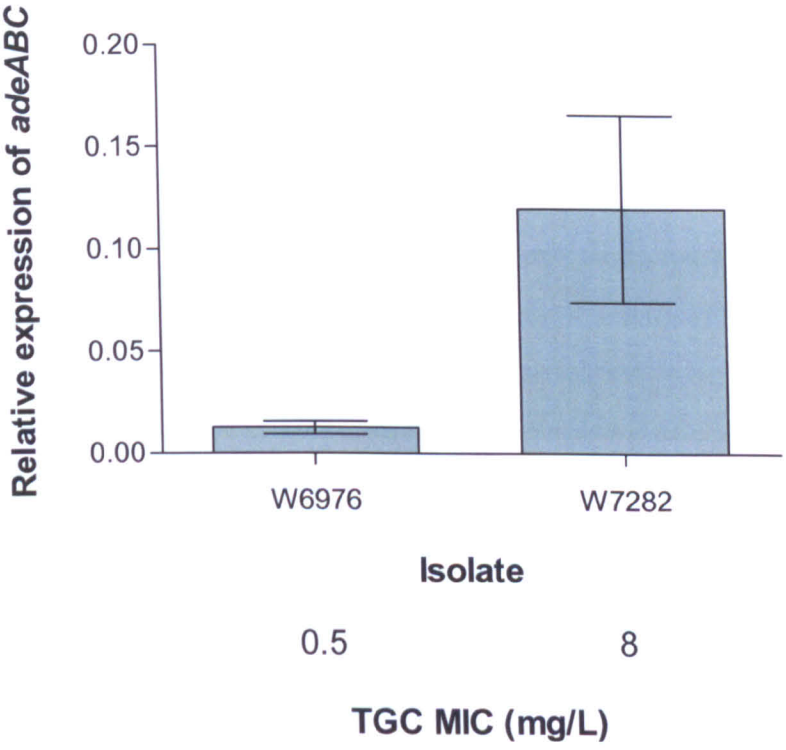

Figure 25. Expression of *adeABC* relative to that of *rpoB* (means ± standard deviations) in the pre- and post-therapy clinical isolates W6976 and W7282. Tigecycline (TGC) MICs are shown.

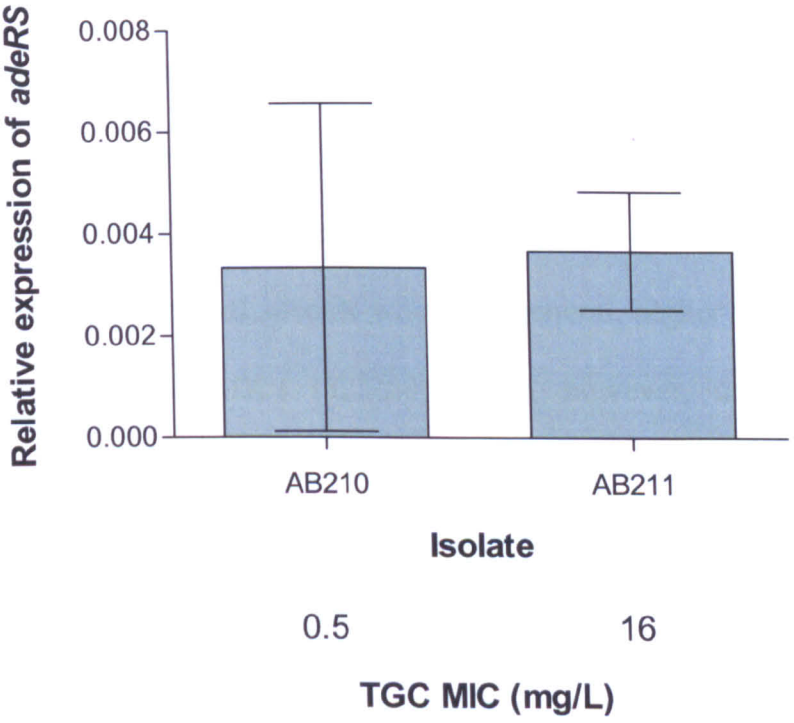

Figure 26. Expression of *adeRS* relative to that of *rpoB* (means ± standard deviations) in the pre- and post-therapy clinical isolates AB210 and AB211. Tigecycline (TGC) MICs are shown.

3.1.4. Effect of varying concentrations of $MnSO_4$ on *adeABC* expression and tigecycline MICs in the clinical isolates AB210 and AB211

Manganese levels in Mueller-Hinton (MH) agar produced by different manufacturers can vary dramatically (82). This variation is known to affect tigecycline MICs for *A. baumannii* and other bacterial species where, in general, higher levels of manganese correlate with increased MICs (82;250). It is, however, unclear exactly how manganese influences tigecycline activity *in vitro*. To investigate the effects of manganese concentration on *adeABC* expression, clinical isolates AB210 and AB211 were grown in Iso-Sensitest broth supplemented with varying concentrations of $MnSO_4$. Addition of 1 mg/ml $MnSO_4$ resulted in elevated (four-fold) tigecycline MICs and increased expression (two-fold) of *adeABC* in both clinical isolates. However, further increases in supplemental $MnSO_4$ (to a final concentration of 2 mg/ml; approximately 0.72 mg/ml free Mn^{2+}) did not result in further increases in MIC or *adeABC* expression in isolate AB210, and led to reduced expression of *adeABC* in isolate AB211 without a concurrent reduction in tigecycline MIC (Figure 27).

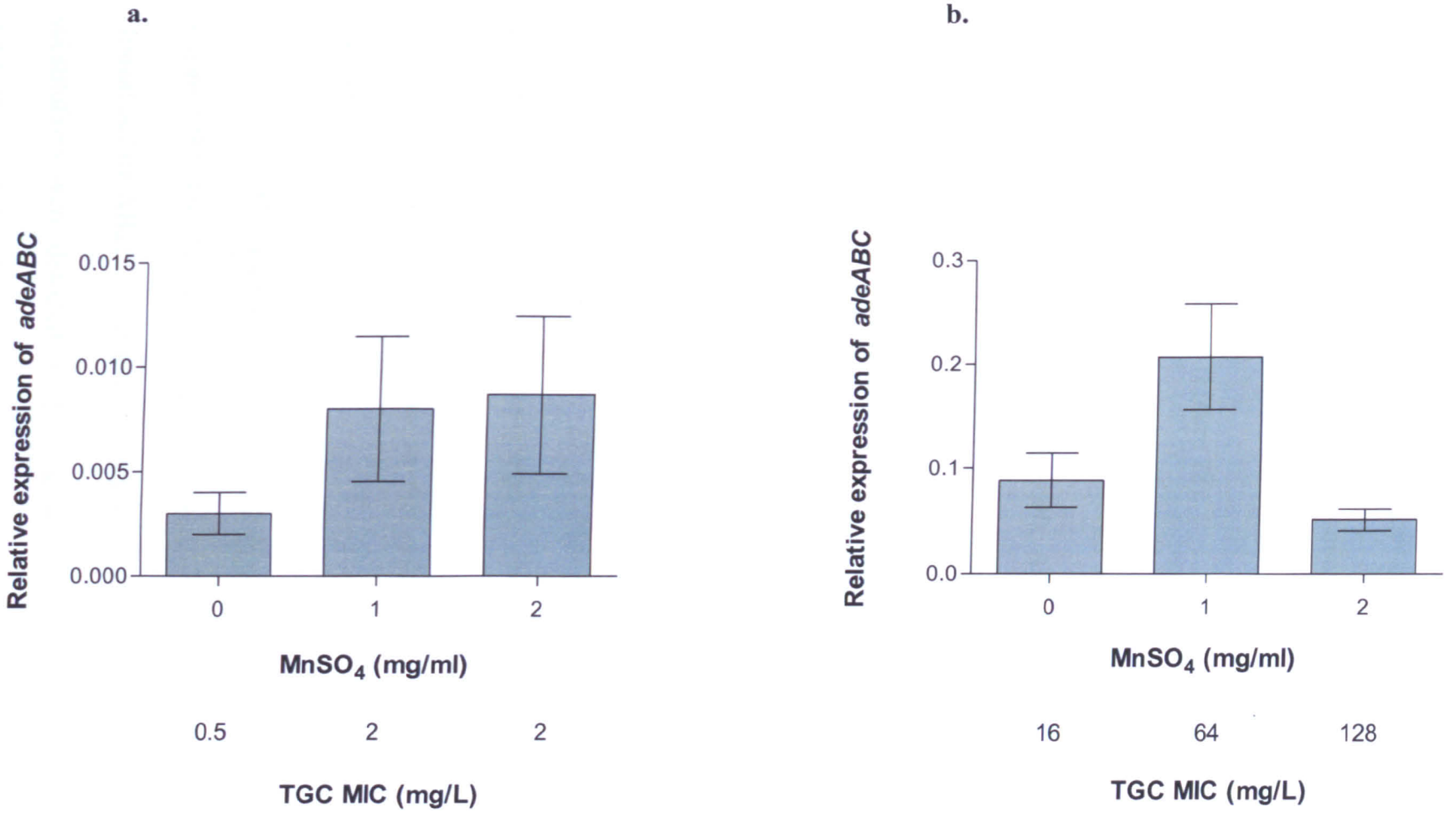

Figure 27. Expression of *adeABC* relative to that of *rpoB* (means ± standard deviations) and tigecycline MICs in the presence of varying concentrations of $MnSO_4$: (a) pre-therapy clinical isolate AB210; (b) post-therapy clinical isolate AB211.

3.1.5. Nucleotide sequencing of the *adeRS* operon

Nucleotide sequence analysis of the regulatory operon *adeRS* in three representatives each of the SE clone and OXA-23 clone 1 revealed a difference at amino acid 62 of the sensor histidine kinase, AdeS, with methionine at this position in OXA-23 clone 1 and isoleucine in the SE clone (Figure 28).

Isoleucine is present at this position in all AdeS sequences available in GenBank (accession numbers: ADM92606; ADM92604; ABX83930; ABX83928; ABX83924; ABX83922; ABX83920; ADP20500; ADP20498; ADP20496; ADP20494; ADP20492; ADP20490; ADP20488; ADP20486; ADP20484; ADP20482; ADP20480; ADP20478; ADP20476; ADP20474; ADP20472; ADP20470; ADP20468; ACM50741; ABQ57261; ABQ57260; ABQ57259; ABQ57258; CAJ77841; ABX83926; ACJ41457; AAR14190; YP_002319440; ACJ57418; YP_002325608; ABO12181; ZP_05827208; EEX04826; ZP_04661879; ZP_07240373; ZP_07235152; ZP_07225668; ZP_06797232; ZP_06781464; AAL14443; CAM86703; YP_001713700).

There were no differences in the amino acid sequences of the response regulator, AdeR.

The *adeRS* operon was also sequenced in both clinical pairs and the mutant AB210-6. An Ala-94→Val substitution in AdeS was found in the resistant clinical isolate AB211 compared with its parent AB210 (Figure 28). Two amino acid substitutions were detected in the laboratory mutant AB210-6: Gly-103→Asp in AdeS (Figure 16) and Ala-91→Val in AdeR (Figure 29). It is notable that the G→A mutation responsible for the latter change was located immediately up-stream of the putative −10 promoter sequence of the *adeABC* operon, located within the *adeR*

coding region (164). A single substitution in AdeS, Ser-8→Arg, was detected in W7282 compared with W6976 though no differences were detected in the response regulator, AdeR.

Figure 28. Amino acid sequence alignment of the sensor histidine kinase, AdeS in AB210, AB211, AB210-6 (OXA-23 clone 1) and all SE clone isolates (n=3). Transmembrane helical regions are underlined. The conserved histidine residue that is the site of autophosphorylation is shown emboldened in red.

```
                  *         20          *         40          *         60
AB210    : MFDHSFSFDCQDKVILVVEDDYDIGDIIENYLKREGMSVIRAMNGKQAIELHASQPIDLI
AB210-6  : ............................................................

                  *         80          *        100          *        120
AB210    : LLDIKLPELNGWEVLNKIRQKAQTPVIMLTALDQDIDKVMALRIGADDFVVKPFNPNEVI
AB210-6  : ............................V...........................

                  *        140          *        160          *        180
AB210    : ARVQAVLRRTQFANKVTNKNKLYKNIEIDTDTHSVYIHSENKKILLNLTLTEYKIISFMI
AB210-6  : ............................................................

                  *        200          *        220          *        240
AB210    : DQPHKVFTRGELMNHCMNDSDALERTVDSHVSKLRKKLEEQGIFQMLINVRGVGYRLDNP
AB210-6  : ............................................................


AB210    : LAVKDDA
AB210-6  : .......
```

Figure 29. Amino acid sequence alignment of the response regulator, AdeR in AB210 and AB210-6. The conserved aspartic acid residue (phosphorylation site) is shown emboldened in red.

3.1.6. Interruption of genes in *A. baumannii*

A. baumannii genes were disrupted by the targeted integration via homologous recombination of suicide plasmids containing internal fragments of the target genes (Materials and Methods section 2.19.3). Previous studies employed suicide vectors containing the pUC origin of replication to inactivate genes in this species (160;164;223). An overview of the strategy used here is shown in Figure 30.

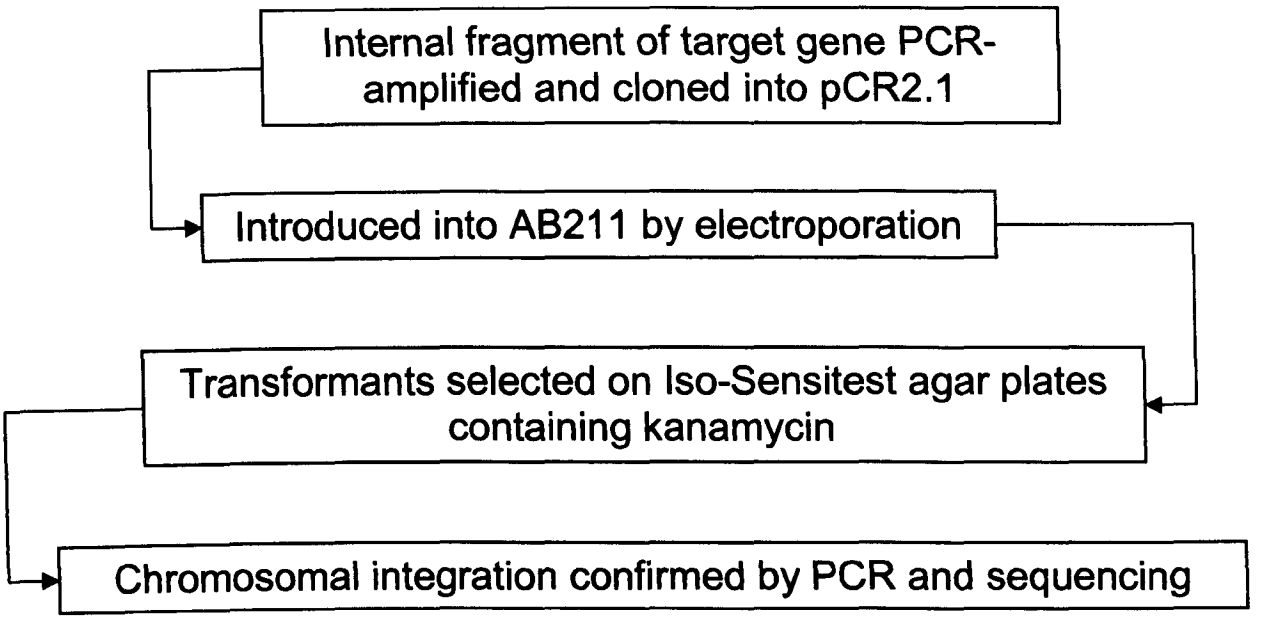

Figure 30. Overview of strategy used to interrupt genes in the clinical isolate AB211.

3.1.6.1. *adeB*

The RND efflux pump gene *adeB* was targeted for inactivation in the post-therapy clinical isolate, AB211 using suicide plasmid, pBK-5 (Figure 13), to assess fully the role of the AdeABC efflux system in the emergence of tigecycline resistance. Aminoglycoside susceptibility in AB211 (kanamycin MIC, 4 mg/L) - most likely due to the loss of *armA* - allowed the kanamycin resistance cassette encoded by pBK-5 to be used as the selectable marker. The integration of pBK-5 into the chromosome was confirmed by PCR followed by sequencing across the site of insertion (Figure 31).

a.

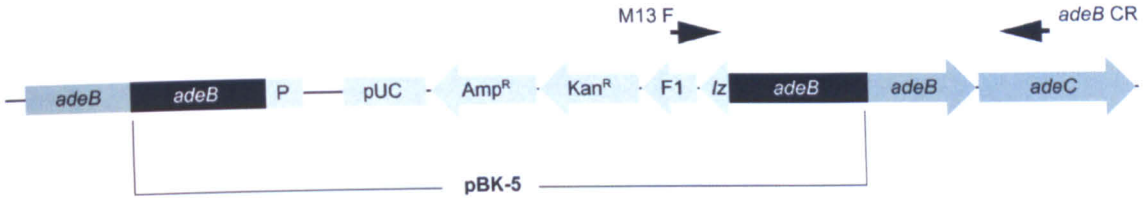

b.

1 2

Figure 31. Confirmation of the chromosomal insertion of pBK-5: (a) schematic of pBK-5 insertion displaying the primers used to perform PCR across the insertion site; (b) agarose gel electrophoresis displaying a 1-Kb DNA ladder in lane 1 and the 3040-bp PCR product in lane 2.

Interruption of *adeB* in the resistant clinical isolate, AB211 with plasmid pBK-5 restored full susceptibility to tigecycline (MIC, 0.5 mg/L; Table 12 and Figure 32). The PFGE profiles of AB211 and AB211Δ*adeB* were consistent (Figure 33).

Figure 32. Tigecycline Etest performed on clinical isolate AB211 and mutant AB211Δ*adeB*.

AB211Δ*adeB*
AB211

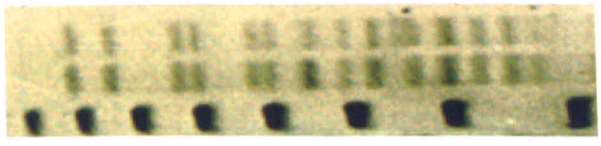

Figure 33. PFGE profiles of *A. baumannii* clinical isolate AB211 and derivative AB211Δ*adeB*.

Table 12. Antibiotic susceptibilities of AB211Δ*adeB*

Isolate	MIC (mg/L)															
	AMP	AUG	AZT	CAR	CLAV	CLOX	CLAX	CTX	CTXC	CAZ	CAZC	CPR	CPRC	FOX	PIP	PTZ
AB211Δ*adeB*	>64	>64	64	>512	>4	>100	256	>256	>32	128	>32	>64	>32	>64	>64	>64
AB211	>64	>64	64	>512	>4	>100	256	>256	>32	64	>32	>64	>32	>64	>64	>64

AMP, ampicillin; AUG, co-amoxiclav; AZT, aztreonam; CAR, carbenicillin; CLAV, clavulanic acid; CLOX, cloxacillin; CLAX, cloxacillin plus cefotaxime; CTX, cefotaxime; CTXC, cefotaxime plus clavulanic acid; CAZ, ceftazidime; CAZC, ceftazidime plus clavulanic acid; CPR, cefpirome, CPRC, cefpirome plus clavulanic acid, FOX, cefoxitin, PIP, piperacillin; PTZ, piperacillin plus tazobactam.

Table 12. Antibiotic susceptibilities of AB211Δ*adeB* cont.

Isolate	MIC (mg/L)														
	EDTA	IME	IM	MEM	ERP	CIP	TOB	AMK	GEN	TET	MIN	TGC	SUB	COL	CHL
AB211Δ*adeB*	>320	>16	>32	>32	>16	>8.0	2	4	8	NT	8	0.5	>32	≤0.5	NT
AB211	>320	>16	>32	>32	>16	>8.0	2	4	8	NT	16	16	32	≤0.5	NT

EDTA, ethylenediaminetetraacetic acid; IME, imipenem plus EDTA; IPM, imipenem; MEM, meropenem; ETP, ertapenem; CIP, ciprofloxacin; TOB, tobramycin; AMK, amikacin; GEN, gentamicin, TET, tetracycline; MIN, minocycline; TGC, tigecycline; SUB, sulbactam; COL, colistin; CHL, chloramphenicol.

3.1.6.2. *adeS*

The regulation of *adeABC* was investigated in clinical isolate AB211 by the targeted disruption of the sensor histidine kinase gene, *adeS* with the suicide plasmids pSK-1 (Figure 14a) and pSK-2 (Figure 14b). These plasmids were introduced separately into electrocompetent AB211 cells. As with the pBK-5 insertion described above, chromosomal integration of pSK-1 and pSK-2 was confirmed by PCR, followed by sequencing across the site of insertion (Figure 34).

a.

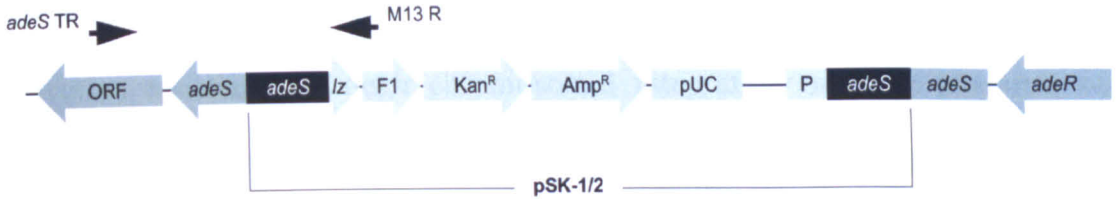

b.

1 2

c.

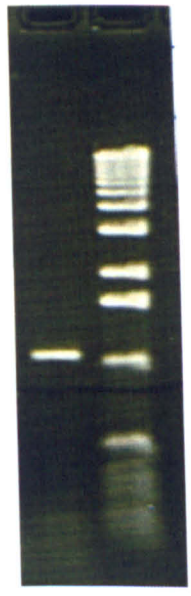

1 2

Figure 34. Confirmation of the chromosomal insertion of pSK-1 and pSK-2: (a) schematic of pSK-1/2 insertion displaying the primers used to perform PCR across the insertion site; (b) agarose gel electrophoresis displaying a 1-Kb DNA ladder in lane 1 and the 1292-bp PCR product in lane 2 (pSK-1); (c) agarose gel electrophoresis displaying a 1-Kb DNA ladder in lane 2 and the 1118-bp PCR product in lane 1 (pSK-2).

Surprisingly, inactivation of *adeS* in the tigecycline-resistant isolate, AB211 with either pSK-1 or pSK-2 did not affect tigecycline MICs. Previous work has suggested that this gene is essential for the expression of *adeABC* (164) and hence tigecycline resistance. Though chromosomal integration of these plasmids within *adeS* was confirmed by PCR and sequencing, it was still possible to PCR-amplify the entire, intact *adeRS* operon from both derivatives. Single colonies were positive both for plasmid integration and intact *adeS*, making interpretation of the phenotypic observations difficult. The reasons for this are unclear. It may be that the chromosomal insertions were unstable. Since the organisms were maintained under selective pressure, this would imply that such cells retained the plasmid extra-chromosomally.

Unsuccessful attempts were made to generate a more stable *adeS* insertion derivative where only the selectable marker gene was integrated, a process that required a double homologous recombination event. Initially, theses attempts were made using the phage λ Red recombination system encoded by pKOBEG, which was used successfully to inactivate *acrB* in the *E. cloacae* clinical isolate TGC-R (section 3.2.5.1). For this purpose, attempts were made to clone the phage λ Red genes into the *E. coli* / *A. baumannii* shuttle vector pAT-RA (63). However, the insertion proved problematic and after efforts to optimise the cloning experiments failed, the strategy was abandoned.

Secondly, attempts were made to construct suicide plasmids using the pUC19 cloning vector containing a kanamycin resistance cassette flanked by regions complementary to *adeS* and the negative selectable marker gene, *ccd*B, which encodes a toxin that interferes with DNA gyrase activity, leading to cell death (26). Cloning of the *ccd*B gene failed despite using a CcdB-resistant commercial strain of

E. coli. Attempts to clone a second selectable marker gene, *sacB* from *Bacillus subtilis* were successful. The *sacB* gene encodes levansucrase, a fructosyltransferase that utilises sucrose to catalyse the synthesis of levan (a fructose polymer) and is involved in sucrose metabolism in *B. subtilis*, but which is lethal to *E. coli* in the presence of 5% sucrose (93). This was considered to be a better negative marker candidate since, unlike *ccd*B, the *sacB* gene product is not lethal unless the growth medium is supplemented with sucrose. Initial investigations demonstrated that the *sacB* gene was fit for purpose as it was lethal to clinical isolate, AB211 only in the presence of 5% sucrose. Unfortunately, time constraints meant that this strategy could not be developed further.

3.2. *E. cloacae*

The HPA's ARMRL has been receiving isolates of *E. cloacae* displaying reduced susceptibility and resistance (MICs $\geq$ 2 mg/L) to tigecycline since 2005. Again, these included instances where resistance emerged during therapy and / or where pairs of clonally related isolates displayed a susceptible / resistant phenotype. Two such cases are described below. The molecular basis of tigecycline resistance was investigated using these clinical pairs and laboratory-selected mutants.

3.2.1. Clinical case reports

3.2.1.1. Case 3

In 2006, a patient presented to a London hospital with a ten-day history of progressively increasing back pain, high fever (40°C) and swelling over the spine. The patient had undergone two previous operations for stabilisation of a lumbar spinal fracture, 20 months, followed by a revision 16 months, prior to this event. An

aspirate revealed two colony variants of *E. cloacae*, which varied in their antibiotic susceptibility patterns. Both appeared sensitive to ciprofloxacin, and an initial empirical regimen was changed to ciprofloxacin (400 mg every 12 h intravenous) on day four after admission. A definitive surgical procedure was performed three days later and one litre of pus and all the metalwork (eight screws and plates) were removed. The same organisms were isolated again but they now showed changes in antibiotic resistance patterns, with one variant now resistant to ciprofloxacin (designated TGC-R) and the other remaining susceptible (designated TGC-S). This pair of isolates was referred to the HPA's ARMRL, where the ciprofloxacin-resistant isolate was found also to be resistant also to tigecycline. Ciprofloxacin was subsequently replaced with meropenem after eight days and the patient slowly recovered after several months of carbapenem therapy. The original source of the infection was not established.

3.2.1.2. Case 4

A patient presented to a hospital in North-West England in 2009 with a three-day history of upper abdominal pain. Acute cholecystitis was diagnosed and was managed with intravenous piperacillin / tazobactam. The patient was admitted for an elective laparoscopy 16 days after initial presentation following an ultrasound, which revealed dilatation of the biliary tree and a gallstone impacted at the neck of the gall bladder. At laparoscopy, a pneumoperitoneum was seen and the surgery was modified to an open cholecystectomy. This was complicated by malrotation of the gut but drains were placed and the patient made a good post-operative recovery. However, two days after surgery the patient became septic and complained of abdominal pain and so underwent a laparotomy where a bowel leak was discovered. An endoscopic

retrograde cholangiopancreatography was performed the next day with large sphincterotomy. Spiking pyrexia led to the piperacillin / tazobactam therapy being restarted but as the organism cultured from drain fluid was resistant, and the patient was switched to ciprofloxacin and metronidazole. On day 10 post-surgery the patient developed severe *Clostridium difficile* infection and was commenced on oral vancomycin. Despite this management they continued to have spiking pyrexia and a CT scan revealed a large psoas collection which was drained percutaneously. Further collections could not be drained and the patient was transferred to another hospital 33 days after admission for CT-guided drainage. This took place two days later and two variants of *E. cloacae* (designated EC390 and EC391) were isolated from drain fluid. Tigecycline therapy was started the next day, but was discontinued amid concerns of resistance. The pair of *E. cloacae* isolates was referred to the HPA's ARMRL, where tigecycline resistance was confirmed in one of them (EC391), whereas the other (EC390) was tigecycline-susceptible. The patient then received a combination of teicoplanin and ertapenem and their condition slowly improved until they were eventually discharged nearly four months after initial presentation. The patient subsequently went on to make a good recovery.

3.2.2. Isolate characterisation and antibiotic susceptibilities

All clinical isolates were identified as *E. cloacae* by API20E. MICs of ciprofloxacin and tigecycline were eight-fold higher for the clinical isolate, TGC-R (4 mg/L for both compounds) than for TGC-S (both 0.5 mg/L; Table 13). Although this clinical pair did not have identical PFGE profiles, analysis of the intermediate laboratory-selected mutants derived from TGC-S (Materials and Methods section 2.18) showed an analogous transition from the tigecycline-susceptible to the tigecycline-resistant

profile; moreover, the PFGE profile of the final laboratory-selected mutant TGC-S7 (ciprofloxacin MIC, 4 mg/L; tigecycline MIC, 32 mg/L) was indistinguishable from that of clinical isolate, TGC-R (Figure 35a). MICs of chloramphenicol, minocycline, and tetracycline also were raised for TGC-R and TGC-S7 relative to TGC-S, whereas those of β-lactams were unaffected, although that of cefpirome was high already (8 mg/L), possibly reflecting AmpC-activity, as based on interpretive reading of wider antibiogram data (Table 13). Interestingly, the laboratory mutant, TGC-S7 displayed a four-, eight- and 16-fold reduction in the MICs of ceftazidime, aztreonam and cefotaxime, respectively, when compared with the parent clinical isolate, TGC-S (Table 13). The reasons for these reductions in the MICs are unknown though it is striking that similar reductions were observed for the laboratory-selected *A. baumannii* mutant AB210-6 (section 3.1.2.2.).

Tigecycline and minocycline MICs were increased 16- and eight-fold, respectively, in clinical isolate, EC391 when compared with isolate, EC390 (Table 13). In contrast with the isolates described above, there was only a two-fold increase in the MIC of ciprofloxacin between EC390 and EC391. The PFGE profiles of the two clinical isolates were identical (Figure 35b).

Table 13. Antibiotic susceptibilities of *E. cloacae* isolates and laboratory mutant

Isolate	MIC (mg/L)															
	AMP	AUG	**AZT**	CAR	CLAV	CLOX	**CLAX**	CTX	CTXC	**CAZ**	**CAZC**	CPR	CPRC	FOX	PIP	PTZ
TGC-S	>64	>64	**16**	512	>4	>100	**1**	128	>32	**32**	**>32**	8	16	>64	64	16
TGC-R	>64	64	16	256	>4	>100	**8**	64	>32	16	>32	8	16	>64	64	16
TGC-S7	>64	64	**2**	128	>4	>100	2	8	>32	**8**	**16**	4	8	>64	16	16
EC390	>64	32	**>64**	256	>4	>100	4	32	32	4	2	1	1	64	>64	>64
EC391	>64	32	**32**	128	>4	>100	4	16	16	2	2	2	2	>64	>64	>64

AMP, ampicillin; AUG, co-amoxiclav; AZT, aztreonam; CAR, carbenicillin; CLAV, clavulanic acid; CLOX, cloxacillin; CLAX, cloxacillin plus cefotaxime; CTX, cefotaxime; CTXC, cefotaxime plus clavulanic acid; CAZ, ceftazidime; CAZC, ceftazidime plus clavulanic acid; CPR, cefpirome, CPRC, cefpirome plus clavulanic acid, FOX, cefoxitin, PIP, piperacillin; PTZ, piperacillin plus tazobactam.

Table 13 cont. Antibiotic susceptibilities of *E. cloacae* isolates and laboratory mutant

Isolate	MIC (mg/L)														
	EDTA	IME	IM	MEM	ERP	CIP	TOB	AMK	GEN	**TET**	**MIN**	**TGC**	SUB	COL	**CHL**
TGC-S	>320	0.5	1	0.125	2	0.5	0.5	2	0.5	**2**	**4**	**0.5**	>32	≤0.5	**8**
TGC-R	>320	0.25	0.25	0.125	2	4	0.5	1	0.5	**16**	**>32**	**4**	>32	≤0.5	**64**
TGC-S7	>320	0.5	0.5	0.25	4	4	0.5	1	0.25	32	>32	**32**	>32	≤0.5	>256
EC390	>320	0.125	0.125	≤0.060	0.25	0.5	1	1	0.5	NT	**4**	**0.5**	>32	≤0.5	NT
EC391	>320	0.06	≤0.060	≤0.060	0.25	0.25	0.5	≤0.5	0.25	NT	**32**	**8**	>32	≤0.5	NT

EDTA, ethylenediaminetetraacetic acid; IME, imipenem plus EDTA; IPM, imipenem; MEM, meropenem; ETP, ertapenem; CIP, ciprofloxacin; TOB, tobramycin; AMK, amikacin; GEN, gentamicin, TET, tetracycline; MIN, minocycline; TGC, tigecycline; SUB, sulbactam; COL, colistin; CHL, chloramphenicol.

a.

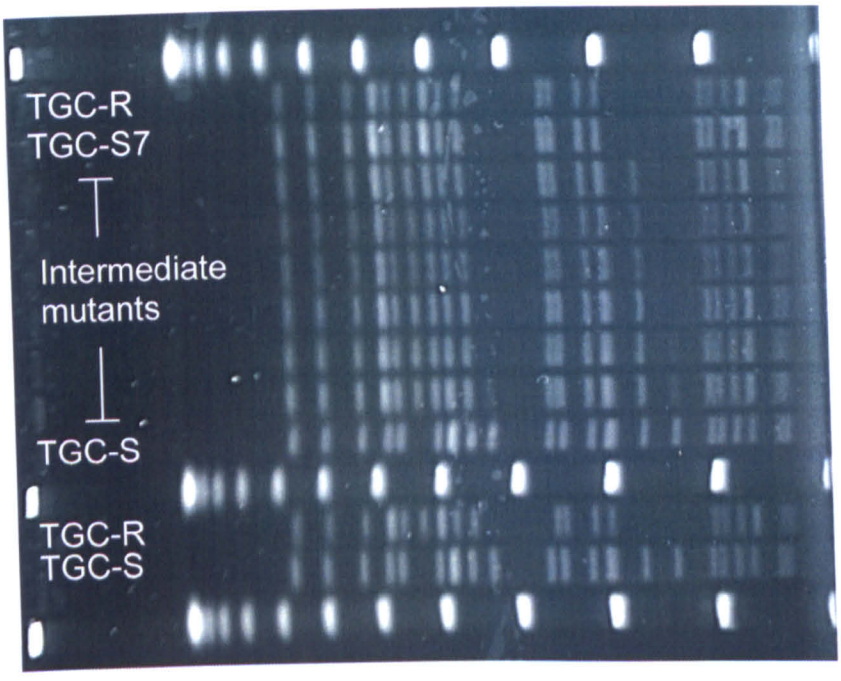

b.

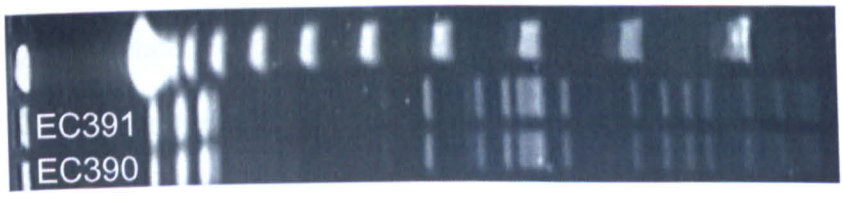

Figure 35. PFGE profiles of *E. cloacae* clinical isolates and mutants: (a) TGC-S, TGC-R and all laboratory-selected mutants; (b) EC390 and EC391.

3.2.3. Analysis of expression of the efflux pump-encoding operon *acrAB* and the global regulatory gene *ramA* in clinical isolates and a laboratory mutant using real-time RT-PCR

To date, tigecycline resistance in *E. cloacae* has been associated with up-regulation of the RND efflux system AcrAB and the global regulator, RamA (127). Expression of *acrAB* and *ramA* was analysed by real-time RT-PCR (Materials and Methods sections 2.15 and 2.20.1).

Relative to the tigecycline-susceptible isolate, TGC-S, expression of *acrAB* and *ramA* was increased four- and 276-fold, respectively, in isolate TGC-R and nine- and 407-fold, respectively, in the laboratory mutant, TGC-S7 (Figures 36 and 37). Expression of *acrAB* was increased five-fold in the post-therapy clinical isolate EC391 when compared with its pre-therapy parent, EC390 (Figure 38). Expression of *ramA* in isolates EC390 and EC391 was not investigated.

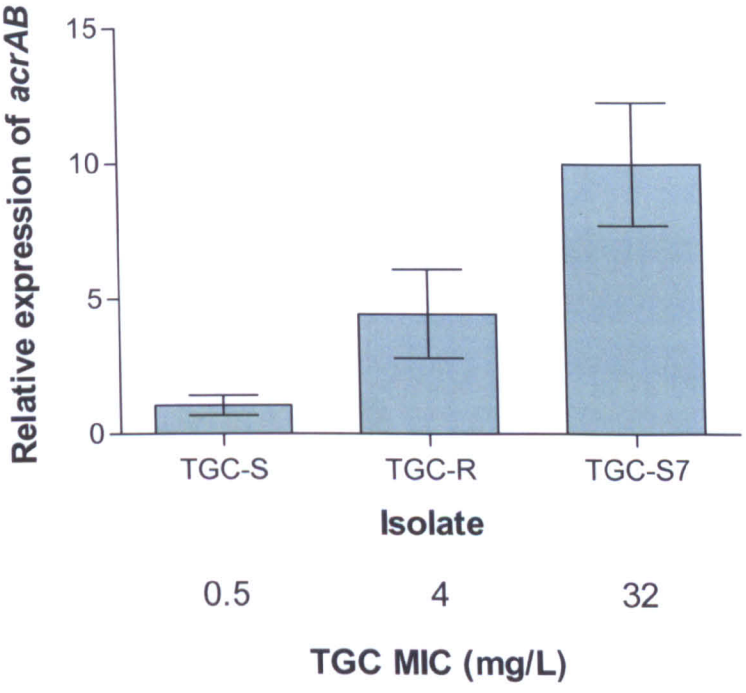

Figure 36. Expression of *acrAB* relative to that of *rpoB* (means ± standard deviations) in the clinical isolates TGC-S and TGC-R, the laboratory mutant TGC-S7. Tigecycline (TGC) MICs are shown.

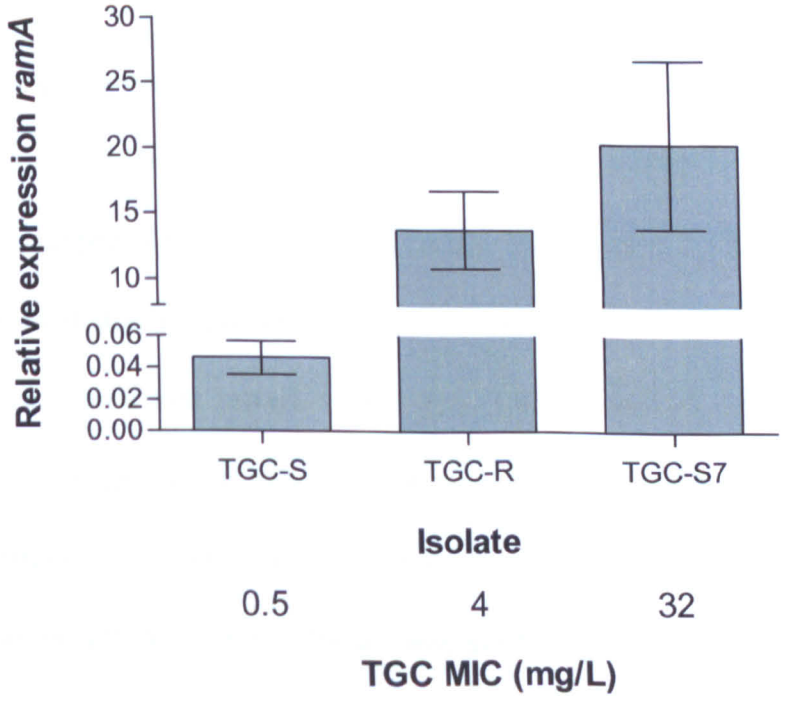

Figure 37. Expression of *ramA* relative to that of *rpoB* (means ± standard deviations) in the clinical isolates TGC-S and TGC-R, the laboratory mutant TGC-S7. Tigecycline (TGC) MICs are shown.

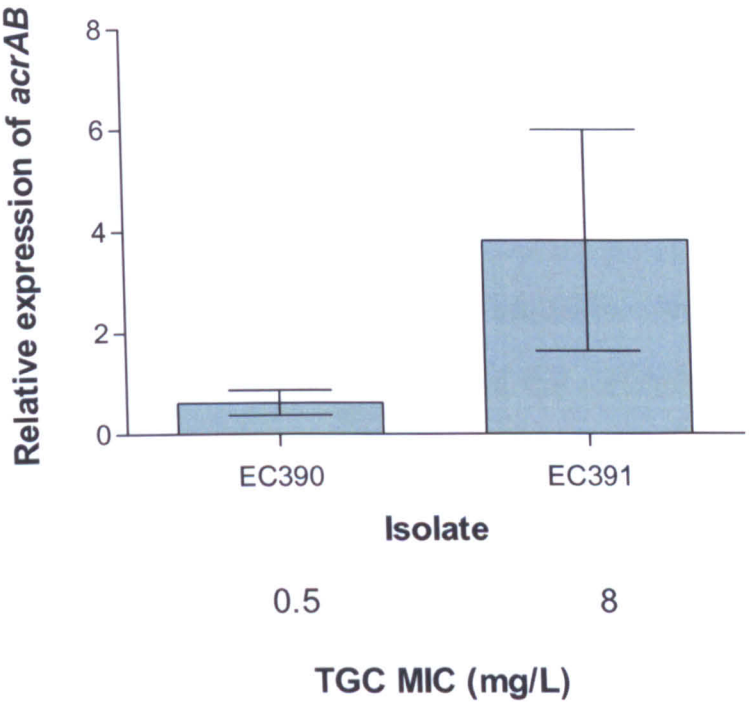

Figure 38. Expression of *acrAB* relative to that of *rpoB* (means ± standard deviations) in the clinical isolates EC390 and EC391. Tigecycline (TGC) MICs are shown.

3.2.4. Overexpression of *ramA* in the clinical isolate TGC-S

Keeney *et al.* previously demonstrated an association between elevated tigecycline MICs and overexpression of *acrAB* and *ramA* in *E. cloacae*. However, no previous experimental evidence has placed *acrAB* definitively in the RamA regulon (127).

To investigate this aspect, *ramA* from isolate TGC-R was overexpressed in isolate TGC-S using the pBAD expression vector (Materials and Methods section 2.20.3). In order to achieve this, the gene first had to be PCR-amplified from *E. cloacae* genomic DNA. Primer design was problematic owing to the fact that there were no publicly-available genome sequence data for this species at the time although, more recently, the complete genome of the *E. cloacae* type strain ATCC 13047 has been published (212). Initial attempts to amplify *ramA* using primers

designed on gene sequences from closely-related species (accession numbers: NC_009436; AJ404625; U19581) were unsuccessful. Nevertheless, although no *E. cloacae ramA* nucleotide sequences were available in GenBank, there was a RamA protein sequence (accession number: P55922) and the reverse primer *ramA* CDS R was designed by reverse-translating this protein sequence. Nucleotide sequence data reported by Komatsu *et al.* were used to design the forward primer, Full *ramA* F (Table 9) (133). The *ramA* gene was then cloned into the pBADS derivative, pBADKM (Figure 18b) generating plasmid pBADKM-R (Figure 18c). The addition of the kanamycin resistance gene to pBADS allowed the pBAD-based expression system to be used with clinical isolate TGC-S owing to the isolate's susceptibility to the aminoglycosides. This would otherwise not have been possible because isolate TGC-S was ampicillin-resistant (Table 13).

Induction of *ramA* expression by increasing the L-arabinose concentration resulted in increased *acrAB* expression (Figure 39). When *ramA* was induced with a relatively high (0.2% w/v) concentration of L-arabinose, *acrAB* was expressed at a higher level than in isolate TGC-R, for which the tigecycline MIC was 4 mg/L [relative *acrAB* expression 7.75 (±1.43) vs. 4.43 (±1.63) for TGC-R].

Comparison of the nucleotide sequence of *ramA* (partial coding region) in isolates TGC-S and TGC-R revealed a His-95→Arg substitution in TGC-R (Figure 40), although this was not selected in TGC-S7, and its significance is therefore uncertain.

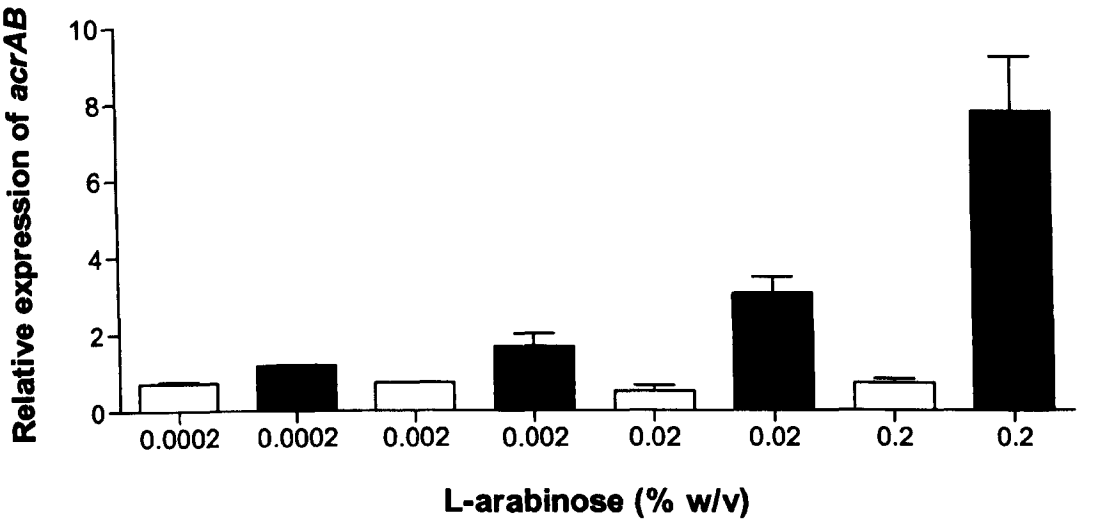

Figure 39. Expression relative to that of *rpoB* (means ± standard deviations) of *acrAB* in TGC-S harbouring either control plasmid, pBADKM (Figure 18b), shown in white or pBADKM-R with cloned *ramA* (Figure 18c) shown in black, in the presence of varying concentrations of L-arabinose.

```
                *         20         *         40         *         60
TGC-S : MTISAQVIDTIVEWIDDNLHQPLRIEEIARHAGYSKWHLQRLFMQYKGESLGRYIRERKL
TGC-R : ............................................................

                *         80         *        100
TGC-S : LMAARDLRESDERVYDICLRYGFDSQQTFTRIFTHTFNQPPGAYRK
TGC-R : ..................................R...........
```

Figure 40. Amino acid sequence alignment of the global regulator, RamA in clinical isolates TGC-S and TGC-R.

3.2.5. Interruption of genes in *E. cloacae*

3.2.5.1. Insertional inactivation of *acrB* in clinical isolate TGC-R

The *acrB* gene in isolate TGC-R was disrupted by insertional inactivation using the helper plasmid pKOBEG (Figure 15) and a linear DNA fragment containing a gentamicin resistance cassette flanked by regions complementary to the target gene (Materials and Methods section 2.20.2.1). An overview of the strategy used is outlined in Figure 41. The susceptibility of TGC-R to the aminoglycosides (Table 13) allowed for the use of gentamicin as the selective agent. The chromosomal insertion of the gentamicin resistance cassette within the *acrB* gene was confirmed by PCR and sequencing across the insertion site (Figure 42).

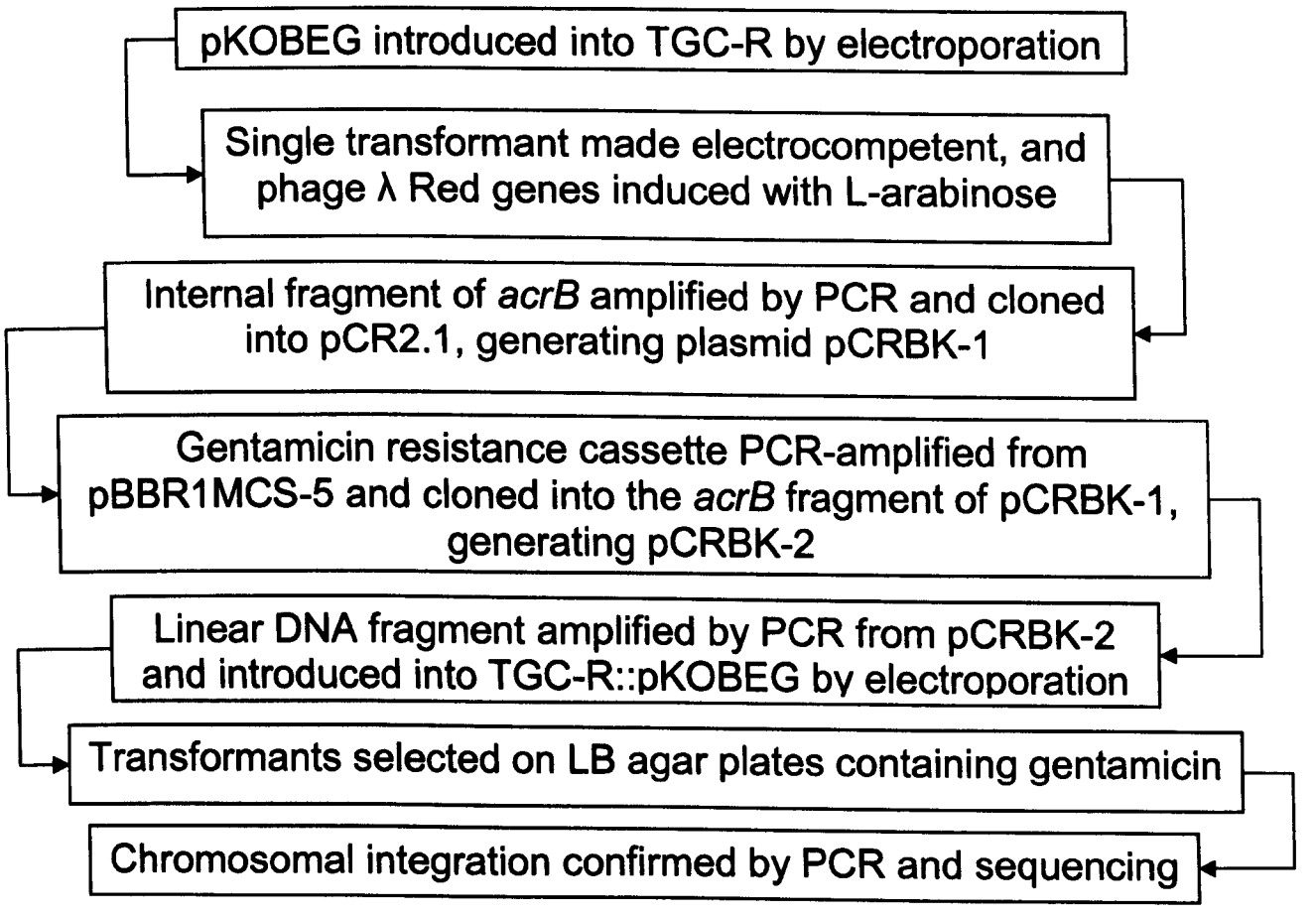

Figure 41. Overview of strategy used to interrupt *acrB* in the clinical isolate TGC-R.

a.

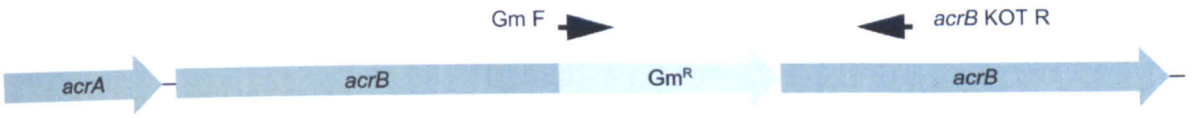

b.

1 2

Figure 42. Confirmation of the chromosomal insertion of the gentamicin resistance cassette from pBBR1MCS-5: (a) schematic of gentamicin cassette insertion displaying the primers used to perform PCR across the insertion site; (b) agarose gel electrophoresis displaying a 1-Kb DNA ladder in lane 1 and the 1405-bp PCR product in lane 2.

Disruption of *acrB* in clinical isolate TGC-R restored full susceptibility to tigecycline (MIC, 0.125; Figure 43 and Table 14), ciprofloxacin, chloramphenicol, and resulted in a large reduction in the MICs of minocycline (≥64-fold) and tetracycline (16-fold) (Table 14). Isolate TGC-R and mutant TGC-RΔ*acrB* had identical PFGE profiles (Figure 44).

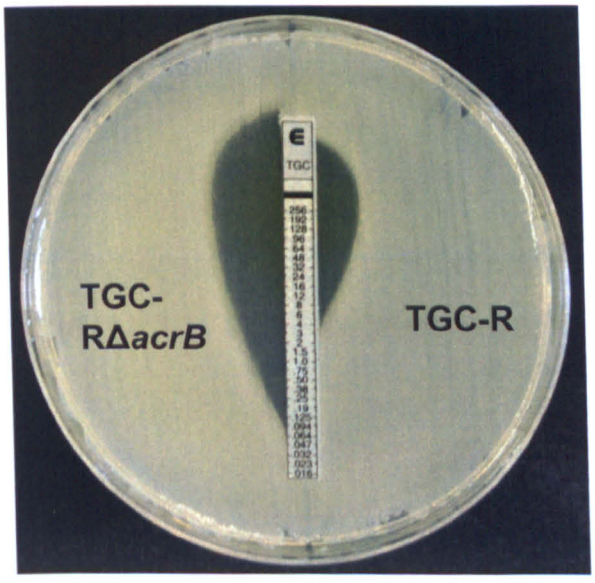

Figure 43. Tigecycline Etest performed on clinical isolate TGC-R and derivative TGC-RΔ*acrB*.

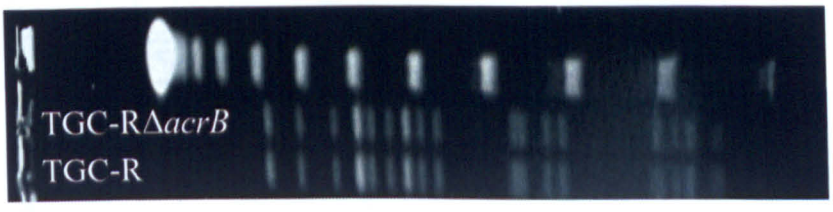

Figure 44. PFGE profiles of *E. cloacae* clinical isolate TGC-R and derivative TGC-RΔ*acrB*.

Table 14. Antibiotic susceptibilities of TGC-RΔ*acrB*

Isolate	MIC (mg/L)															
	AMP	AUG	AZT	CAR	CLAV	**CLOX**	**CLAX**	CTX	CTXC	CAZ	CAZC	CPR	CPRC	FOX	PIP	PTZ
TGC-RΔ*acrB*	>64	64	8	512	>4	**≤100**	**≤0.125**	128	>32	16	>32	8	8	>64	32	16
TGC-R	>64	64	16	256	>4	**>100**	**8**	64	>32	16	>32	8	16	>64	64	16

AMP, ampicillin; AUG, co-amoxiclav; AZT, aztreonam; CAR, carbenicillin; CLAV, clavulanic acid; CLOX, cloxacillin; CLAX, cloxacillin plus cefotaxime; CTX, cefotaxime; CTXC, cefotaxime plus clavulanic acid; CAZ, ceftazidime; CAZC, ceftazidime plus clavulanic acid; CPR, cefpirome, CPRC, cefpirome plus clavulanic acid, FOX, cefoxitin, PIP, piperacillin; PTZ, piperacillin plus tazobactam.

Table 14. Antibiotic susceptibilities of TGC-RΔ*acrB* cont.

Isolate	MIC (mg/L)														
	EDTA	**IME**	IM	MEM	ERP	**CIP**	TOB	AMK	**GEN**	**TET**	**MIN**	**TGC**	SUB	COL	**CHL**
TGC-RΔ*acrB*	>320	**1**	0.5	0.125	4	**0.25**	0.5	1	**4**	**1**	**1**	**0.125**	>32	1	**4**
TGC-R	>320	**0.25**	0.25	0.125	2	**4**	0.5	1	**0.5**	**16**	**>32**	**4**	>32	≤0.5	**64**

EDTA, ethylenediaminetetraacetic acid; IME, imipenem plus EDTA; IPM, imipenem; MEM, meropenem; ETP, ertapenem; CIP, ciprofloxacin; TOB, tobramycin; AMK, amikacin; GEN, gentamicin, TET, tetracycline; MIN, minocycline; TGC, tigecycline; SUB, sulbactam; COL, colistin; CHL, chloramphenicol

3.2.5.2. Insertional inactivation of *acrB* in clinical isolate EC391

To confirm the role of AcrAB in tigecycline resistance in EC391, the *acrB* gene was inactivated by the targeted insertion of suicide plasmid, pRSACRB (Figure 17; Materials and Methods section 2.20.2.2). Although the phage λ Red functions encoded by pKOBEG were employed successfully to inactivate *acrB* in clinical isolate TGC-R (section 3.2.5.1), a different approach was taken with isolate EC391. This was because the pKOBEG system proved somewhat cumbersome and inefficient.

A suicide plasmid system based upon the R6Kγ origin of replication (*ori*) was considered a better alternative (section 3.3.4) (132). Figure 45 shows an overview of the strategy used. Isolate EC391 remained susceptible to the aminoglycosides (Table 13) which allowed for the use of kanamycin as the selective agent. Chromosomal integration of pRSACRB was confirmed by PCR and sequencing across the insertion site (Figure 46).

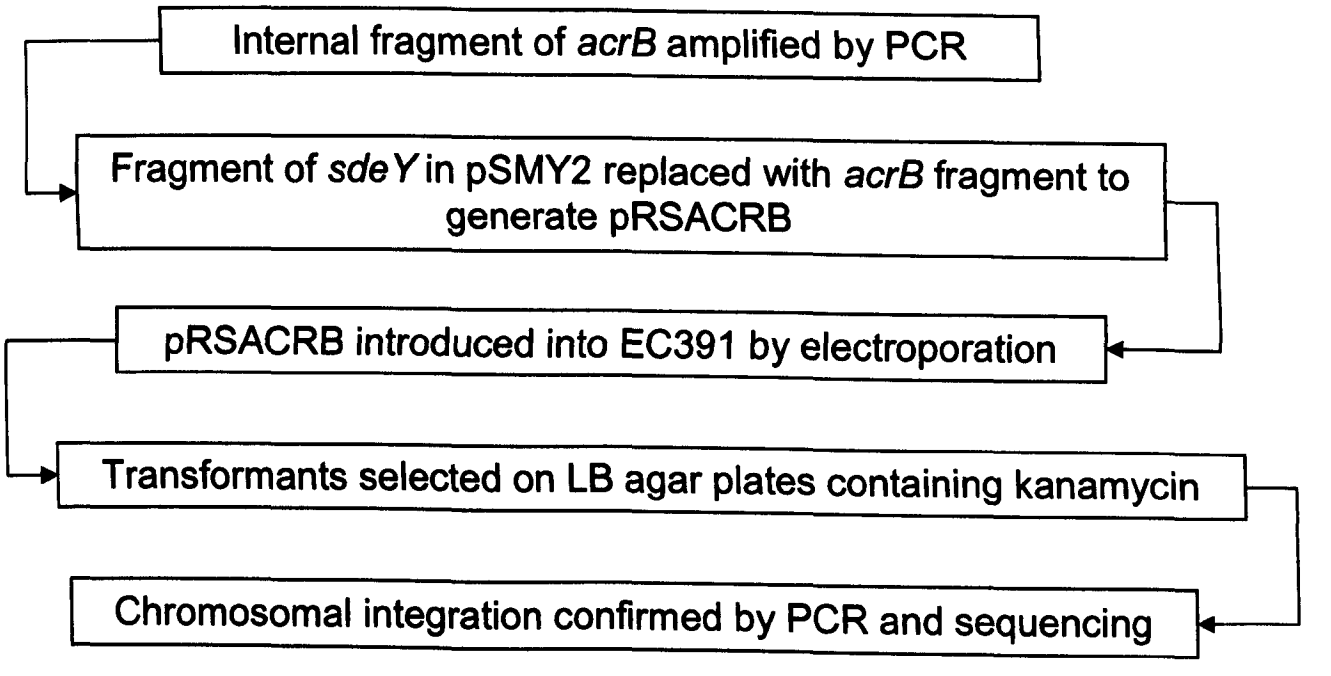

Figure 45. Overview of strategy used to interrupt *acrB* in clinical isolate, EC391.

a.

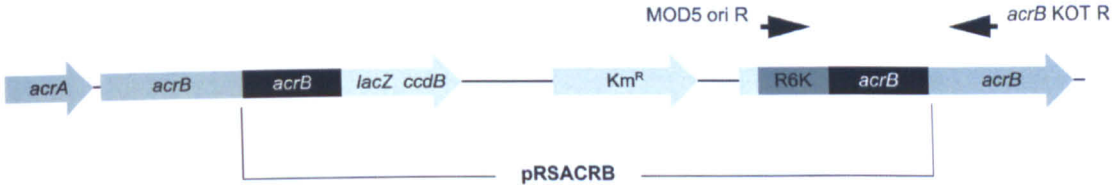

b.

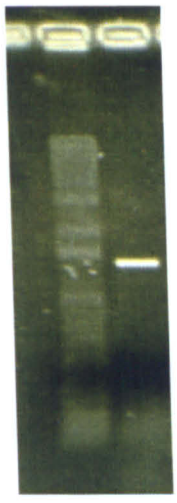

Figure 46. Confirmation of the chromosomal insertion of suicide plasmid, pRSACRB: (a) schematic of gentamicin cassette insertion displaying the primers used to perform PCR across the insertion site; (b) agarose gel electrophoresis displaying a 1-Kb DNA ladder in lane 1 and the 1540-bp PCR product in lane 2.

Disruption of *acrB* in clinical isolate, EC391 restored full susceptibility to tigecycline (MIC, 0.125; Figure 47). The PFGE profiles of EC391 and EC391Δ*acrB* were consistent (Figure 48).

Figure 47. Tigecycline Etest performed on clinical isolate EC391 and derivative EC391Δ*acrB*.

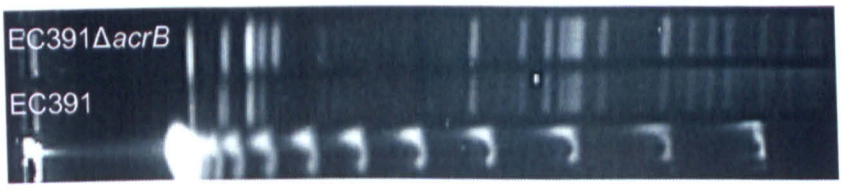

Figure 48. PFGE profiles of *E. cloacae* clinical isolate EC391 and derivative EC391Δ*acrB*.

3.3. *S. marcescens*

There were no tigecycline-resistant clinical isolates of *S. marcescens* available in ARMRL's collection until the isolate described in case 5 (section 3.3.1.1) was referred in 2009. Since the mechanisms of tigecycline resistance in this species were unknown, the molecular basis of such resistance was investigated using the clinical isolate described below and laboratory-selected mutants.

3.3.1. Clinical case reports

3.3.1.1. Case 5

Clinical isolate SM346 was recovered from the urine of a patient hospitalised for assessment in North-East England in 2009. They received no antimicrobial therapy while in hospital.

3.3.2. Isolate characterisation and antibiotic susceptibilities

Isolate SM346 was identified as *S. marcescens* by API20E; MICs were 16 mg/L of tigecycline and 64 mg/L of tetracycline, compared with 0.25 mg/L and 16 mg/L for the type strain, NCTC 10211. Tigecycline resistance could be selected by serial passage of the latter strain (Materials and Methods section 2.18), and MICs of tigecycline and tetracycline for an intermediate mutant, 10211-6, and the ultimate mutant, 10211-10, were 8 and 64, and 256 and >256 mg/L, respectively. Mutant 10211-10 also showed 16-fold increases in the MICs of ciprofloxacin (0.25 mg/L to 4 mg/L) and cefpirome (0.5 mg/L to 8 mg/L). Similarly, a mutant selected from *S. marcescens* NCTC 10211 during exposure to tetracycline (10211-TC7) showed a 16-fold increase in tigecycline MIC when compared with the parent strain, though no increases in the MICs of ciprofloxacin or cefpirome were observed (Table 15). The

type strain 10211 and its laboratory mutant 10211-10 had identical PFGE profiles (Figure 49).

a.

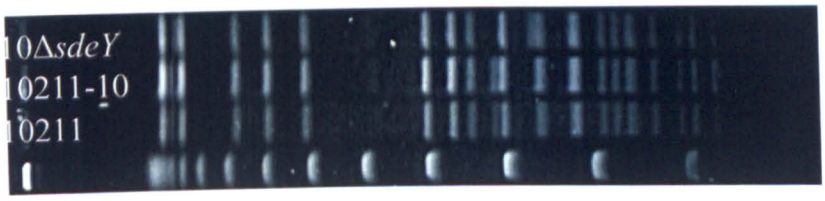

b.

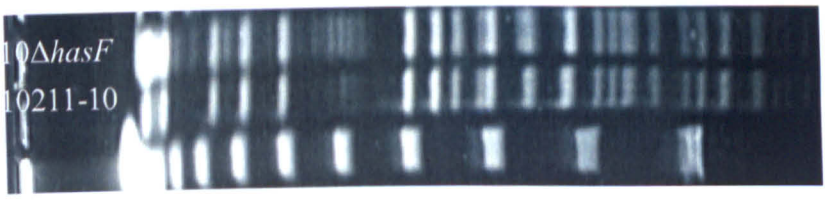

Figure 49. PFGE profiles of the *S. marcescens* type strain and derivatives: (a) NCTC 10211, the laboratory-selected mutant 10211-10 and derivative 10211-10Δ*sdeY*; (b) 10211-10 and derivative 10211-10Δ*hasF*.

Table 15. Antibiotic susceptibilities of *S. marcescens* isolates and laboratory mutants

Isolate	MIC (mg/L)															
	AMP	AUG	AZT	CAR	CLAV	CLOX	**CLAX**	CTX	**CTXC**	**CAZ**	**CAZC**	**CPR**	**CPRC**	FOX	**PIP**	**PTZ**
SM346	>64	64	4	128	>4	>100	16	32	32	4	2	2	2	>64	32	32
NCTC 10211	>64	>64	4	512	>4	>100	**1**	8	**32**	**0.5**	**4**	**0.5**	**1**	>64	**64**	**32**
10211-6	>64	64	1	128	>4	>100	1	4	**8**	**2**	**1**	1	2	>64	**8**	**4**
10211-10	>64	64	1	256	>4	>100	**4**	4	16	**4**	4	**8**	**4**	>64	**16**	**16**
10211-TC7	>64	>64	0.5	128	>4	>100	1	4	16	1	2	0.5	1	>64	**16**	**8**

AMP, ampicillin; AUG, co-amoxiclav; AZT, aztreonam; CAR, carbenicillin; CLAV, clavulanic acid; CLOX, cloxacillin; CLAX, cloxacillin plus cefotaxime; CTX, cefotaxime; CTXC, cefotaxime plus clavulanic acid; CAZ, ceftazidime; CAZC, ceftazidime plus clavulanic acid; CPR, cefpirome, CPRC, cefpirome plus clavulanic acid, FOX, cefoxitin, PIP, piperacillin; PTZ, piperacillin plus tazobactam.

Table 15 cont. Antibiotic susceptibilities of *S. marcescens* isolates and laboratory mutants

Isolate	MIC (mg/L)														
	EDTA	IME	IM	MEM	ERP	**CIP**	**TOB**	AMK	**GEN**	**TET**	**MIN**	TGC	SUB	COL	CHL
SM346	>320	0.5	1	≤0.060	1	>8.0	>32	2	>32	64	>32	**16**	>32	>32	NT
NCTC 10211	>320	1	2	0.125	0.25	**0.25**	**32**	16	**8**	**16**	**16**	**0.25**	>32	>32	NT
10211-6	>320	1	2	≤0.060	0.5	**1**	**8**	8	4	**256**	**>32**	**8**	>32	>32	NT
10211-10	>320	1	2	0.25	0.5	**4**	16	16	**2**	**>256**	**>32**	**64**	>32	>32	NT
10211-TC7	>320	1	2	≤0.060	0.5	0.25	16	8	**2**	**>256**	**>32**	**4**	>32	>32	NT

EDTA, ethylenediaminetetraacetic acid; IME, imipenem plus EDTA; IPM, imipenem; MEM, meropenem; ETP, ertapenem; CIP, ciprofloxacin; TOB, tobramycin; AMK, amikacin; GEN, gentamicin, TET, tetracycline; MIN, minocycline; TGC, tigecycline; SUB, sulbactam; COL, colistin; CHL, chloramphenicol.

3.3.3. Analysis of expression of the efflux pump-encoding operons *sdeAB*, *sdeCDE* and *sdeXY* in the type strain NCTC 10211 and laboratory mutant 10211-10 using real-time RT-PCR

The mechanisms of tigecycline resistance in *S. marcescens* were unknown although resistance in other Enterobacteriaceae species had been associated with up-regulation of the RND efflux transporter, AcrAB (127;128;224). Three RND systems have been described to date in *S. marcescens*, namely SdeAB (135), SdeCDE (22) and SdeXY (42). When a BLAST search was performed of the assembled (but unpublished) genome sequence of *S. marcescens* Db11 (Sanger Institute *S. marcescens* BLAST Server available at http://www.sanger.ac.uk/cgi-bin/blast/submitblast/s_marcescens) using an *E. cloacae acrB* sequence (accession number: AM287287) the results indicated that the *sdeY* gene was the most similar to this at the nucleotide level, with 79% identity.

The potential of efflux by RND-type transporters as a mechanism of tigecycline resistance in *S. marcescens* was investigated by analysis of expression of *sdeAB*, *sdeCDE* and *sdeXY* in type strain NCTC 10211 and laboratory mutant 10211-10.

Compared with NCTC 10211, mutant 10211-10 overexpressed all of the three RND efflux systems studied, but the increase in expression of *sdeXY* was reproducibly higher (*c.* 11-fold) than the 2-3-fold increases for the *sdeAB* and *sdeCDE* pumps (Figures 50, 51 and 52). Expression of *sdeXY* was also raised in clinical isolate, SM346 and intermediate mutant, 10211-6 (tigecycline MIC, 8 mg/L) as compared with NCTC 10211. Likewise, the mutant selected during exposure to tetracycline, 10211-TC7, showed a modest (c. two-fold) increase in *sdeXY* expression compared with NCTC 10211 (Figure 52).

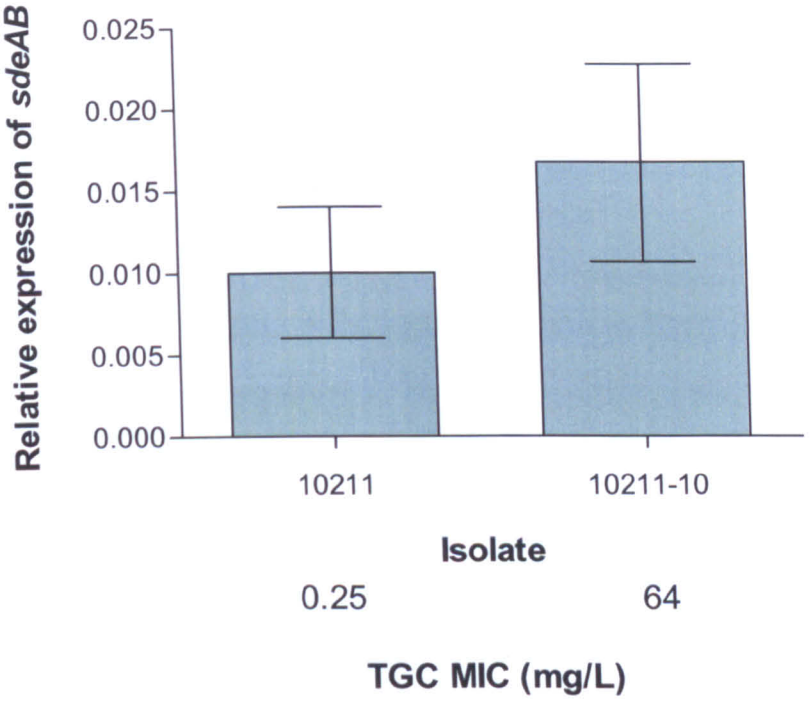

Figure 50. Expression of *sdeAB* relative to that of *rpoB* (means ± standard deviations) in the type strain NCTC 10211 and the laboratory mutant, 10211-10. Tigecycline (TGC) MICs are shown.

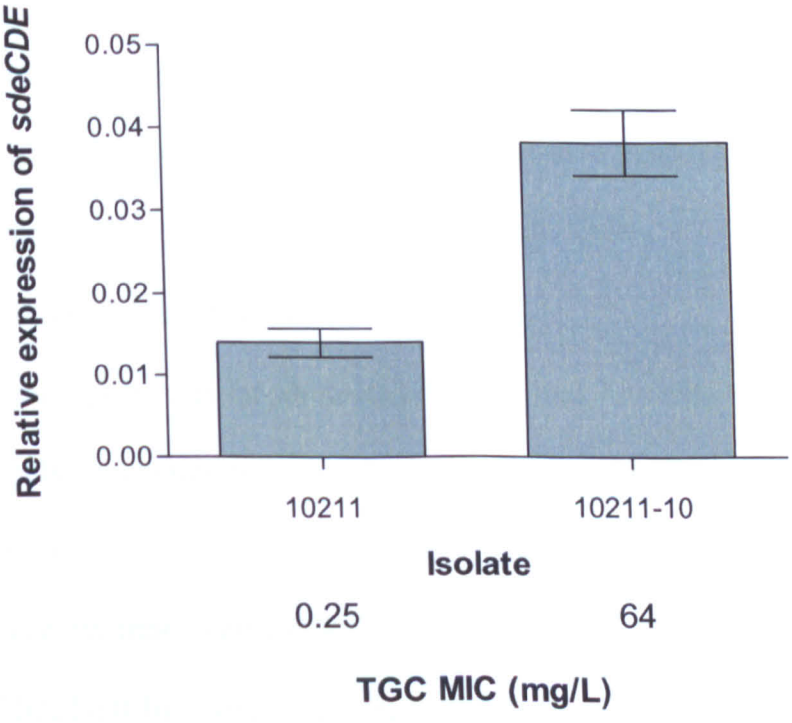

Figure 51. Expression of *sdeCDE* relative to that of *rpoB* (means ± standard deviations) in the type strain NCTC 10211 and the laboratory mutant, 10211-10. Tigecycline (TGC) MICs are shown.

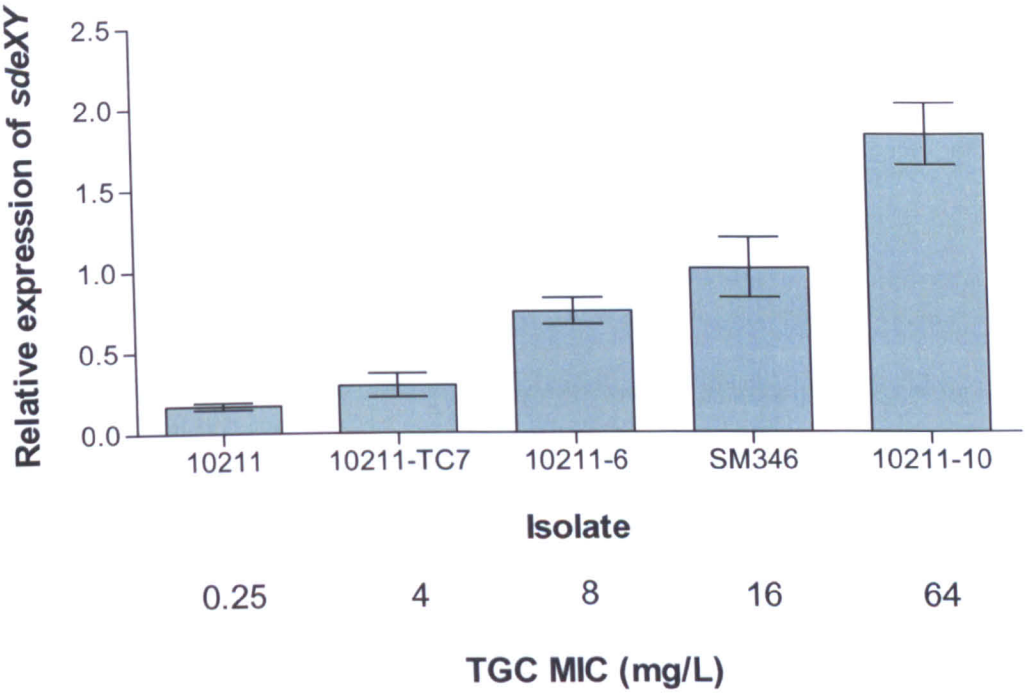

Figure 52. Expression of *sdeXY* relative to that of *rpoB* (means ± standard deviations) in the clinical isolate SM346, the type strain NCTC 10211 and derivatives. Tigecycline (TGC) MICs are shown.

3.3.4. Interruption of genes in *S. marcescens*

The efflux pump-encoding operon *sdeXY* and the *tolC* homologue, *hasF* were targeted for disruption in the final laboratory mutant, 10211-10 to investigate their involvement in tigecycline resistance.

The *hasF* gene was targeted because previous work has indicated that HasF may be the only outer-membrane channel involved in energy-dependent efflux in *S. marcescens* (136).

Initially, attempts were made to modify the phage λ Red recombination system for use in 10211-10 by cloning a kanamycin resistance marker into pKOBEG and generating a linear DNA fragment containing a gentamicin resistance cassette flanked by regions complementary to *sdeY*. Although pKOBEG replication was observed in

10211-10 under kanamycin pressure, multiple attempts to inactivate *sdeY* using this system were unsuccessful.

A suicide plasmid system was then considered; however, pUC-derived plasmids, like those used to inactivate genes in *A. baumannii* (section 3.1.4) were not suitable, as they replicate in *S. marcescens*. The origin of replication of plasmid R6K was considered a viable alternative, as its function is dependent upon the replication initiator (Rep) protein, π, which is encoded by the *pir* gene (132). Plasmids containing this origin of replication do not replicate in bacteria that lack the *pir* gene, including *S. marcescens*. The R6K *ori* was first used successfully in a suicide construct to inactivate the *toxR* gene of *Vibrio cholerae* (173), and has also been used to inactivate efflux pump genes in *S. marcescens* (22). The strategies employed to interrupt the *sdeY* and *hasF* genes of *S. marcescens* are shown in Figures 53 and 54, respectively. Chromosomal integration of pSMY-2 and pHASF was confirmed by PCR and sequencing across the insertion site (Figures 55 and 56).

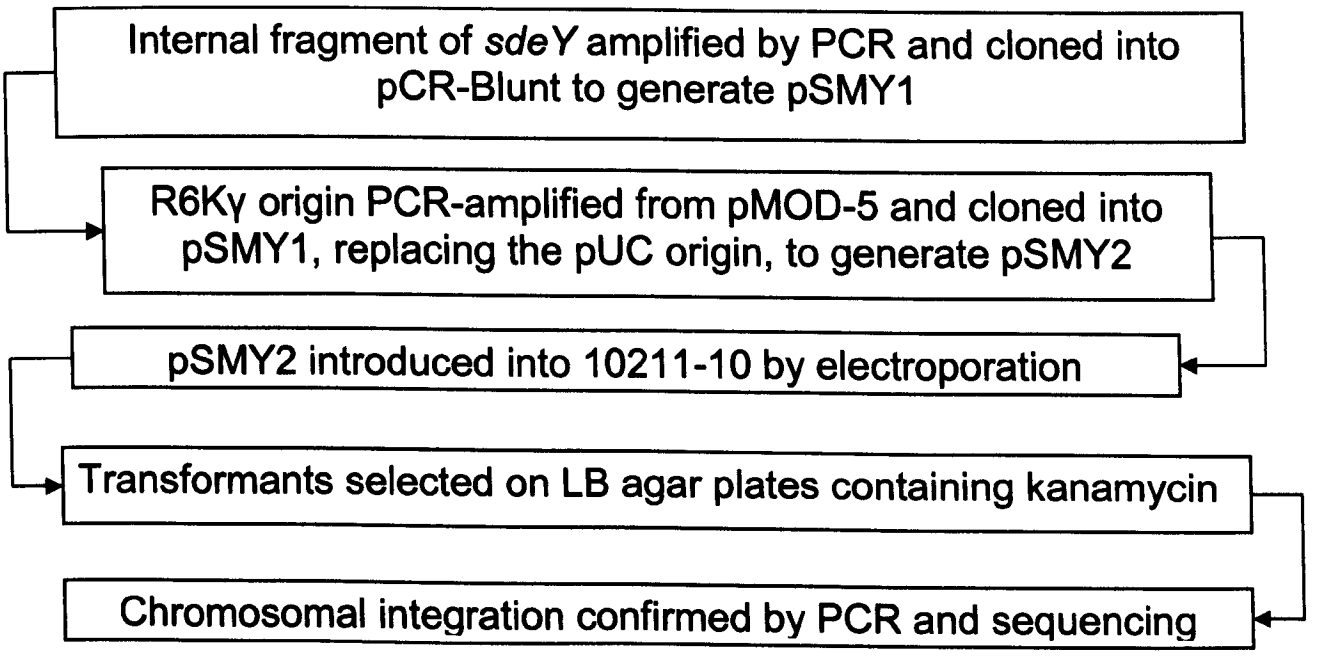

Figure 53. Overview of strategy used to disrupt *sdeY* in the laboratory mutant 10211-10.

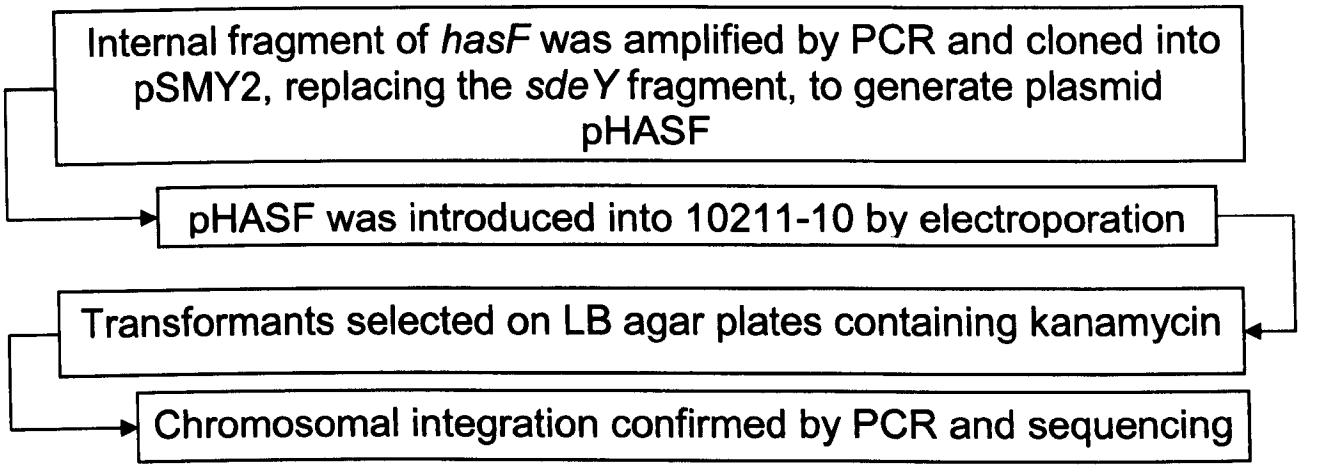

Figure 54. Overview of strategy used to disrupt *hasF* in the laboratory mutant 10211-10.

a.

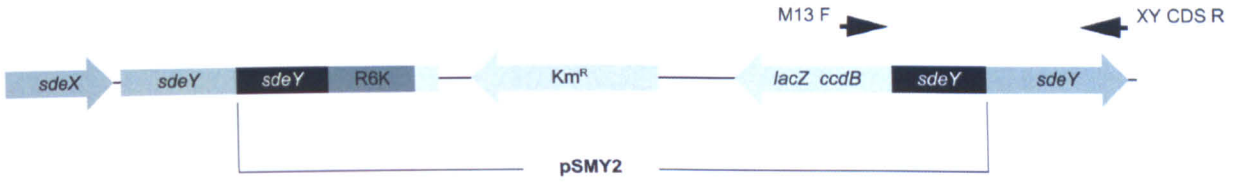

b.

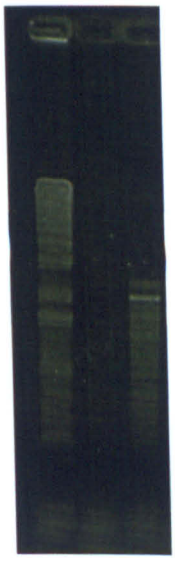

1 2 3

Figure 55. Confirmation of the chromosomal insertion of suicide plasmid, pSMY2: (a) schematic of pSMY2 insertion displaying the primers used to perform PCR across the insertion site; (b) agarose gel electrophoresis displaying a 1-Kb DNA ladder in lane 1 and the 2260-bp PCR product in lane 3.

a.

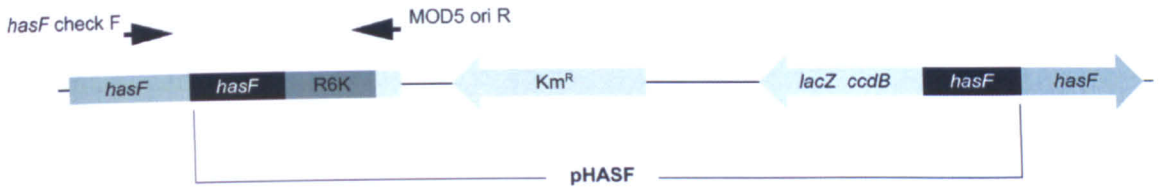

b.

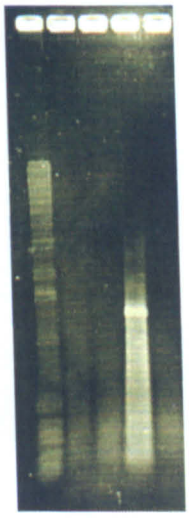

1 2 3 4

Figure 56. Confirmation of the chromosomal insertion of suicide plasmid, pHASF: (a) schematic of pHASF insertion displaying the primers used to perform PCR across the insertion site; (b) agarose gel electrophoresis displaying a 1-Kb DNA ladder in lane 1 and the 1372-bp PCR product in lane 4.

Interruption of either *sdeY* or *hasF* in the laboratory mutant 10211-10 restored full susceptibility to tigecycline (MIC, 0.125; Figures 57 and 58; Table 16). MICs of ciprofloxacin, cefpirome and tetracycline also were markedly reduced to below the values for the 'wild-type' parent, NCTC 10211. MIC shifts were much less marked for meropenem, but followed the same general trend, being increased for mutant 10211-10 but reduced by inactivation of *sdeY* or *hasF*. Compared with 10211-10 the

ceftazidime MIC was reduced eight- and 16-fold in derivatives 10211-10Δ*sdeY* and 10211-10Δ*hasF*, respectively, whilst the MIC of cefotaxime was reduced (eight-fold) for 10211-10Δ*hasF* only. Interruption of *hasF* resulted in a reduction in the MICs of aztreonam, carbenicillin, cefoxitin, piperacillin and minocycline (Table 16).

Figure 57. Tigecycline Etest performed on laboratory mutant 10211-10 and derivative 10211-10Δ*sdeY*.

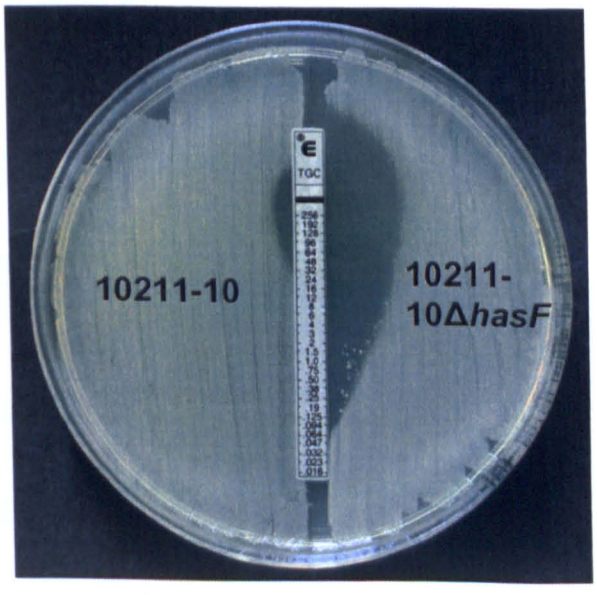

Figure 58. Tigecycline Etest performed on laboratory mutant 10211-10 and mutant 10211-10Δ*hasF*.

Table 16. Antibiotic susceptibilities of 10211-10Δ*sdeY* and 10211-10Δ*hasF*

Isolate	MIC (mg/L)															
	AMP	AUG	**AZT**	**CAR**	CLAV	CLOX	**CLAX**	**CTX**	**CTXC**	**CAZ**	**CAZC**	**CPR**	**CPRC**	**FOX**	**PIP**	**PTZ**
10211-10Δ*sdeY*	>64	>64	1	256	>4	>100	≤0.125	8	32	**0.5**	2	≤0.125	0.5	64	32	16
10211-10Δ*hasF*	64	64	**≤0.125**	**≤16**	>4	>100	**≤0.125**	**0.5**	**2**	**0.25**	**0.125**	**≤0.125**	**≤0.060**	**32**	**2**	**≤1.0**
10211-10	>64	64	**1**	**256**	>4	>100	**4**	**4**	**16**	**4**	**4**	**8**	**4**	**>64**	**16**	**16**

AMP, ampicillin; AUG, co-amoxiclav; AZT, aztreonam; CAR, carbenicillin; CLAV, clavulanic acid; CLOX, cloxacillin; CLAX, cloxacillin plus cefotaxime; CTX, cefotaxime; CTXC, cefotaxime plus clavulanic acid; CAZ, ceftazidime; CAZC, ceftazidime plus clavulanic acid; CPR, cefpirome, CPRC, cefpirome plus clavulanic acid, FOX, cefoxitin, PIP, piperacillin; PTZ, piperacillin plus tazobactam.

Table 16 cont. Antibiotic susceptibilities of 10211-10Δ*sdeY* and 10211-10Δ*hasF*

Isolate	MIC (mg/L)													
	EDTA	IME	IM	**MEM**	ERP	**CIP**	TOB	AMK	GEN	**TET**	**MIN**	**TGC**	SUB	COL	CHL
10211-10Δ*sdeY*	>320	2	2	**≤0.060**	0.25	**≤0.125**	8	8	2	**1**	32	**0.125**	>32	>32	NT
10211-10Δ*hasF*	>320	2	4	**≤0.060**	0.25	**≤0.125**	8	8	2	**2**	**16**	**0.125**	>32	>32	NT
10211-10	>320	1	2	**0.25**	0.5	**4**	16	16	2	**>256**	**>32**	**64**	>32	>32	NT

EDTA, ethylenediaminetetraacetic acid; IME, imipenem plus EDTA; IPM, imipenem; MEM, meropenem; ETP, ertapenem; CIP, ciprofloxacin; TOB, tobramycin; AMK, amikacin; GEN, gentamicin, TET, tetracycline; MIN, minocycline; TGC, tigecycline; SUB, sulbactam; COL, colistin; CHL, chloramphenicol.

3.4. Screening of tigecycline-resistant isolates for the *tet*(X) gene by PCR

Tigecycline-resistant (MIC, ≥ 4 mg/L) clinical isolates of all species used in this thesis (n=5) were screened by PCR for the presence of *tet*(X) (281). Tet(X) is a flavin-dependent mono-oxygenase known to modify tigecycline (175). The *tet*(X) gene was not detected in any of the organisms tested, although the positive control strain gave a PCR product of the correct size (Figure 59).

1 2 3 4

Figure 59. Agarose gel electrophoresis displaying a 123-bp DNA ladder in lane 1 and the results of *tet*(X) PCR performed on the *E. coli* positive control strain Em24 pBSJ (275) (lane 2) and clinical isolates AB211 (lane 3) and W7282 (lane 4).

4. Discussion

At the beginning of the studentship in the spring of 2007, tigecycline had been licensed in the US for less than two years and in Europe for only a year. It was the first new tetracycline derivative to be marketed in over three decades and was the first-in-class glycylcycline antimicrobial to be approved for clinical use. Around the time of its launch, on the basis of its *in vitro* activity and performance in clinical trials, there was expectation that it would find use in the treatment of infections caused by MDR pathogens, including many Gram-negative species (153). However, by 2006 (the year tigecycline was licensed in Europe) there was already evidence that tigecycline is a substrate of chromosomally-encoded RND-type efflux systems of *P. aeruginosa*, *M. morganii*, *P. mirabilis* and *K. pneumoniae* (61;222;224;267). There were also warning signs of the propensity of tigecycline to select for resistance, as evidenced by data from phase III trials that documented five instances of emerging tigecycline resistance in a number of Gram-negative species, namely, *K. pneumoniae* (two instances), *M. morganii*, *E. cloacae* and *A. baumannii* (153).

In this study, isolates of Enterobacteriaceae (*E. cloacae* and *S. marcescens*) and *A. baumannii* referred to ARMRL that displayed resistance to tigecycline ($\geq$ 4 mg/L) were characterised, and efflux by RND systems was investigated as a possible mechanism.

4.1. *A. baumannii*

Reports of resistance to tigecycline in *A. baumannii* are worrying, given the MDR nature of the majority of clinical isolates of this species, in addition to its propensity to persist in the nosocomial environment. Of particular concern are reports of resistance in representatives of epidemic, carbapenem-resistant lineages where

tigecycline is usually one of the few agents to remain active *in vitro*, along with colistin, to which resistance has also been documented (59). It therefore was considered particularly important to investigate the emergence of tigecycline resistance during tigecycline therapy in representatives of one of the UK's most successful carbapenem-resistant lineages, OXA-23 clone 1.

The first task was to confirm both the identity of the *A. baumannii* isolates described in Table 2 and their tigecycline MICs (Results sections 3.1.1.1 and 3.1.1.2; Tables 2 and 11). Identification to genus level was achieved using API20NE, although phenotypic tests such as this do not distinguish between members of the *A. calcoaceticus-A. baumannii* complex very well (94). A relatively simple method for confirming an isolate as *A. baumannii* is detection by PCR of the $bla_{\text{OXA-51-like}}$ gene, which has been shown to be intrinsic to the species (261). This was chosen as a simpler and cheaper alternative to other molecular methods of species-level identification such as sequencing of the 16S – 23S rRNA gene spacer region (Results section 3.1.2) (40). However, since the completion of the practical element of this study, the $bla_{\text{OXA-51-like}}$ gene has been detected in a clinical isolate of *A. nosocomialis* (formerly known as *Acinetobacter* genomic species 13TU) and so can no longer be considered an absolutely reliable species-specific marker (140;183). All isolates were then assigned to OXA-23 clone 1, the SE clone or the ACB20 clone by analysis of their PFGE profiles (Results section 3.1.2). PFGE identification within these clusters also confirmed their species identity as *A. baumannii*.

Susceptibility testing was performed by agar dilution or by Etest according to BSAC guidelines on Iso-Sensitest agar (Materials and Methods section 2.5). Care was taken to prepare media containing tigecycline on the day of use to avoid the potential for artificially high MICs resulting from the inactivation of tigecycline by oxidation in

aged media (112). There has been some controversy surrounding the methods for determining tigecycline susceptibility *in vitro* when using Mueller Hinton (MH) media (82;250). Significantly different zone diameters were observed when tigecycline disc diffusion susceptibility testing was performed using MH agar supplied by different manufacturers (250). Subsequently, it was found that elevated tigecycline MICs correlated with higher concentrations of manganese in the medium (82). The reasons for this effect are unclear, though it was postulated that it may be due to induction of RND transporters by manganese (82). This aspect was investigated using clinical isolates AB210 and AB211 (Results section 3.1.4).

Evidence that tigecycline is a substrate of the AdeABC efflux transporter was first published in 2007, less than a month after the beginning of the PhD studentship (197;223). I therefore decided to focus on this mechanism when investigating the emergence of resistance in clinical isolates of *A. baumannii*.

Since up-regulation of AdeABC had been linked with elevated tigecycline MICs in other studies (197;223) the real-time RT-PCR assay described by Peleg *et al.* (197) was used to investigate expression of *adeABC*. However, problems with DNA contamination in the RT-negative controls were encountered when using the multi-copy 16S rRNA gene as the reference housekeeping gene according to the published assay (197). It was also observed that the 16S rRNA reactions had consistently low but variable C_T values. As a result the assay was redesigned using the single copy-gene, *rpoB* as the reference housekeeping gene, using primers designed in highly conserved regions, as evidenced by multiple sequence alignment. An on-column DNase treatment step was introduced into the RNA extraction protocol (Materials and Methods section 2.8) to ensure the purity of RNA extracts.

The post-therapy, tigecycline-resistant clinical isolate, AB211 and its tigecycline-susceptible, pre-therapy counterpart, AB210 had been referred to ARMRL in 2005 (Results section 3.1.1.1). PFGE analysis confirmed them as OXA-23 clone 1 representatives (Figure 21a) and *in vitro* susceptibility testing confirmed tigecycline resistance and susceptibility in AB211 and AB210, respectively (Table 11).

Using the modified assay described above, RT-PCR identified overexpression of this efflux system in the tigecycline-resistant clinical isolate, AB211 and the laboratory-selected, tigecycline-resistant mutant, AB210-6 compared with the pre-therapy, tigecycline-susceptible clinical isolate, AB210 (Results section 3.1.3). There was an association between increasing tigecycline MIC and elevated expression of *adeABC* (Figure 24). These data were in agreement with previous reports (197;223) and suggested involvement of the AdeABC efflux system in the mutational emergence of tigecycline resistance, under tigecycline selection pressure, both *in vitro* and *in vivo*.

Real-time RT-PCR data suggested that up-regulation of the RND transporter AdeABC was responsible for the tigecycline-resistant phenotype. To assess fully the role of this pump in the emergence of resistance in AB211 it was decided to attempt to silence the system by targeting the *adeB* for inactivation (Materials and Methods section 2.19.3.1.1).

A number of strategies exist for the inactivation of genes in Gram-negative bacteria, though most of these have been developed for use in *E. coli* (17). At the time of choosing a strategy for the inactivation of *adeB* in 2008, all the studies that reported on the inactivation of *A. baumannii* genes described either: (i) the chromosomal integration of suicide plasmids encoding a selectable marker (antibiotic resistance) gene, mediated by a single homologous recombination event or (ii)

integration of the selectable marker gene only, which was similarly encoded on a suicide plasmid but which relied upon a double homologous recombination event (160;164;223). An alternative PCR-based method has since been described (14).

The simplest of the suicide plasmid-based approaches is integration of an entire plasmid within the gene of interest, which disrupts the coding region and inactivates the gene. This was the approach adopted by Ruzin *et al.* to inactivate *adeB* (223) and, on this basis, the suicide vector pBK-5 was constructed (Materials and Methods section 2.19.3.1.1). Plasmid pBK-5 contains ampicillin and kanamycin resistance genes only (Figure 13) and so can only be used to inactivate *adeB* in isolates with relatively low MICs for one or both of these agents whereas isolates of OXA-23 clone 1 are usually resistant to ampicillin and the aminoglycosides (49). Fortuitously, the kanamycin MIC for post-therapy isolate AB211 was 4 mg/L, which allowed for selection of mutants using this agent (Results section 3.1.4.1). However, the laboratory mutant, AB210-6 was resistant to both agents and so was not amenable to such genetic manipulation (Table 11). Inactivation of *adeB* in AB211 resulted in a reduction in tigecycline MICs to the pre-therapy level (Table 12). This result suggested that up-regulation of AdeABC was the sole mechanism of tigecycline resistance in this case.

By this time there was published evidence that tigecycline is also a substrate of the AdeIJK transporter of *A. baumannii* (56), but given the evidence above, efflux by this RND pump was not investigated as a possible mechanism of resistance.

After establishing that up-regulation of AdeABC was the sole mechanism of tigecycline resistance in clinical isolate AB211 and most likely also in laboratory mutant AB210-6, the next question to be addressed was how the pump had come to be up-regulated. Expression of *adeABC* is controlled by the divergently co-transcribed,

two-component signal transduction system, AdeRS (164). Analysis of *adeRS* expression by real-time PCR revealed no differences in expression between AB210 and AB211, indicating that differential expression of the regulatory operon was not responsible for AdeABC up-regulation (Figure 26).

Specific amino acid substitutions in both the sensor histidine kinase, AdeS and its cognate response regulator, AdeR have been associated with constitutive expression of *adeABC* (51;164). Nucleotide sequencing of *adeRS* in AB210, AB211 and AB210-6 did not identify any of the previously reported mutations, but did predict the presence of an Ala-94→Val substitution in AdeS in the tigecycline-resistant clinical isolate, AB211 compared with AB210. A Gly-103→Asp substitution in AdeS and an Ala-91→Val change in AdeR were also identified in the tigecycline-resistant laboratory mutant, AB210-6 compared with its susceptible parent, AB210 (Results section 3.1.5). The Ala/Val-91 and Gly/Asp-103 residues of AdeS are located in the HAMP (histidine kinase, adenylyl cyclase, methyl-accepting chemotaxis protein, and phosphatase) linker domain. This is potentially relevant, as the HAMP domain of the NarX sensor kinase of *E. coli* is thought to play an active part in transmembrane signal transduction (13) whilst mutations in the linker domain of the $VanS_B$ sensor histidine kinase have been associated with glycopeptide resistance in enterococci as a result of induction of the *vanB* gene cluster (64). The Ala/Val-91 residue of AdeR is located in the signal receiver domain, one position downstream of a residue that appears to be important for the co-ordination of Mg^{2+}, which is required for the phosphorylation of the conserved aspartic acid residue. The G→A point mutation responsible for the Ala-91→Val substitution in AdeR was located within the promoter region of the *adeABC* operon (Results section 3.1.5). These mutations may

explain the elevated level of *adeABC* transcript observed in AB211 and the even higher level of expression seen in AB210-6 compared with AB210.

Previous work demonstrated that inactivation of *adeRS* results in susceptibility to known substrates of AdeABC in *A. baumannii*, including the aminoglycosides, suggesting that AdeR positively regulates *adeABC* expression (164). Therefore, it was attempted to explore further the role of AdeRS in the overexpression of *adeABC* observed in clinical isolate AB211 by taking advantage of the relatively low kanamycin MIC. Suicide plasmids, pSK-1 and pSK-2 (Figure 14) were used in an attempt to inactivate the *adeRS* operon. The strategy was the same as that used to inactivate *adeB* (Figure 30). Although previous work has shown that functional AdeRS is required for AdeABC activity (164), no change in tigecycline MIC was observed upon interruption of *adeS* (Results section 3.1.6.2). This result led to assessment of the integrity of the *adeRS* locus in the Δ*adeS* 'mutant' by PCR; this appeared to be intact despite evidence that the pSK-1/2 insertion was successful (Figure 34). In a study describing a PCR-based method of gene interruption in *A. baumannii*, it was found that when an outer membrane protein gene was disrupted using a suicide plasmid, 40% of the population reverted to wild-type after 10 passages without selection pressure (14) and it seems likely that the chromosomal insertions of pSK-1/2 were similarly unstable even under selection pressure. Since further attempts to inactivate *adeS* had to be abandoned due to time constraints (Results section 3.1.6.2), the nature of *adeABC* regulation by AdeRS was not investigated further in clinical isolate AB211.

As noted earlier, it has been documented that increasing levels of manganese in the susceptibility testing medium can lead to increases in tigecycline MICs, and induction of RND transporters has been proposed as a possible mechanism (82).

Clinical isolates AB210 and AB211 displayed elevated tigecycline MICs when the medium was supplemented with $MnSO_4$. AB211 was more affected than AB210 by higher levels of $MnSO_4$ in terms of increases in tigecycline MIC (Figure 27). $MnSO_4$ supplementation appeared to affect *adeABC* expression in both isolates though not in a manner that could explain the observed tigecycline MICs (Figure 27). There was no correlation between level of *adeABC* expression and MIC in the case of AB211 (Figure 27). The mechanism(s) by which manganese affects the *in vitro* activity of tigecycline versus *A. baumannii* therefore remains obscure.

In 2009, ARMRL received a further pre- and post-treatment clinical pair of *A. baumannii* isolates where tigecycline resistance had been reported in the post-therapy isolate, W7282 while the pre-therapy isolate, W6976 was susceptible to this agent (Results section 3.1.1.2; Table 11). Further *in vitro* susceptibility testing of these two isolates confirmed the tigecycline MICs, and PFGE analysis identified both as representatives of OXA-23 clone 1 (Figure 21b).

Given the body of evidence available at that time that suggested that up-regulation of AdeABC was the major tigecycline resistance mechanism in *A. baumannii*, the expression of *adeABC* in W6976 and W7282 was assessed. Real-time RT-PCR identified overexpression of *adeABC* in the post-therapy isolate, W7282 suggesting that AdeABC activity was responsible for the tigecycline-resistant phenotype (Figure 25).

Unlike clinical isolate AB211, isolate W7282 retained resistance to the aminoglycosides (Table 11). This meant that it was not possible to use pBK-5 or any other pCR2.1 derivative encoding only ampicillin and kanamycin resistance genes for the inactivation of *adeB*. Non-antibiotic selection markers were considered for use, including a potassium tellurite resistance cassette that was used successfully in other

Gram-negative species (227). However, since isolates W6976 and W7282 were not referred to ARMRL until 2009, the remaining time for laboratory work was limited, it was considered that construction of further suicide vectors for the inactivation of *adeB* was not a priority given that existing evidence from this and other studies suggested the observed *adeABC* overexpression was most likely responsible for tigecycline resistance in W7282.

The mechanism of *adeABC* overexpression in W7282 relative to W6976 was investigated by analysis of the nucleotide sequence of *adeRS* in both isolates. Initially, no differences were detected between the two isolates, although subsequent whole-genome shotgun sequencing analysis (section 4.1.1) identified a Ser-8→Arg substitution in AdeS in W7282 relative to W6976 (Results section 3.1.5). This residue is not located in any conserved domain and its biological significance remains uncertain. Nevertheless, since it was the only difference identified in the *adeRS* locus between the two isolates it could be that it was responsible for *adeABC* overexpression.

In summary, the emergence of tigecycline resistance in two representative isolates of the epidemic, carbapenem-resistant lineage, OXA-23 clone 1 during tigecycline therapy was investigated. In both instances the tigecycline resistance phenotype was associated with up-regulation of AdeABC and, in the case of AB211, the role of this pump in the emergence of resistance was confirmed by insertional inactivation of *adeB*. These data are in agreement with previous reports that have also suggested that tigecycline is a substrate of AdeABC (197;223). Taken together, it appears that up-regulation of this RND efflux system is currently the major mechanism of tigecycline resistance in this species.

OXA-23 clone 1 belongs to the internationally-disseminated European clone II. This is the first report of tigecycline resistance emerging during therapy in the widespread UK lineage, OXA-23 clone 1. Such resistance is concerning since the OXA-23 clone 1 lineage is already resistant to carbapenems and all other drugs except polymyxins. Moreover, both patients were being treated for intra-abdominal infections, which are a licensed indication for tigecycline, whereas previous reports of emerging tigecycline resistance have mostly concerned off-label use (11;210).

Distinct lineages of *A. baumannii* have different modal tigecycline MICs. Using multiple representatives of the OXA-23 clone 1, SE and ACB20 clones, it was demonstrated that an association exists between a higher modal tigecycline MIC and elevated expression of *adeABC* (Figures 22 and 23; Results section 3.1.3.1). These data support the hypothesis that differential expression of *adeABC* underlies not only intra-clone but also inter-clone variation in tigecycline MICs.

Nucleotide sequence analysis of the *adeRS* operon in multiple representatives each of the SE clone and OXA-23 clone 1 revealed a difference at amino acid 62 of the sensor histidine kinase, AdeS, with methionine at this position in OXA-23 clone 1 and isoleucine in the SE clone, as in all AdeS sequences available in GenBank (Results section 3.1.5). Met/Ile-62 is located in the second transmembrane helix of AdeS, of which the HAMP linker domain is an extension. The presence of Ile or Met-62 may therefore affect susceptibility to tigecycline and so could explain the observed difference in modal tigecycline MIC between these two lineages.

4.1.1. Whole-genome sequencing

The recent availability of rapid and inexpensive whole-genome sequencing permits detailed investigation of genetic differences between pairs of bacterial isolates. In *A. baumannii* whole-genome studies have thus far focused either on comparing distinct antibiotic-susceptible and MDR strains (4,5), or related isolates from different patients (2). The results of these and other similar studies (7) point to a high degree of genome plasticity, the rapid emergence of antibiotic resistance, and significant genetic differences between closely-related isolates.

Since the completion of the practical component of the studentship, the case study isolates AB210, AB211, W6976 and W7282 have been subjected to whole-genome sequencing as part of an on-going collaborative project investigating the genomics of *Acinetobacter* sp.

Eighteen putative single nucleotide polymorphisms (SNPs) were detected between AB210 and AB211. Of these, nine were non-synonymous including one missense mutation. Several of these were located within genes predicted to be involved in core biological functions, including translation, nucleic acid biosynthesis, α-ketoglutarate and arabinose transport, environmental sensing (the signal transduction histidine kinase gene, *adeS* which had been previously identified), and signalling.

Three contigs in AB210 were not covered by reads in AB211. One of these putative deletions disrupted the coding sequence of the DNA mismatch repair gene, *mutS*. The deleted regions comprised of genes encoding for transcriptional regulators, ion channels and transporters, a class A β-lactamase enzyme, components of a type VI secretion system (degenerate in both isolates) and an EAL domain-containing protein

among others. One of the regions included a class 1 integron containing the aminoglycoside resistance genes, *aac(6')-Ib*, *aadA* and *armA* (previously confirmed as absent from AB211 by PCR), the absence of which is consistent with the change in aminoglycoside resistance between AB210 and AB211, with MICs of tobramycin, amikacin and gentamicin reduced at least eight-fold in AB211 (Table 11).

In contrast to the AB210/AB211 pair, there were relatively few genetic differences between W6976 and W7282. No large structural changes were identified, though a total of six putative SNPs were detected between the two isolates, of which two were non-synonymous, with one located in a gene of unknown function and the other resulting in the Ser-8→Arg substitution in AdeS (Results section 3.1.5). This mutation was not detected by Sanger sequencing when the nucleotide sequence of *adeRS* was originally investigated in this thesis. However, in the light of the whole-genome sequence data the nucleotide sequence of *adeS* was investigated a second time and the SNP was subsequently confirmed by Sanger sequencing of PCR amplicons. The reasons for the original error remain unclear. However, analysis of the repeat sequencing chromatograms identified a double peak at the SNP position (Figure 60). It could be that there was a mixed population of bacterial cells, with a proportion harbouring the wild-type allele.

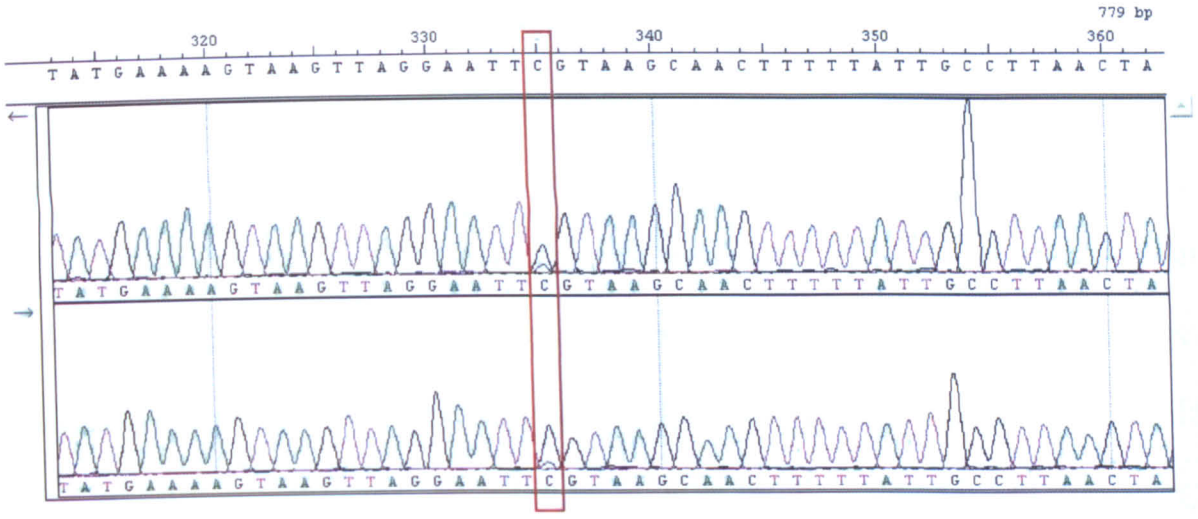

Figure 60. Alignment of forward and reverse chromatograms displaying part of *adeS* from W7282. The SNP responsible for the Ser-8→Arg substitution is boxed in red.

Whole-genome sequencing gave insight into the nature of genetic changes between isolates under selection pressure through antibiotic therapy and a hostile host environment. This work demonstrated significant differences between AB210 and AB211 but relatively few between W6976 and W7282 suggesting that other factors, in addition to tigecycline pressure, played a role in selecting for the differences observed between the Case 1 isolates. The PFGE profiles of the two pairs were not identical (Figure 21, page XX) and therefore suggested the existence of genetic differences between the isolates. However, it is clear from the whole-genome sequencing data that standard molecular typing methods cannot be relied upon to predict the wider phenotypic characteristics of *A. baumannii* clinical isolates.

4.2. *E. cloacae*

The emergence of tigecycline resistance in *E. cloacae* was investigated using the two pairs of clinical isolates described in Results section 3.2.1. In contrast to the *A. baumannii* clinical pairs, neither patient had received tigecycline prior to the recovery

of the tigecycline-resistant isolates (Results section 3.2.1.1 and 3.2.1.2). This suggests that selection pressure other than tigecycline therapy can select for a tigecycline resistant phenotype in this species.

Clinical isolates TGC-S (tigecycline-susceptible) and TGC-R (tigecycline-resistant) had been referred to ARMRL in 2006. Initial characterisation of these two isolates confirmed their identity and tigecycline MICs (Results section 3.2.2; Table 13). Some differences were observed in their PFGE profiles, which led to there being some debate over whether or not they were representatives of the same strain (Results section 3.2.2). However, analysis of the profiles of the laboratory-selected mutants that were derived from TGC-S demonstrated that *in vitro* tigecycline exposure could select for the genetic events responsible for the changes in PFGE profile from TGC-S to TGC-R (Figure 35).

Evidence that tigecycline is a substrate of the *E. cloacae* AcrAB efflux transporter was published in the spring of 2007, just prior to the beginning of the studentship (127;200). Therefore, expression of *acrAB* was investigated in clinical isolates TGC-S and TGC-R using the real-time RT-PCR assay developed by Doumith *et al.* (72). Both TGC-R (the post-therapy isolate) and the tigecycline-resistant laboratory mutant, TGC-S7 overexpressed *acrAB* compared with TGC-S (Results section 3.2.3). Indeed there was a stepwise association between increasing tigecycline MIC and elevated expression of *acrAB* (Figure 36).

The *acrB* gene of TGC-R was targeted for inactivation in order to confirm involvement of AcrAB in tigecycline resistance. The strategy of integrating pCR2.1-based suicide plasmids into the chromosome that was employed to inactivate genes in *A. baumannii* (section 4.1) was not suitable for use in *E. cloacae* due to plasmid replication. Instead, *acrB* was interrupted using a linear DNA fragment containing a

gentamicin resistance cassette flanked by regions complementary to the target using the helper plasmid pKOBEG (Figure 15), which encodes the bacteriophage λ Red functions (41;203), using a modified version of the methods described by Perez *et al.* (200) (Figure 41). The *acrB* gene was disrupted in TGC-R using this approach and tigecycline susceptibility was restored (Table 14; Figure 43), confirming the role of AcrAB up-regulation in the emergence of resistance in this isolate and providing further evidence that tigecycline is a substrate of the AcrAB transporter of *E. cloacae.*

In addition to restoring susceptibility to tigecycline, inactivation of AcrAB in isolate TGC-R affected the MICs of other agents demonstrating that ciprofloxacin, tetracycline, chloramphenicol and minocycline are also substrates of this efflux system (section 3.2.5.1; Table 14). These data are in agreement with published reports where AcrAB has been inactivated in clinical isolates of *E. cloacae* (127;200). The eight-fold increase in gentamicin MIC observed for mutant TGC-RΔ*acrB* relative to its parent clinical isolate, TGC-R, is most likely the result of the chromosomal integration of the gentamicin resistance cassette used to select for insertion mutants (Figure 42; Table 14).

Keeney *et al.* previously demonstrated an association between up-regulated AcrAB and overexpression of the AraC-type transcriptional regulator, RamA in *E. cloacae* (127). In this study, real-time RT-PCR identified a similar relationship between *acrAB* and *ramA* expression, with the latter being overexpressed in TGC-R and TGC-S7 compared with TGC-S (Results section 3.2.3; Figure 37).

In *K. pneumoniae* and *S. enterica* serovar Typhimurium, RamA has been shown to positively regulate expression of *acrAB*, as demonstrated by transposon mutagenesis and targeted gene knockout studies (16;224). However, no previous experimental evidence has placed *acrAB* definitively in the RamA regulon in *E.*

cloacae. To investigate this possibility, *ramA* was overexpressed in clinical isolate TGC-S using the pBAD expression vector which, under certain induction conditions, resulted in increased *acrAB* expression at levels sufficient to confer tigecycline resistance (Results section 3.2.4; Figure 39). These data confirm that up-regulation of AcrAB, mediated by RamA activation, was the factor conferring tigecycline resistance in TGC-R. The mechanism(s) of *ramA* overexpression in TGC-R and TGC-S7 was not investigated due to time constraints, but in *K. pneumoniae* and *S. enterica* serovar Hadar, genetic events that result in non-functional RamR have been implicated (101;102).

The significance of the His-95→Arg substitution in RamA detected in TGC-R relative to TGC-S remains unclear (Results section 3.2.4). However, it was not selected for in the tigecycline-resistant mutant, TGC-S7, which overexpressed *ramA* (Figure 37), nor is His/Arg-95 located in a conserved domain. Taken together, these data indicate that the His-95→Arg substitution was not responsible for *ramA* overexpression in TGC-R.

The further tigecycline-susceptible clinical isolate, *E. cloacae* EC390 and its tigecycline-resistant counterpart, EC391, recovered from the same patient, were referred to ARMRL in 2009. Characterisation of these isolates confirmed their identity, tigecycline MICs, and PFGE profiling established that both isolates belonged to the same strain (Results section 3.2.2; Table 13; Figure 35b).

Since up-regulation of AcrAB was responsible for tigecycline resistance in clinical isolate TGC-R, efflux by this transporter was investigated as a possible mechanism of tigecycline resistance in clinical isolate EC391 by monitoring expression of *acrAB* using the same real-time RT-PCR assay (72). Overexpression of

the pump operon was identified in isolate EC391 compared with EC390 (Figure 38), once again implicating AcrAB in tigecycline resistance in *E. cloacae*.

As with isolate TGC-R, susceptibility to the aminoglycosides allowed for selection of Δ*acrB* mutants of EC391 (Table 13). However, in the case of EC391, a suicide plasmid-based approach was used to inactivate *acrB* due to the inefficiency of the pKOBEG-based method (Results section 3.2.5.2; Figure 34). The suicide plasmid pRSACRB (Figure 17) contained a kanamycin resistance cassette (which allowed for the selection of mutants using this agent) and the conditional origin of replication, R6Kγ (Results section 3.3.4). Interruption of *acrB* in EC391 with pRSACRB restored susceptibility to tigecycline and confirmed the role of AcrAB in resistance. This result is consistent with that of TGC-R as well as previous studies, which report that tigecycline is a substrate of this efflux system (127;200). To my knowledge, this is the first report of an *E. cloacae* gene being interrupted using this method.

The mechanism of AcrAB up-regulation in isolate EC391 was not investigated due to time constraints.

In summary, the *in vivo* emergence of tigecycline resistance in two isolates of *E. cloacae* was investigated. In both cases, up-regulation of the RND transporter AcrAB was responsible for the resistance. RamA was implicated in the up-regulation of AcrAB in one case though was not investigated in the other. In contrast to the *A. baumannii* cases, neither patient received tigecycline before the resistant isolates were recovered (Results section 3.2.1). Thus, factors other than tigecycline pressure can select for resistance to this agent in *E. cloacae*. The emergence of tigecycline resistance described in case 3 was associated with ciprofloxacin therapy. This is the first report of emergence of resistance to tigecycline associated with ciprofloxacin therapy, rather than tigecycline therapy. Ciprofloxacin is known to be a substrate of

AcrAB in *E. cloacae* (200) and it is possible that exposure to this agent selected for AcrAB up-regulation, which resulted in cross-resistance to tigecycline. The potential to select cross-resistance to relatively new antimicrobials such as tigecycline through the use of established front-line therapies is of concern in the clinic. Ciprofloxacin therapy may also have contributed to the emergence of resistance described in case 4 though the situation is less clear given that the patient received other drugs and that the organism was isolated only once, in contrast to case 3. In addition, the ciprofloxacin MIC for the tigecycline-resistant isolate, EC391 was not elevated compared with EC390 (Table 13) despite the overexpression of *acrAB* observed in the former and in contrast to the case 3 isolates. The reasons for this remain unclear. It could be that mutations in *acrB*, which altered the substrate specificity of the pump, were responsible though this would require experimental determination. Importantly, it is assumed that EC390 is the parent of EC391 although the possibility that the patient was concurrently infected with two variants of the same PFGE-defined strain cannot be excluded.

4.3. *S. marcescens*

Clinical isolate SM346 was referred to ARMRL in 2009 and was the only tigecycline-resistant clinical isolate of this species available for study. Characterisation of this isolate confirmed its identification and tigecycline-resistant phenotype (Results section 3.2; Table 15).

The mechanism(s) of tigecycline resistance in *S. marcescens* have not been described although, since up-regulation of RND transporters had been implicated in such resistance in other Enterobacteriaceae (127;128;224), this mechanism was investigated.

Real-time RT-PCR assays were designed to target the RND component gene of the three characterised RND systems of *S. marcescens*, namely SdeAB, SdeCDE and SdeXY (22;42;135). Expression of these genes was monitored in the tigecycline-susceptible type strain, *S. marcescens* NCTC 10211 and its final laboratory-selected, tigecycline-resistant derivative, 10211-10 (Materials and Methods section 2.21). Mutant 10211-10 overexpressed all of the three RND efflux systems studied compared with NCTC 10211, but the increase in expression of *sdeXY* was reproducibly higher than the modest increases for *sdeAB* and *sdeCDE* (Figures 50-52). Expression of *sdeXY* was also monitored in clinical isolate SM346, the intermediate mutant, 10211-6 and the tetracycline-selected, tigecycline-resistant derivative of NCTC 10211, 10211-TC7. These investigations identified an association between increasing tigecycline MIC and elevated expression of *sdeXY* (Results section 3.3.3; Figure 52), suggesting that tigecycline is a substrate of the SdeXY transporter, and pointing to a role for this efflux system in tigecycline resistance.

It was not possible to use clinical isolate SM346 in *sdeY* knockout studies due to its resistance to the aminoglycosides used to select for mutants (Table 15). Therefore, to confirm the role of SdeXY in tigecycline resistance, the *sdeY* gene was targeted for inactivation in the laboratory mutant, 10211-10 (Figure 53). Interruption of *sdeY* in 10211-10 by suicide plasmid pSMY2 restored susceptibility to tigecycline, confirming the role of SdeXY in tigecycline resistance in this mutant (Results section 3.3.3; Table 16; Figure 57).

The outer membrane channel(s) are poorly defined in *S. marcescens*, though the TolC homologue HasF is implicated as one exit portal in energy-dependent efflux (136). On this basis, the potential of HasF to act as the outer membrane channel in a functioning tripartite complex with SdeX and SdeY was investigated by insertional

inactivation of *hasF* in the laboratory mutant 10211-10 using the suicide plasmid pHASF and the same strategy employed to inactivate *sdeY* (Figure 54). Interruption of either *sdeY* or *hasF* reduced the MICs of tigecycline, ciprofloxacin, cefpirome, and tetracycline markedly, to below the values for the 'wild-type' parent (Tables 15 and 16). These data strongly suggest that up-regulated SdeXY-HasF efflux was responsible for tigecycline resistance in *S. marcescens*, and that intrinsic efflux pump activity is responsible for the lower susceptibility of the species to ciprofloxacin (modal MIC 0.125 mg/L compared with 0.016 mg/L for *E. coli*; EUCAST).

4.4. Tigecycline: six years in the clinic

Since its introduction into clinical use in 2005 there have been a number of concerning reports on the emergence of tigecycline resistance and non-susceptibility during therapy in Gram-negative (55;199;210) and, more rarely, Gram-positive species (113;275). Even before these there were the reports of emerging resistance observed during phase III trials (section 4).

Besides those described in this thesis, there have been two reports of resistance emerging during tigecycline therapy in *A. baumannii* (199;210). The first details two cases where patients developed bacteraemia while receiving tigecycline: (i) as empiric monotherapy after developing a fever following a lumbar laminectomy and (ii) for a wound infection and where tigecycline-resistant isolates of *A. baumannii* were recovered from blood cultures in both instances (MICs, 4 and 16 mg/L, respectively) (199). The authors observed potentiation of tigecycline activity in the presence of the EPI, PAβN, suggesting efflux as a mechanism of resistance (199). This report highlights the potential of tigecycline to select for resistant organisms in the bloodstream due to its relatively low C_{max}. Of note, both tigecycline-resistant isolates

were susceptible to imipenem. This is in contrast with the cases of emerging resistance in *A. baumannii* described in this thesis, where resistance emerged in a lineage resistant to carbapenems owing to production of an OXA carbapenemase (Table 11), and where both patients received tigecycline for an approved indication (Results section 3.1.1). The second literature report of emerging resistance in *A. baumannii* described a patient with HAP (not an approved indication) who was treated with tigecycline (210). *A. baumannii* was recovered from sputum and tigecycline MICs for the pre- and post-therapy isolates were 2 and 24 mg/L, respectively. Tigecycline MIC rises (0.75 to 2 mg/L) during tigecycline therapy were also noted in the case of a patient who received the drug for HAP and empyema caused by a KPC carbapenemase-producing strain of *K. pneumoniae* (55). In the UK, the non-susceptibility rate for tigecycline in *Klebsiella* spp. is high (17.7%) relative to other Enterobacteriaceae (111) and although the reason(s) for the MIC increase was not investigated, other reports have implicated up-regulation of AcrAB in *Klebsiella* as well as in the genera studied here (220;224).

Tigecycline is licensed for the treatment of cSSSI, cIAI and of CAP in the US. However, clinicians are tempted to use tigecycline for other, often severe infections because of its broad-spectrum activity and also because of the lack of therapeutic options, especially in the case of infections caused by MDR Gram-negative pathogens. Indeed, data from a recent South American study indicate that the majority of tigecycline prescriptions are for off-label indications (68.5%) in that region and that the most frequent off-label use was for VAP (53).

There are mixed reports on the clinical efficacy of tigecycline in the off-label treatment of severe infection, including HAP and VAP. In a retrospective study of tigecycline monotherapy for infections caused by MDR *A. baumannii* and *K.*

pneumoniae in Greece, overall successful clinical outcome was observed in 81.8% of cases and 90.5% in the HAP/VAP group (204). Another retrospective study of patients treated with tigecycline for *A. baumannii* infection demonstrated positive clinical outcome in 68% of cases, though the authors noted that three patients developed bacteraemia while receiving tigecycline which, in one case, was caused by *K. pneumoniae* (97). In 2010, the US FDA issued a Drug Safety Communication warning that there was an increased mortality risk associated with the use of tigecycline in the treatment of various serious infections compared to that of other drugs (262), further fuelling the debate on the efficacy of tigecycline in the treatment of such infections.

It is clear that there are legitimate concerns over the use of tigecycline for the treatment of serious infections caused by MDR pathogens and in some respects the drug has already proved to be a disappointment in this regard. There is hope that new tetracycline analogues, such as the fluorocycline, TP-434 (Tetraphase), which is currently entering phase II clinical trials, will be prove to be more efficacious. In a recent study, this compound displayed greater *in vitro* activity versus MDR Gram-negative organisms than tigecycline (90) and there is evidence that it has oral bioavailability in humans (141). However, there are currently no data on whether or not TP-434 is vulnerable to efflux by RND transporters.

4.5. Further work

Time constraints meant that detailed investigations of a number of interesting aspects were not possible. Although the molecular mechanism of tigecycline resistance was elucidated in each isolate studied, some important questions remain. Lines of enquiry that should be pursued if further funding were to become available are detailed below.

Although evidence exists that the two-component regulatory system, AdeRS controls expression of *adeABC* in *A. baumannii* (164), the data presented here (Results section 3.1.5) and elsewhere indicate that other regulatory mechanisms remain to be found (197). Evidence from studies of *E. coli* and other Gram-negative species suggests that the regulation of RND efflux systems is complex, often involving multiple regulatory elements (98). In addition to investigating the possibility of involvement of other regulatory systems, the precise mechanism of transcriptional control by AdeRS remains to be fully elucidated. For instance, it is unclear which specific ligand(s) activate AdeS and how amino acid substitutions that have been associated with constitutive *adeABC* expression actually affect the biological activity of the sensor kinase.

Comparative genomic analysis demonstrated considerable genetic differences between clinical isolates AB210 and AB211 (section 4.1.1). It seems likely that these differences will have phenotypic effects that extend beyond the antibiogram and that raise questions concerning the relative fitness of these isolates. It would be interesting to assess the *in vivo* performance of susceptible and resistant isolates using an animal model of *A. baumannii* infection such as that described by Peleg *et al.* (198). Analysis of the whole-genome sequence of AB211 revealed that the *mutS* gene was interrupted, suggesting that this isolate may display a hypermutator phenotype (section 4.1.1). This hypothesis should be experimentally investigated to assess the possible implications for the emergence of antibiotic resistance.

This study provided evidence that demonstrated, for the first time that, *acrAB* is part of the RamA regulon in *E. cloacae* (Results section 3.2.4). However, the mechanism(s) of RamA up-regulation remains to be elucidated and this should be investigated to gain a fuller understanding of the molecular events that can lead to

acrAB overexpression and hence tigecycline resistance. Such increased knowledge of global regulatory elements may also shed light on the reasons for the reduction in the MICs of some β-lactams observed for the laboratory-selected mutant, TGC-S7 (Table 13). This phenomenon was also observed for the *A. baumannii* laboratory-selected mutant, AB210-6 (Table 11) and is evidence for changes in global regulatory networks in the species.

Efflux as a mechanism of resistance to tigecycline in *S. marcescens* was investigated here and it was shown for the first time that the SdeXY-HasF complex was responsible for such resistance in a laboratory-selected mutant (Results section 3.3). Although real-time RT-PCR data indicated that this mechanism may also be responsible for resistance in a clinical isolate, this remains to be confirmed with knockout mutagenesis studies using tigecycline-resistant clinical isolates. In addition, the mechanism(s) of *sdeXY* overexpression remain obscure.

4.6. Conclusions

Tigecycline retains good *in vitro* activity against many problematic nosocomial Gram-negative pathogens. Despite concerns over its efficacy in the treatment of severe infections it is an important addition to the antimicrobial arsenal given the small number of new agents with any Gram-negative coverage entering clinical use. However, data presented here, as well as literature evidence, indicate that it is vulnerable to efflux by RND-type transporters, and that this mechanism often underlies mutational resistance in Enterobacteriaceae (127;128;220) and *A. baumannii* (197;223), as well as the intrinsic resistance of *P. aeruginosa* and *P. mirabilis* (61;267). In contrast to the acquired tetracycline resistance mechanisms described, there is no literature evidence of horizontal transfer of tigecycline resistance. The results of this study support the hypothesis that tigecycline resistance in clinical isolates of Gram-negative bacteria arises as a result of the up-regulated activity of intrinsic efflux systems. Thus, there exists the potential for any strain to develop resistance that possess a functioning RND efflux system of which tigecycline is a substrate. Despite this, tigecycline-resistant isolates of some species, notably *E. coli*, are encountered only rarely in the clinic. Further studies are necessary to gain a fuller understanding of the factors responsible for the emergence of efflux-mediated tigecycline resistance.

RND-type transporters are ubiquitous in Gram-negative species and their up-regulation can result in resistance to multiple antimicrobial agents, as demonstrated here. Since agents other than tigecycline can select for up-regulated efflux, limiting the use of tigecycline alone may not prevent further cases of resistance emerging.

References

(1) Abril C, Brodard I, Perreten V. Two novel antibiotic resistance genes, *tet*(44) and *ant(6)-Ib*, are located within a transferable pathogenicity island in *Campylobacter fetus* subsp. *fetus*. Antimicrob Agents Chemother 2010; 54 (7): 3052-3055.

(2) Adams MD, Chan ER, Molyneaux ND, Bonomo RA. Genomewide analysis of divergence of antibiotic resistance determinants in closely related isolates of *Acinetobacter baumannii*. Antimicrob Agents Chemother 2010; 54 (9): 3569-3577.

(3) Akama H, Kanemaki M, Yoshimura M, Tsukihara T, Kashiwagi T, Yoneyama H et al. Crystal structure of the drug discharge outer membrane protein, OprM, of *Pseudomonas aeruginosa*: dual modes of membrane anchoring and occluded cavity end. J Biol Chem 2004; 279 (51): 52816-52819.

(4) Akama H, Matsuura T, Kashiwagi S, Yoneyama H, Narita S, Tsukihara T et al. Crystal structure of the membrane fusion protein, MexA, of the multidrug transporter in *Pseudomonas aeruginosa*. J Biol Chem 2004; 279 (25): 25939-25942.

(5) Aleksandrov A, Simonson T. Molecular dynamics simulations of the 30S ribosomal subunit reveal a preferred tetracycline binding site. J Am Chem Soc 2008; 130 (4): 1114-1115.

(6) Alekshun MN, Levy SB. Regulation of chromosomally mediated multiple antibiotic resistance: the mar regulon. Antimicrob Agents Chemother 1997; 41 (10): 2067-2075.

(7) Alekshun MN, Levy SB. Alteration of the repressor activity of MarR, the negative regulator of the *Escherichia coli marRAB* locus, by multiple chemicals in vitro. J Bacteriol 1999; 181 (15): 4669-4672.

(8) Andersen C, Koronakis E, Bokma E, Eswaran J, Humphreys D, Hughes C et al. Transition to the open state of the TolC periplasmic tunnel entrance. Proc Natl Acad Sci U S A 2002; 99 (17): 11103-11108.

(9) Andrews JM. BSAC standardized disc susceptibility testing method (version 10). J Antimicrob Chemother 2011; doi: 10.1093/jac/dkr359.

(10) Anokhina MM, Barta A, Nierhaus KH, Spiridonova VA, Kopylov AM. Mapping of the second tetracycline binding site on the ribosomal small subunit of *E.coli*. Nucleic Acids Res 2004; 32 (8): 2594-2597.

(11) Anthony KB, Fishman NO, Linkin DR, Gasink LB, Edelstein PH, Lautenbach E. Clinical and microbiological outcomes of serious infections with multidrug-resistant gram-negative organisms treated with tigecycline. Clin Infect Dis 2008; 46 (4): 567-570.

(12) Aono R, Tsukagoshi N, Yamamoto M. Involvement of outer membrane protein TolC, a possible member of the *mar-sox* regulon, in maintenance and improvement of organic solvent tolerance of *Escherichia coli* K-12. J Bacteriol 1998; 180 (4): 938-944.

(13) Appleman JA, Stewart V. Mutational analysis of a conserved signal-transducing element: the HAMP linker of the *Escherichia coli* nitrate sensor NarX. J Bacteriol 2003; 185 (1): 89-97.

(14) Aranda J, Poza M, Pardo BG, Rumbo S, Rumbo C, Parreira JR et al. A rapid and simple method for constructing stable mutants of *Acinetobacter baumannii*. BMC Microbiol 2010; 10: 279.

(15) Argast M, Beck CF. Tetracycline uptake by susceptible *Escherichia coli* cells. Arch Microbiol 1985; 141 (3): 260-265.

(16) Bailey AM, Ivens A, Kingsley R, Cottell JL, Wain J, Piddock LJ. RamA, a member of the AraC/XylS family, influences both virulence and efflux in *Salmonella enterica* serovar Typhimurium. J Bacteriol 2010; 192 (6): 1607-1616.

(17) Balbas P, Gosset G. Chromosomal editing in *Escherichia coli*. Vectors for DNA integration and excision. Mol Biotechnol 2001; 19 (1): 1-12.

(18) Baranova N, Nikaido H. The *baeSR* two-component regulatory system activates transcription of the yegMNOB (mdtABCD) transporter gene cluster in *Escherichia coli* and increases its resistance to novobiocin and deoxycholate. J Bacteriol 2002; 184 (15): 4168-4176.

(19) Bassetti M, Ginocchio F, Mikulska M. New treatment options against Gram-negative organisms. Crit Care 2011; 15 (2): 215.

(20) Bauer G, Berens C, Projan SJ, Hillen W. Comparison of tetracycline and tigecycline binding to ribosomes mapped by dimethylsulphate and drug-

directed Fe2+ cleavage of 16S rRNA. J Antimicrob Chemother 2004; 53 (4): 592-599.

(21) Bazzini S, Udine C, Sass A, Pasca MR, Longo F, Emiliani G et al. Deciphering the role of RND efflux transporters in *Burkholderia cenocepacia*. PLoS ONE 2011; 6 (4): e18902.

(22) Begic S, Worobec EA. Characterization of the *Serratia marcescens* SdeCDE multidrug efflux pump studied via gene knockout mutagenesis. Can J Microbiol 2008; 54 (5): 411-416.

(23) Begic S, Worobec EA. The role of the *Serratia marcescens* SdeAB multidrug efflux pump and TolC homologue in fluoroquinolone resistance studied via gene-knockout mutagenesis. Microbiology 2008; 154 (Pt 2): 454-461.

(24) Bergallo C, Jasovich A, Teglia O, Oliva ME, Lentnek A, de Wouters L et al. Safety and efficacy of intravenous tigecycline in treatment of community-acquired pneumonia: results from a double-blind randomized phase 3 comparison study with levofloxacin. Diagn Microbiol Infect Dis 2009; 63 (1): 52-61.

(25) Bergeron J, Ammirati M, Danley D, James L, Norcia M, Retsema J et al. Glycylcyclines bind to the high-affinity tetracycline ribosomal binding site and evade Tet(M)- and Tet(O)-mediated ribosomal protection. Antimicrob Agents Chemother 1996; 40 (9): 2226-2228.

(26) Bernard P, Couturier M. Cell killing by the F plasmid CcdB protein involves poisoning of DNA-topoisomerase II complexes. J Mol Biol 1992; 226 (3): 735-745.

(27) Bina XR, Lavine CL, Miller MA, Bina JE. The AcrAB RND efflux system from the live vaccine strain of *Francisella tularensis* is a multiple drug efflux system that is required for virulence in mice. FEMS Microbiol Lett 2008; 279 (2): 226-233.

(28) Bohnert JA, Schuster S, Fahnrich E, Trittler R, Kern WV. Altered spectrum of multidrug resistance associated with a single point mutation in the *Escherichia coli* RND-type MDR efflux pump YhiV (MdtF). J Antimicrob Chemother 2007; 59 (6): 1216-1222.

(29) Bohnert JA, Schuster S, Seeger MA, Fahnrich E, Pos KM, Kern WV. Site-directed mutagenesis reveals putative substrate binding residues in the *Escherichia coli* RND efflux pump AcrB. J Bacteriol 2008; 190 (24): 8225-8229.

(30) Bonomo RA, Szabo D. Mechanisms of multidrug resistance in *Acinetobacter* species and *Pseudomonas aeruginosa*. Clin Infect Dis 2006; 43 Suppl 2: S49-S56.

(31) Bradford PA, Weaver-Sands DT, Petersen PJ. *In vitro* activity of tigecycline against isolates from patients enrolled in phase 3 clinical trials of treatment for complicated skin and skin-structure infections and complicated intra-abdominal infections. Clin Infect Dis 2005; 41 Suppl 5: S315-S332.

(32) Bratu S, Landman D, Martin DA, Georgescu C, Quale J. Correlation of antimicrobial resistance with beta-lactamases, the OmpA-like porin, and efflux pumps in clinical isolates of *Acinetobacter baumannii* endemic to New York City. Antimicrob Agents Chemother 2008; 52 (9): 2999-3005.

(33) Breedt J, Teras J, Gardovskis J, Maritz FJ, Vaasna T, Ross DP et al. Safety and efficacy of tigecycline in treatment of skin and skin structure infections: results of a double-blind phase 3 comparison study with vancomycin-aztreonam. Antimicrob Agents Chemother 2005; 49 (11): 4658-4666.

(34) Brodersen DE, Clemons WM, Jr., Carter AP, Morgan-Warren RJ, Wimberly BT, Ramakrishnan V. The structural basis for the action of the antibiotics tetracycline, pactamycin, and hygromycin B on the 30S ribosomal subunit. Cell 2000; 103 (7): 1143-1154.

(35) Brown MG, Mitchell EH, Balkwill DL. Tet 42, a novel tetracycline resistance determinant isolated from deep terrestrial subsurface bacteria. Antimicrob Agents Chemother 2008; 52 (12): 4518-4521.

(36) Buckley AM, Webber MA, Cooles S, Randall LP, La Ragione RM, Woodward MJ et al. The AcrAB-TolC efflux system of *Salmonella enterica* serovar Typhimurium plays a role in pathogenesis. Cell Microbiol 2006; 8 (5): 847-856.

(37) Bunikis I, Denker K, Ostberg Y, Andersen C, Benz R, Bergstrom S. An RND-type efflux system in *Borrelia burgdorferi* is involved in virulence and resistance to antimicrobial compounds. PLoS Pathog 2008; 4 (2): e1000009.

(38) Casino P, Rubio V, Marina A. The mechanism of signal transduction by two-component systems. Curr Opin Struct Biol 2010; 20 (6): 763-771.

(39) Chan YY, Chua KL. The *Burkholderia pseudomallei* BpeAB-OprB efflux pump: expression and impact on quorum sensing and virulence. J Bacteriol 2005; 187 (14): 4707-4719.

(40) Chang HC, Wei YF, Dijkshoorn L, Vaneechoutte M, Tang CT, Chang TC. Species-level identification of isolates of the *Acinetobacter calcoaceticus-Acinetobacter baumannii* complex by sequence analysis of the 16S-23S rRNA gene spacer region. J Clin Microbiol 2005; 43 (4): 1632-1639.

(41) Chaveroche MK, Ghigo JM, d'Enfert C. A rapid method for efficient gene replacement in the filamentous fungus *Aspergillus nidulans*. Nucleic Acids Res 2000; 28 (22): E97.

(42) Chen J, Kuroda T, Huda MN, Mizushima T, Tsuchiya T. An RND-type multidrug efflux pump SdeXY from *Serratia marcescens*. J Antimicrob Chemother 2003; 52 (2): 176-179.

(43) Chen L, Chen ZL, Liu JH, Zeng ZL, Ma JY, Jiang HX. Emergence of RmtB methylase-producing *Escherichia coli* and *Enterobacter cloacae* isolates from pigs in China. J Antimicrob Chemother 2007; 59 (5): 880-885.

(44) Chopra I, Hawkey PM, Hinton M. Tetracyclines, molecular and clinical aspects. J Antimicrob Chemother 1992; 29 (3): 245-277.

(45) Chopra I, Roberts M. Tetracycline antibiotics: mode of action, applications, molecular biology, and epidemiology of bacterial resistance. Microbiol Mol Biol Rev 2001; 65 (2): 232-260.

(46) Chu YW, Chau SL, Houang ET. Presence of active efflux systems AdeABC, AdeDE and AdeXYZ in different *Acinetobacter* genomic DNA groups. J Med Microbiol 2006; 55 (Pt 4): 477-478.

(47) Chubiz LM, Rao CV. Aromatic acid metabolites of *Escherichia coli* K-12 can induce the *marRAB* operon. J Bacteriol 2010; 192 (18): 4786-4789.

(48) Clewell DB, Flannagan SE, Jaworski DD. Unconstrained bacterial promiscuity: the Tn916-Tn1545 family of conjugative transposons. Trends Microbiol 1995; 3 (6): 229-236.

(49) Coelho JM, Turton JF, Kaufmann ME, Glover J, Woodford N, Warner M et al. Occurrence of carbapenem-resistant *Acinetobacter baumannii* clones at multiple hospitals in London and Southeast England. J Clin Microbiol 2006; 44 (10): 3623-3627.

(50) Connell SR, Tracz DM, Nierhaus KH, Taylor DE. Ribosomal protection proteins and their mechanism of tetracycline resistance. Antimicrob Agents Chemother 2003; 47 (12): 3675-3681.

(51) Coyne S, Guigon G, Courvalin P, Perichon B. Screening and quantification of the expression of antibiotic resistance genes in *Acinetobacter baumannii* with a microarray. Antimicrob Agents Chemother 2010; 54 (1): 333-340.

(52) Coyne S, Rosenfeld N, Lambert T, Courvalin P, Perichon B. Overexpression of resistance-nodulation-cell division pump AdeFGH confers multidrug resistance in *Acinetobacter baumannii*. Antimicrob Agents Chemother 2010; 54 (10): 4389-4393.

(53) Curcio D, Vargas SW, Ugarte US, Varon F, Rojas SJ, Paz CC et al. Tigecycline treatment of critically ill patients: the Latin user experience. Curr Clin Pharmacol 2011; 6 (1): 18-25.

(54) Dailidiene D, Bertoli MT, Miciuleviciene J, Mukhopadhyay AK, Dailide G, Pascasio MA et al. Emergence of tetracycline resistance in *Helicobacter pylori*: multiple mutational changes in 16S ribosomal DNA and other genetic loci. Antimicrob Agents Chemother 2002; 46 (12): 3940-3946.

(55) Daly MW, Riddle DJ, Ledeboer NA, Dunne WM, Ritchie DJ. Tigecycline for treatment of pneumonia and empyema caused by carbapenemase-producing *Klebsiella pneumoniae*. Pharmacotherapy 2007; 27 (7): 1052-1057.

(56) Damier-Piolle L, Magnet S, Bremont S, Lambert T, Courvalin P. AdeIJK, a resistance-nodulation-cell division pump effluxing multiple antibiotics in *Acinetobacter baumannii*. Antimicrob Agents Chemother 2008; 52 (2): 557-562.

(57) Dartois N, Castaing N, Gandjini H, Cooper A. Tigecycline versus levofloxacin for the treatment of community-acquired pneumonia: European experience. J Chemother 2008; 20 Suppl 1: 28-35.

(58) Daurel C, Fiant AL, Bremont S, Courvalin P, Leclercq R. Emergence of an *Enterobacter hormaechei* strain with reduced susceptibility to tigecycline under tigecycline therapy. Antimicrob Agents Chemother 2009; 53 (11): 4953-4954.

(59) David MD, Gill MJ. Potential for underdosing and emergence of resistance in *Acinetobacter baumannii* during treatment with colistin. J Antimicrob Chemother 2008; 61 (4): 962-964.

(60) De Rossi E, Blokpoel MC, Cantoni R, Branzoni M, Riccardi G, Young DB et al. Molecular cloning and functional analysis of a novel tetracycline resistance determinant, *tet*(V), from *Mycobacterium smegmatis*. Antimicrob Agents Chemother 1998; 42 (8): 1931-1937.

(61) Dean CR, Visalli MA, Projan SJ, Sum PE, Bradford PA. Efflux-mediated resistance to tigecycline (GAR-936) in *Pseudomonas aeruginosa* PAO1. Antimicrob Agents Chemother 2003; 47 (3): 972-978.

(62) Deguchi T, Yasuda M, Nakano M, Ozeki S, Kanematsu E, Nishino Y et al. Detection of mutations in the *gyrA* and *parC* genes in quinolone-resistant clinical isolates of *Enterobacter cloacae*. J Antimicrob Chemother 1997; 40 (4): 543-549.

(63) Del Mar TM, Beceiro A, Perez A, Velasco D, Moure R, Villanueva R et al. Cloning and functional analysis of the gene encoding the 33- to 36-kilodalton outer membrane protein associated with carbapenem resistance in *Acinetobacter baumannii*. Antimicrob Agents Chemother 2005; 49 (12): 5172-5175.

(64) Depardieu F, Podglajen I, Leclercq R, Collatz E, Courvalin P. Modes and modulations of antibiotic resistance gene expression. Clin Microbiol Rev 2007; 20 (1): 79-114.

(65) Dessi A, Puddu M, Testa M, Marcialis MA, Pintus MC, Fanos V. *Serratia marcescens* infections and outbreaks in neonatal intensive care units. J Chemother 2009; 21 (5): 493-499.

(66) Diaz-Torres ML, McNab R, Spratt DA, Villedieu A, Hunt N, Wilson M et al. Novel tetracycline resistance determinant from the oral metagenome. Antimicrob Agents Chemother 2003; 47 (4): 1430-1432.

(67) Dijkshoorn L, Aucken H, Gerner-Smidt P, Janssen P, Kaufmann ME, Garaizar J et al. Comparison of outbreak and nonoutbreak *Acinetobacter baumannii* strains by genotypic and phenotypic methods. J Clin Microbiol 1996; 34 (6): 1519-1525.

(68) Dijkshoorn L, Nemec A, Seifert H. An increasing threat in hospitals: multidrug-resistant *Acinetobacter baumannii*. Nat Rev Microbiol 2007; 5 (12): 939-951.

(69) Doi Y, Yokoyama K, Yamane K, Wachino J, Shibata N, Yagi T et al. Plasmid-mediated 16S rRNA methylase in *Serratia marcescens* conferring high-level resistance to aminoglycosides. Antimicrob Agents Chemother 2004; 48 (2): 491-496.

(70) Domain F, Bina XR, Levy SB. Transketolase A, an enzyme in central metabolism, derepresses the *marRAB* multiple antibiotic resistance operon of

Escherichia coli by interaction with MarR. Mol Microbiol 2007; 66 (2): 383-394.

(71) Domain F, Levy SB. GyrA interacts with MarR to reduce repression of the *marRAB* operon in *Escherichia coli*. J Bacteriol 2010; 192 (4): 942-948.

(72) Doumith M, Ellington MJ, Livermore DM, Woodford N. Molecular mechanisms disrupting porin expression in ertapenem-resistant *Klebsiella* and *Enterobacter* spp. clinical isolates from the UK. J Antimicrob Chemother 2009; 63 (4): 659-667.

(73) Drew D, Klepsch MM, Newstead S, Flaig R, De Gier JW, Iwata S et al. The structure of the efflux pump AcrB in complex with bile acid. Mol Membr Biol 2008; 25 (8): 677-682.

(74) Edgar R, Bibi E. MdfA, an *Escherichia coli* multidrug resistance protein with an extraordinarily broad spectrum of drug recognition. J Bacteriol 1997; 179 (7): 2274-2280.

(75) Elkins CA, Mullis LB. Mammalian steroid hormones are substrates for the major RND- and MFS-type tripartite multidrug efflux pumps of *Escherichia coli*. J Bacteriol 2006; 188 (3): 1191-1195.

(76) Elkins CA, Nikaido H. Substrate specificity of the RND-type multidrug efflux pumps AcrB and AcrD of Escherichia coli is determined predominantly by two large periplasmic loops. J Bacteriol 2002; 184 (23): 6490-6498.

(77) Ellis-Grosse EJ, Babinchak T, Dartois N, Rose G, Loh E. The efficacy and safety of tigecycline in the treatment of skin and skin-structure infections: results of 2 double-blind phase 3 comparison studies with vancomycin-aztreonam. Clin Infect Dis 2005; 41 Suppl 5: S341-S353.

(78) Esterly J, Richardson CL, Eltoukhy NS, Qi C, Scheetz MH. Genetic mechanisms of antimicrobial resistance of *Acinetobacter baumannii* . Ann Pharmacother 2011; doi: 10.1345/aph.1P084.

(79) Fagon JY, Chastre J, Domart Y, Trouillet JL, Gibert C. Mortality due to ventilator-associated pneumonia or colonization with *Pseudomonas* or *Acinetobacter* species: assessment by quantitative culture of samples obtained by a protected specimen brush. Clin Infect Dis 1996; 23 (3): 538-542.

(80) Federici L, Du D, Walas F, Matsumura H, Fernandez-Recio J, McKeegan KS et al. The crystal structure of the outer membrane protein VceC from the bacterial pathogen *Vibrio cholerae* at 1.8 A resolution. J Biol Chem 2005; 280 (15): 15307-15314.

(81) Ferhat M, Atlan D, Vianney A, Lazzaroni JC, Doublet P, Gilbert C. The TolC protein of *Legionella pneumophila* plays a major role in multi-drug resistance and the early steps of host invasion. PLoS ONE 2009; 4 (11): e7732.

(82) Fernandez-Mazarrasa C, Mazarrasa O, Calvo J, del Arco A, Martinez-Martinez L. High concentrations of manganese in Mueller-Hinton agar

increase MICs of tigecycline determined by Etest. J Clin Microbiol 2009; 47 (3): 827-829.

(83) FINLAND M, JONES WF, Jr., BARNES MW. Occurrence of serious bacterial infections since introduction of antibacterial agents. J Am Med Assoc 1959; 170: 2188-2197.

(84) Fishbain J, Peleg AY. Treatment of *Acinetobacter* infections. Clin Infect Dis 2010; 51 (1): 79-84.

(85) Fleming A. On the antibacterial action of cultures of a penicillium, with special reference to their use in the isolation of *B. influenzae*. 1929. Bull World Health Organ 2001; 79 (8): 780-790.

(86) Fluit AC, Florijn A, Verhoef J, Milatovic D. Presence of tetracycline resistance determinants and susceptibility to tigecycline and minocycline. Antimicrob Agents Chemother 2005; 49 (4): 1636-1638.

(87) Fomin P, Beuran M, Gradauskas A, Barauskas G, Datsenko A, Dartois N et al. Tigecycline is efficacious in the treatment of complicated intra-abdominal infections. Int J Surg 2005; 3 (1): 35-47.

(88) Fralick JA. Evidence that TolC is required for functioning of the Mar/AcrAB efflux pump of *Escherichia coli*. J Bacteriol 1996; 178 (19): 5803-5805.

(89) Freire AT, Melnyk V, Kim MJ, Datsenko O, Dzyublik O, Glumcher F et al. Comparison of tigecycline with imipenem/cilastatin for the treatment of hospital-acquired pneumonia. Diagn Microbiol Infect Dis 2010; 68 (2): 140-151.

(90) Fyfe C, Grossman T, O'Brien W, Achorn C, Sutcliffe J. The novel broad-spectrum fluorocycline TP-434 is active against MDR Gram-negative pathogens. In: Abstracts of the 21st ECCMID/27th ICC, Milan, Italy, 7-10 May 2011. Clin Microbiol Infect 2011; 17 (S4): S108-S668.

(91) Gales AC, Jones RN. Antimicrobial activity and spectrum of the new glycylcycline, GAR-936 tested against 1,203 recent clinical bacterial isolates. Diagn Microbiol Infect Dis 2000; 36 (1): 19-36.

(92) Galimand M, Courvalin P, Lambert T. Plasmid-mediated high-level resistance to aminoglycosides in Enterobacteriaceae due to 16S rRNA methylation. Antimicrob Agents Chemother 2003; 47 (8): 2565-2571.

(93) Gay P, Le Coq D, Steinmetz M, Berkelman T, Kado CI. Positive selection procedure for entrapment of insertion sequence elements in gram-negative bacteria. J Bacteriol 1985; 164 (2): 918-921.

(94) Gerner-Smidt P, Tjernberg I, Ursing J. Reliability of phenotypic tests for identification of *Acinetobacter* species. J Clin Microbiol 1991; 29 (2): 277-282.

(95) Gerrits MM, Berning M, Van Vliet AH, Kuipers EJ, Kusters JG. Effects of 16S rRNA gene mutations on tetracycline resistance in *Helicobacter pylori*. Antimicrob Agents Chemother 2003; 47 (9): 2984-2986.

(96) Gerrits MM, de Zoete MR, Arents NL, Kuipers EJ, Kusters JG. 16S rRNA mutation-mediated tetracycline resistance in *Helicobacter pylori*. Antimicrob Agents Chemother 2002; 46 (9): 2996-3000.

(97) Gordon NC, Wareham DW. A review of clinical and microbiological outcomes following treatment of infections involving multidrug-resistant *Acinetobacter baumannii* with tigecycline. J Antimicrob Chemother 2009; 63 (4): 775-780.

(98) Grkovic S, Brown MH, Skurray RA. Regulation of bacterial drug export systems. Microbiol Mol Biol Rev 2002; 66 (4): 671-701.

(99) Hachler H, Cohen SP, Levy SB. *marA*, a regulated locus which controls expression of chromosomal multiple antibiotic resistance in *Escherichia coli*. J Bacteriol 1991; 173 (17): 5532-5538.

(100) Hejazi A, Falkiner FR. *Serratia marcescens*. J Med Microbiol 1997; 46 (11): 903-912.

(101) Hentschke M, Christner M, Sobottka I, Aepfelbacher M, Rohde H. Combined *ramR* mutation and presence of a Tn1721-associated tet(A) variant in a clinical isolate of *Salmonella enterica* serovar Hadar resistant to tigecycline. Antimicrob Agents Chemother 2010; 54 (3): 1319-1322.

(102) Hentschke M, Wolters M, Sobottka I, Rohde H, Aepfelbacher M. *ramR* mutations in clinical isolates of *Klebsiella pneumoniae* with reduced susceptibility to tigecycline. Antimicrob Agents Chemother 2010; 54 (6): 2720-2723.

(103) Hentschke M, Wolters M, Sobottka I, Rohde H, Aepfelbacher M. *ramR* mutations in clinical isolates of *Klebsiella pneumoniae* with reduced susceptibility to tigecycline. Antimicrob Agents Chemother 2010; 54 (6): 2720-2723.

(104) Henwood CJ, Gatward T, Warner M, James D, Stockdale MW, Spence RP et al. Antibiotic resistance among clinical isolates of *Acinetobacter* in the UK, and *in vitro* evaluation of tigecycline (GAR-936). J Antimicrob Chemother 2002; 49 (3): 479-487.

(105) Higgins MK, Bokma E, Koronakis E, Hughes C, Koronakis V. Structure of the periplasmic component of a bacterial drug efflux pump. Proc Natl Acad Sci U S A 2004; 101 (27): 9994-9999.

(106) Higgins PG, Dammhayn C, Hackel M, Seifert H. Global spread of carbapenem-resistant *Acinetobacter baumannii*. J Antimicrob Chemother 2010; 65 (2): 233-238.

(107) Hirakata Y, Srikumar R, Poole K, Gotoh N, Suematsu T, Kohno S et al. Multidrug efflux systems play an important role in the invasiveness of *Pseudomonas aeruginosa*. J Exp Med 2002; 196 (1): 109-118.

(108) Hirakawa H, Inazumi Y, Masaki T, Hirata T, Yamaguchi A. Indole induces the expression of multidrug exporter genes in *Escherichia coli*. Mol Microbiol 2005; 55 (4): 1113-1126.

(109) Hirakawa H, Takumi-Kobayashi A, Theisen U, Hirata T, Nishino K, Yamaguchi A. AcrS/EnvR represses expression of the *acrAB* multidrug efflux genes in *Escherichia coli*. J Bacteriol 2008; 190 (18): 6276-6279.

(110) Ho PL, Ho AY, Chow KH, Lai EL, Ching P, Seto WH. Epidemiology and clonality of multidrug-resistant *Acinetobacter baumannii* from a healthcare region in Hong Kong. J Hosp Infect 2010; 74 (4): 358-364.

(111) Hope R, Mushtaq S, James D, Pllana T, Warner M, Livermore DM. Tigecycline activity: low resistance rates but problematic disc breakpoints revealed by a multicentre sentinel survey in the UK. J Antimicrob Chemother 2010; 65 (12): 2602-2609.

(112) Hope R, Warner M, Mushtaq S, Ward ME, Parsons T, Livermore DM. Effect of medium type, age and aeration on the MICs of tigecycline and classical tetracyclines. J Antimicrob Chemother 2005; 56 (6): 1042-1046.

(113) Hornsey M, Wareham DW, Turton J, Martin K, Pike R, David M et al. Emergence of tigecycline and linezolid resistance in a vancomycin-resistant isolate of *Enterococcus faecium*. In: Abstracts of the 21st ECCMID/27th ICC, Milan, Italy, 7-10 May 2011. Clin Microbiol Infect 2011; 17 (S4): S233-S234.

(114) Hossain A, Ferraro MJ, Pino RM, Dew RB, III, Moland ES, Lockhart TJ et al. Plasmid-mediated carbapenem-hydrolyzing enzyme KPC-2 in an *Enterobacter* sp. Antimicrob Agents Chemother 2004; 48 (11): 4438-4440.

(115) Hu Z, Zhao WH. Identification of plasmid- and integron-borne *blaIMP-1* and *blaIMP-10* in clinical isolates of *Serratia marcescens*. J Med Microbiol 2009; 58 (Pt 2): 217-221.

(116) Huang L, Sun L, Xu G, Xia T. Differential susceptibility to carbapenems due to the AdeABC efflux pump among nosocomial outbreak isolates of *Acinetobacter baumannii* in a Chinese hospital. Diagn Microbiol Infect Dis 2008; 62 (3): 326-332.

(117) Huys G, Cnockaert M, Nemec A, Swings J. Sequence-based typing of *adeB* as a potential tool to identify intraspecific groups among clinical strains of multidrug-resistant *Acinetobacter baumannii*. J Clin Microbiol 2005; 43 (10): 5327-5331.

(118) Huys G, Cnockaert M, Vaneechoutte M, Woodford N, Nemec A, Dijkshoorn L et al. Distribution of tetracycline resistance genes in genotypically related and unrelated multiresistant *Acinetobacter baumannii* strains from different European hospitals. Res Microbiol 2005; 156 (3): 348-355.

(119) Iredell J, Thomas L, Power D, Mendes E. Tigecycline resistance in Australian antibiotic-resistant Gram-negative bacteria. J Antimicrob Chemother 2007; 59 (4): 816-818.

(120) Jacoby GA. AmpC beta-lactamases. Clin Microbiol Rev 2009; 22 (1): 161-82.

(121) Jawad A, Seifert H, Snelling AM, Heritage J, Hawkey PM. Survival of *Acinetobacter baumannii* on dry surfaces: comparison of outbreak and sporadic isolates. J Clin Microbiol 1998; 36 (7): 1938-1941.

(122) Jeong SH, Lee K, Chong Y, Yum JH, Lee SH, Choi HJ et al. Characterization of a new integron containing VIM-2, a metallo- beta-lactamase gene cassette, in a clinical isolate of *Enterobacter cloacae*. J Antimicrob Chemother 2003; 51 (2): 397-400.

(123) Jerse AE, Sharma ND, Simms AN, Crow ET, Snyder LA, Shafer WM. A gonococcal efflux pump system enhances bacterial survival in a female

mouse model of genital tract infection. Infect Immun 2003; 71 (10): 5576-5582.

(124) Joly-Guillou ML. Clinical impact and pathogenicity of *Acinetobacter*. Clin Microbiol Infect 2005; 11 (11): 868-873.

(125) Jones CS, Osborne DJ, Stanley J. Enterobacterial tetracycline resistance in relation to plasmid incompatibility. Mol Cell Probes 1992; 6 (4): 313-317.

(126) Kaase M, Nordmann P, Wichelhaus TA, Gatermann SG, Bonnin RA, Poirel L. NDM-2 carbapenemase in *Acinetobacter baumannii* from Egypt. J Antimicrob Chemother 2011; 66 (6): 1260-1262.

(127) Keeney D, Ruzin A, Bradford PA. RamA, a Transcriptional Regulator, and AcrAB, an RND-Type Efflux Pump, are Associated with Decreased Susceptibility to Tigecycline in *Enterobacter cloacae*. Microb Drug Resist 2007; 13 (1): 1-6.

(128) Keeney D, Ruzin A, McAleese F, Murphy E, Bradford PA. MarA-mediated overexpression of the AcrAB efflux pump results in decreased susceptibility to tigecycline in *Escherichia coli*. J Antimicrob Chemother 2008; 61 (1): 46-53.

(129) Kim JH, Cho EH, Kim KS, Kim HY, Kim YM. Cloning and nucleotide sequence of the DNA gyrase gyrA gene from *Serratia marcescens* and characterization of mutations in gyrA of quinolone-resistant clinical isolates. Antimicrob Agents Chemother 1998; 42 (1): 190-193.

(130) Kobayashi N, Nishino K, Yamaguchi A. Novel macrolide-specific ABC-type efflux transporter in *Escherichia coli*. J Bacteriol 2001; 183 (19): 5639-5644.

(131) Kobayashi T, Nonaka L, Maruyama F, Suzuki S. Molecular evidence for the ancient origin of the ribosomal protection protein that mediates tetracycline resistance in bacteria. J Mol Evol 2007; 65 (3): 228-235.

(132) Kolter R, Inuzuka M, Helinski DR. Trans-complementation-dependent replication of a low molecular weight origin fragment from plasmid R6K. Cell 1978; 15 (4): 1199-1208.

(133) Komatsu T, Ohta M, Kido N, Arakawa Y, Ito H, Mizuno T et al. Molecular characterization of an *Enterobacter cloacae* gene (*romA*) which pleiotropically inhibits the expression of *Escherichia coli* outer membrane proteins. J Bacteriol 1990; 172 (7): 4082-4089.

(134) Koronakis V, Sharff A, Koronakis E, Luisi B, Hughes C. Crystal structure of the bacterial membrane protein TolC central to multidrug efflux and protein export. Nature 2000; 405 (6789): 914-919.

(135) Kumar A, Worobec EA. Cloning, sequencing, and characterization of the SdeAB multidrug efflux pump of *Serratia marcescens*. Antimicrob Agents Chemother 2005; 49 (4): 1495-1501.

(136) Kumar A, Worobec EA. HasF, a TolC-homolog of *Serratia marcescens*, is involved in energy-dependent efflux. Can J Microbiol 2005; 51(6):497-500.

(137) Kumarasamy KK, Toleman MA, Walsh TR, Bagaria J, Butt F, Balakrishnan R et al. Emergence of a new antibiotic resistance mechanism in India, Pakistan, and the UK: a molecular, biological, and epidemiological study. Lancet Infect Dis 2010; 10 (9): 597-602.

(138) Lee HK, Park YJ, Kim JY, Chang E, Cho SG, Chae HS et al. Prevalence of decreased susceptibility to carbapenems among *Serratia marcescens*, *Enterobacter cloacae*, and *Citrobacter freundii* and investigation of carbapenemases. Diagn Microbiol Infect Dis 2005; 52 (4): 331-336.

(139) Lee Y, Yum JH, Kim CK, Yong D, Jeon EH, Jeong SH et al. Role of OXA-23 and AdeABC efflux pump for acquiring carbapenem resistance in an *Acinetobacter baumannii* strain carrying the *blaOXA-66* gene. Ann Clin Lab Sci 2010; 40 (1): 43-48.

(140) Lee YT, Turton JF, Chen TL, Wu RC, Chang WC, Fung CP et al. First identification of *blaOXA-51-like* in non-baumannii *Acinetobacter* spp. J Chemother 2009; 21 (5): 514-520.

(141) Leighton A, Zupanets I, Bezugla N, Plamondon L, Macdonald G, Sutcliffe J. Broad-spectrum fluorocycline TP-434 has oral bioavailability in humans. In: Abstracts of the 21st ECCMID/27th ICC, Milan, Italy, 7-10 May 2011. Clin Microbiol Infect 2011; 17 (S4): S108-S668.

(142) Leung E, Weil DE, Raviglione M, Nakatani H. The WHO policy package to combat antimicrobial resistance. Bull World Health Organ 2011; 89 (5): 390-392.

(143) Levy SB, McMurry LM, Barbosa TM, Burdett V, Courvalin P, Hillen W et al. Nomenclature for new tetracycline resistance determinants. Antimicrob Agents Chemother 1999; 43 (6): 1523-1524.

(144) Levy SB, McMurry LM, Burdett V, Courvalin P, Hillen W, Roberts MC et al. Nomenclature for tetracycline resistance determinants. Antimicrob Agents Chemother 1989; 33 (8): 1373-1374.

(145) Li XZ, Nikaido H. Efflux-mediated drug resistance in bacteria: an update. Drugs 2009; 69 (12): 1555-1623.

(146) Li XZ, Nikaido H, Poole K. Role of *mexA-mexB-oprM* in antibiotic efflux in *Pseudomonas aeruginosa*. Antimicrob Agents Chemother 1995; 39 (9): 1948-1953.

(147) Li XZ, Poole K, Nikaido H. Contributions of MexAB-OprM and an EmrE homolog to intrinsic resistance of *Pseudomonas aeruginosa* to aminoglycosides and dyes. Antimicrob Agents Chemother 2003; 47 (1): 27-33.

(148) Lin HT, Bavro VN, Barrera NP, Frankish HM, Velamakanni S, van Veen HW et al. MacB ABC transporter is a dimer whose ATPase activity and macrolide-binding capacity are regulated by the membrane fusion protein MacA. J Biol Chem 2009; 284 (2): 1145-1154.

(149) Lin J, Sahin O, Michel LO, Zhang Q. Critical role of multidrug efflux pump CmeABC in bile resistance and in vivo colonization of *Campylobacter jejuni*. Infect Immun 2003; 71 (8): 4250-4259.

(150) Lin L, Ling BD, Li XZ. Distribution of the multidrug efflux pump genes, *adeABC*, *adeDE* and *adeIJK*, and class 1 integron genes in multiple-antimicrobial-resistant clinical isolates of *Acinetobacter baumannii-Acinetobacter calcoaceticus* complex. Int J Antimicrob Agents 2009; 33 (1): 27-32.

(151) Lin YC, Chen TL, Ju HL, Chen HS, Wang FD, Yu KW et al. Clinical characteristics and risk factors for attributable mortality in *Enterobacter cloacae* bacteremia. J Microbiol Immunol Infect 2006; 39 (1): 67-72.

(152) Livak KJ, Schmittgen TD. Analysis of relative gene expression data using real-time quantitative PCR and the 2(-Delta Delta C(T)) Method. Methods 2001; 25 (4): 402-408.

(153) Livermore DM. Tigecycline: what is it, and where should it be used? J Antimicrob Chemother 2005; 56 (4): 611-614.

(154) Lolans K, Rice TW, Munoz-Price LS, Quinn JP. Multicity outbreak of carbapenem-resistant *Acinetobacter baumannii* isolates producing the carbapenemase OXA-40. Antimicrob Agents Chemother 2006; 50 (9): 2941-2945.

(155) Lomovskaya O, Warren MS, Lee A, Galazzo J, Fronko R, Lee M et al. Identification and characterization of inhibitors of multidrug resistance efflux pumps in *Pseudomonas aeruginosa*: novel agents for combination therapy. Antimicrob Agents Chemother 2001; 45 (1): 105-116.

(156) Lowman W, Kalk T, Menezes CN, John MA, Grobusch MP. A case of community-acquired *Acinetobacter baumannii* meningitis - has the threat moved beyond the hospital? J Med Microbiol 2008; 57 (Pt 5): 676-678.

(157) Ma D, Alberti M, Lynch C, Nikaido H, Hearst JE. The local repressor AcrR plays a modulating role in the regulation of *acrAB* genes of *Escherichia coli* by global stress signals. Mol Microbiol 1996; 19 (1): 101-112.

(158) Ma D, Cook DN, Alberti M, Pon NG, Nikaido H, Hearst JE. Molecular cloning and characterization of *acrA* and *acrE* genes of *Escherichia coli*. J Bacteriol 1993; 175 (19): 6299-6313.

(159) Ma D, Cook DN, Alberti M, Pon NG, Nikaido H, Hearst JE. Genes *acrA* and *acrB* encode a stress-induced efflux system of *Escherichia coli*. Mol Microbiol 1995; 16 (1): 45-55.

(160) Magnet S, Courvalin P, Lambert T. Resistance-nodulation-cell division-type efflux pump involved in aminoglycoside resistance in *Acinetobacter baumannii* strain BM4454. Antimicrob Agents Chemother 2001; 45 (12): 3375-3380.

(161) Mahamoud A, Chevalier J, Alibert-Franco S, Kern WV, Pages JM. Antibiotic efflux pumps in Gram-negative bacteria: the inhibitor response strategy. J Antimicrob Chemother 2007; 59 (6): 1223-1229.

(162) Mak JK, Kim MJ, Pham J, Tapsall J, White PA. Antibiotic resistance determinants in nosocomial strains of multidrug-resistant *Acinetobacter baumannii*. J Antimicrob Chemother 2009; 63 (1): 47-54.

(163) Manzur A, Tubau F, Pujol M, Calatayud L, Dominguez MA, Pena C et al. Nosocomial outbreak due to extended-spectrum-beta-lactamase- producing *Enterobacter cloacae* in a cardiothoracic intensive care unit. J Clin Microbiol 2007; 45 (8): 2365-2369.

(164) Marchand I, Damier-Piolle L, Courvalin P, Lambert T. Expression of the RND-type efflux pump AdeABC in *Acinetobacter baumannii* is regulated by the AdeRS two-component system. Antimicrob Agents Chemother 2004; 48 (9): 3298-3304.

(165) Martin RG, Gillette WK, Martin NI, Rosner JL. Complex formation between activator and RNA polymerase as the basis for transcriptional activation by MarA and SoxS in *Escherichia coli*. Mol Microbiol 2002; 43 (2): 355-370.

(166) Martin RG, Rosner JL. Binding of purified multiple antibiotic-resistance repressor protein (MarR) to *mar* operator sequences. Proc Natl Acad Sci U S A 1995; 92 (12): 5456-5460.

(167) McAleese F, Petersen P, Ruzin A, Dunman PM, Murphy E, Projan SJ et al. A novel MATE family efflux pump contributes to the reduced susceptibility of laboratory-derived *Staphylococcus aureus* mutants to tigecycline. Antimicrob Agents Chemother 2005; 49 (5): 1865-1871.

(168) McDermott PF, McMurry LM, Podglajen I, Dzink-Fox JL, Schneiders T, Draper MP et al. The *marC* gene of *Escherichia coli* is not involved in multiple antibiotic resistance. Antimicrob Agents Chemother 2008; 52 (1): 382-383.

(169) Meagher AK, Ambrose PG, Grasela TH, Ellis-Grosse EJ. Pharmacokinetic/pharmacodynamic profile for tigecycline-a new glycylcycline antimicrobial agent. Diagn Microbiol Infect Dis 2005; 52 (3): 165-171.

(170) Middlemiss JK, Poole K. Differential impact of MexB mutations on substrate selectivity of the MexAB-OprM multidrug efflux pump of *Pseudomonas aeruginosa*. J Bacteriol 2004; 186 (5): 1258-1269.

(171) Mikolosko J, Bobyk K, Zgurskaya HI, Ghosh P. Conformational flexibility in the multidrug efflux system protein AcrA. Structure 2006; 14 (3): 577-587.

(172) Milatovic D, Schmitz FJ, Verhoef J, Fluit AC. Activities of the glycylcycline tigecycline (GAR-936) against 1,924 recent European clinical bacterial isolates. Antimicrob Agents Chemother 2003; 47 (1): 400-404.

(173) Miller VL, Mekalanos JJ. A novel suicide vector and its use in construction of insertion mutations: osmoregulation of outer membrane proteins and virulence determinants in *Vibrio cholerae* requires *toxR*. J Bacteriol 1988; 170 (6): 2575-2583.

(174) Mima T, Joshi S, Gomez-Escalada M, Schweizer HP. Identification and characterization of TriABC-OpmH, a triclosan efflux pump of *Pseudomonas aeruginosa* requiring two membrane fusion proteins. J Bacteriol 2007; 189 (21): 7600-7609.

(175) Moore IF, Hughes DW, Wright GD. Tigecycline is modified by the flavin-dependent monooxygenase TetX. Biochemistry 2005; 44 (35): 11829-11835.

(176) Morita Y, Kataoka A, Shiota S, Mizushima T, Tsuchiya T. NorM of *Vibrio parahaemolyticus is* an Na(+)-driven multidrug efflux pump. J Bacteriol 2000; 182 (23): 6694-6697.

(177) Morita Y, Kodama K, Shiota S, Mine T, Kataoka A, Mizushima T et al. NorM, a putative multidrug efflux protein, of *Vibrio parahaemolyticus* and its homolog in *Escherichia coli*. Antimicrob Agents Chemother 1998; 42 (7): 1778-1782.

(178) Murakami S, Nakashima R, Yamashita E, Matsumoto T, Yamaguchi A. Crystal structures of a multidrug transporter reveal a functionally rotating mechanism. Nature 2006; 443 (7108): 173-179.

(179) Murakami S, Nakashima R, Yamashita E, Yamaguchi A. Crystal structure of bacterial multidrug efflux transporter AcrB. Nature 2002; 419 (6907): 587-593.

(180) Naas T, Vandel L, Sougakoff W, Livermore DM, Nordmann P. Cloning and sequence analysis of the gene for a carbapenem-hydrolyzing class A beta-lactamase, Sme-1, from *Serratia marcescens* S6. Antimicrob Agents Chemother 1994; 38 (6): 1262-1270.

(181) Nara T, Kouyama T, Kurata Y, Kikukawa T, Miyauchi S, Kamo N. Anti-parallel membrane topology of a homo-dimeric multidrug transporter, EmrE. J Biochem 2007; 142 (5): 621-625.

(182) Navon-Venezia S, Leavitt A, Carmeli Y. High tigecycline resistance in multidrug-resistant *Acinetobacter baumannii*. J Antimicrob Chemother 2007; 59 (4): 772-774.

(183) Nemec A, Krizova L, Maixnerova M, van der Reijden TJ, Deschaght P, Passet V et al. Genotypic and phenotypic characterization of the *Acinetobacter calcoaceticus-Acinetobacter baumannii* complex with the proposal of *Acinetobacter pittii* sp. nov. (formerly *Acinetobacter* genomic species 3) and *Acinetobacter nosocomialis* sp. nov. (formerly *Acinetobacter* genomic species 13TU). Res Microbiol 2011; 162 (4): 393-404.

(184) Ng LK, Martin I, Alfa M, Mulvey M. Multiplex PCR for the detection of tetracycline resistant genes. Mol Cell Probes 2001; 15 (4): 209-215.

(185) Nikaido E, Shirosaka I, Yamaguchi A, Nishino K. Regulation of the AcrAB multidrug efflux pump in *Salmonella enterica* serovar Typhimurium in response to indole and paraquat. Microbiology 2011; 157 (Pt 3): 648-655.

(186) Nikaido E, Yamaguchi A, Nishino K. AcrAB multidrug efflux pump regulation in *Salmonella enterica* serovar Typhimurium by RamA in response to environmental signals. J Biol Chem 2008; 283 (35): 24245-24253.

(187) Nishino K, Honda T, Yamaguchi A. Genome-wide analyses of *Escherichia coli* gene expression responsive to the BaeSR two-component regulatory system. J Bacteriol 2005; 187 (5): 1763-1772.

(188) Nishino K, Latifi T, Groisman EA. Virulence and drug resistance roles of multidrug efflux systems of *Salmonella enterica* serovar Typhimurium. Mol Microbiol 2006; 59 (1): 126-141.

(189) Nonaka L, Suzuki S. New Mg^{2+}-dependent oxytetracycline resistance determinant *tet 34* in *Vibrio* isolates from marine fish intestinal contents. Antimicrob Agents Chemother 2002; 46 (5): 1550-1552.

(190) Olliver A, Valle M, Chaslus-Dancla E, Cloeckaert A. Role of an *acrR* mutation in multidrug resistance of in vitro-selected fluoroquinolone-resistant mutants of *Salmonella enterica* serovar Typhimurium. FEMS Microbiol Lett 2004; 238 (1): 267-272.

(191) Pages JM, Amaral L. Mechanisms of drug efflux and strategies to combat them: challenging the efflux pump of Gram-negative bacteria. Biochim Biophys Acta 2009; 1794 (5): 826-833.

(192) Pages JM, Masi M, Barbe J. Inhibitors of efflux pumps in Gram-negative bacteria. Trends Mol Med 2005; 11 (8): 382-389.

(193) Park YJ, Lee S, Yu JK, Woo GJ, Lee K, Arakawa Y. Co-production of 16S rRNA methylases and extended-spectrum beta-lactamases in AmpC-producing *Enterobacter cloacae*, *Citrobacter freundii* and *Serratia marcescens* in Korea. J Antimicrob Chemother 2006; 58 (4): 907-908.

(194) Paterson DL. Resistance in gram-negative bacteria: Enterobacteriaceae. Am J Infect Control 2006; 34 (5 Suppl 1): S20-S28.

(195) Patterson AJ, Rincon MT, Flint HJ, Scott KP. Mosaic tetracycline resistance genes are widespread in human and animal fecal samples. Antimicrob Agents Chemother 2007; 51 (3): 1115-1118.

(196) Pei XY, Hinchliffe P, Symmons MF, Koronakis E, Benz R, Hughes C et al. Structures of sequential open states in a symmetrical opening transition of the TolC exit duct. Proc Natl Acad Sci U S A 2011; 108 (5): 2112-2117.

(197) Peleg AY, Adams J, Paterson DL. Tigecycline efflux as a mechanism for nonsusceptibility in *Acinetobacter baumannii*. Antimicrob Agents Chemother 2007; 51 (6): 2065-2069.

(198) Peleg AY, Jara S, Monga D, Eliopoulos GM, Moellering RC, Jr., Mylonakis E. *Galleria mellonella* as a model system to study *Acinetobacter baumannii* pathogenesis and therapeutics. Antimicrob Agents Chemother 2009; 53 (6): 2605-2609.

(199) Peleg AY, Potoski BA, Rea R, Adams J, Sethi J, Capitano B et al. *Acinetobacter baumannii* bloodstream infection while receiving tigecycline: a cautionary report. J Antimicrob Chemother 2007; 59 (1): 128-131.

(200) Perez A, Canle D, Latasa C, Poza M, Beceiro A, Del Mar TM et al. Cloning, nucleotide sequencing, and analysis of the AcrAB-TolC efflux pump of *Enterobacter cloacae* and determination of its involvement in antibiotic resistance in a clinical isolate. Antimicrob Agents Chemother 2007; 51 (9): 3247-3253.

(201) Petersen PJ, Jacobus NV, Weiss WJ, Sum PE, Testa RT. *In vitro* and *in vivo* antibacterial activities of a novel glycylcycline, the 9-t-butylglycylamido derivative of minocycline (GAR-936). Antimicrob Agents Chemother 1999; 43 (4): 738-744.

(202) Poole K, Krebes K, McNally C, Neshat S. Multiple antibiotic resistance in *Pseudomonas aeruginosa*: evidence for involvement of an efflux operon. J Bacteriol 1993; 175 (22): 7363-7372.

(203) Poteete AR. What makes the bacteriophage lambda Red system useful for genetic engineering: molecular mechanism and biological function. FEMS Microbiol Lett 2001; 201 (1): 9-14.

(204) Poulakou G, Kontopidou FV, Paramythiotou E, Kompoti M, Katsiari M, Mainas E et al. Tigecycline in the treatment of infections from multidrug resistant Gram-negative pathogens. J Infect 2009; 58 (4): 273-284.

(205) Projan SJ. Francis Tally and the discovery and development of tigecycline: a personal reminiscence. Clin Infect Dis 2010; 50 (S1): S24-S25.

(206) Rahmati S, Yang S, Davidson AL, Zechiedrich EL. Control of the AcrAB multidrug efflux pump by quorum-sensing regulator SdiA. Mol Microbiol 2002; 43 (3): 677-685.

(207) Rajendran R, Quinn RF, Murray C, McCulloch E, Williams C, Ramage G. Efflux pumps may play a role in tigecycline resistance in *Burkholderia* species. Int J Antimicrob Agents 2010; 36 (2): 151-154.

(208) Rasmussen BA, Gluzman Y, Tally FP. Inhibition of protein synthesis occurring on tetracycline-resistant, TetM-protected ribosomes by a novel class of tetracyclines, the glycylcyclines. Antimicrob Agents Chemother 1994; 38 (7): 1658-1660.

(209) Reffay M, Gambin Y, Benabdelhak H, Phan G, Taulier N, Ducruix A et al. Tracking membrane protein association in model membranes. PLoS ONE 2009; 4 (4): e5035.

(210) Reid GE, Grim SA, Aldeza CA, Janda WM, Clark NM. Rapid development of *Acinetobacter baumannii* resistance to tigecycline. Pharmacotherapy 2007; 27 (8): 1198-1201.

(211) Reinert RR, Low DE, Rossi F, Zhang X, Wattal C, Dowzicky MJ. Antimicrobial susceptibility among organisms from the Asia/Pacific Rim, Europe and Latin and North America collected as part of TEST and the in vitro activity of tigecycline. J Antimicrob Chemother 2007; 60 (5): 1018-1029.

(212) Ren Y, Ren Y, Zhou Z, Guo X, Li Y, Feng L et al. Complete genome sequence of *Enterobacter cloacae* subsp. *cloacae* type strain ATCC 13047. J Bacteriol 2010; 192 (9): 2463-2464.

(213) Renau TE, Leger R, Flamme EM, Sangalang J, She MW, Yen R et al. Inhibitors of efflux pumps in *Pseudomonas aeruginosa* potentiate the activity of the fluoroquinolone antibacterial levofloxacin. J Med Chem 1999; 42 (24): 4928-4931.

(214) Rieg S, Huth A, Kalbacher H, Kern WV. Resistance against antimicrobial peptides is independent of *Escherichia coli* AcrAB, *Pseudomonas aeruginosa* MexAB and *Staphylococcus aureus* NorA efflux pumps. Int J Antimicrob Agents 2009; 33 (2): 174-176.

(215) Robenshtok E, Paul M, Leibovici L, Fraser A, Pitlik S, Ostfeld I et al. The significance of *Acinetobacter baumannii* bacteraemia compared with *Klebsiella pneumoniae* bacteraemia: risk factors and outcomes. J Hosp Infect 2006; 64 (3): 282-287.

(216) Roberts MC. Update on acquired tetracycline resistance genes. FEMS Microbiol Lett 2005; 245 (2): 195-203.

(217) Ross JI, Eady EA, Cove JH, Cunliffe WJ. 16S rRNA mutation associated with tetracycline resistance in a Gram-positive bacterium. Antimicrob Agents Chemother 1998; 42 (7): 1702-1705.

(218) Rouquette-Loughlin CE, Balthazar JT, Shafer WM. Characterization of the MacA-MacB efflux system in *Neisseria gonorrhoeae*. J Antimicrob Chemother 2005; 56 (5): 856-860.

(219) Ruiz N, Montero T, Hernandez-Borrell J, Vinas M. The role of *Serratia marcescens* porins in antibiotic resistance. Microb Drug Resist 2003; 9 (3): 257-264.

(220) Ruzin A, Immermann FW, Bradford PA. Real-time PCR and statistical analyses of *acrAB* and *ramA* expression in clinical isolates of *Klebsiella pneumoniae*. Antimicrob Agents Chemother 2008; 52 (9): 3430-3432.

(221) Ruzin A, Immermann FW, Bradford PA. RT-PCR and statistical analyses of adeABC expression in clinical isolates of *Acinetobacter calcoaceticus-Acinetobacter baumannii* complex. Microb Drug Resist 2010; 16 (2): 87-89.

(222) Ruzin A, Keeney D, Bradford PA. AcrAB efflux pump plays a role in decreased susceptibility to tigecycline in *Morganella morganii*. Antimicrob Agents Chemother 2005; 49 (2): 791-793.

(223) Ruzin A, Keeney D, Bradford PA. AdeABC multidrug efflux pump is associated with decreased susceptibility to tigecycline in *Acinetobacter calcoaceticus-Acinetobacter baumannii* complex. J Antimicrob Chemother 2007; 59 (5): 1001-1004.

(224) Ruzin A, Visalli MA, Keeney D, Bradford PA. Influence of transcriptional activator RamA on expression of multidrug efflux pump AcrAB and tigecycline susceptibility in *Klebsiella pneumoniae*. Antimicrob Agents Chemother 2005; 49 (3): 1017-1022.

(225) Sacchidanand S, Penn RL, Embil JM, Campos ME, Curcio D, Ellis-Grosse E et al. Efficacy and safety of tigecycline monotherapy compared with vancomycin plus aztreonam in patients with complicated skin and skin structure infections: Results from a phase 3, randomized, double-blind trial. Int J Infect Dis 2005; 9 (5): 251-261.

(226) Saier MH, Jr., Paulsen IT. Phylogeny of multidrug transporters. Semin Cell Dev Biol 2001; 12 (3): 205-213.

(227) Sanchez-Romero JM, Diaz-Orejas R, De L, V. Resistance to tellurite as a selection marker for genetic manipulations of *Pseudomonas* strains. Appl Environ Microbiol 1998; 64 (10): 4040-4046.

(228) Schnappinger D, Hillen W. Tetracyclines: antibiotic action, uptake, and resistance mechanisms. Arch Microbiol 1996; 165 (6): 359-369.

(229) Schuldiner S, Lebendiker M, Yerushalmi H. EmrE, the smallest ion-coupled transporter, provides a unique paradigm for structure-function studies. J Exp Biol 1997; 200 (Pt 2): 335-341.

(230) Seeger MA, Schiefner A, Eicher T, Verrey F, Diederichs K, Pos KM. Structural asymmetry of AcrB trimer suggests a peristaltic pump mechanism. Science 2006; 313 (5791): 1295-1298.

(231) Seeger MA, von Ballmoos C, Eicher T, Brandstatter L, Verrey F, Diederichs K et al. Engineered disulfide bonds support the functional rotation mechanism of multidrug efflux pump AcrB. Nat Struct Mol Biol 2008; 15 (2): 199-205.

(232) Sennhauser G, Bukowska MA, Briand C, Grutter MG. Crystal structure of the multidrug exporter MexB from *Pseudomonas aeruginosa*. J Mol Biol 2009; 389 (1): 134-145.

(233) Shafer WM, Qu X, Waring AJ, Lehrer RI. Modulation of *Neisseria gonorrhoeae* susceptibility to vertebrate antibacterial peptides due to a member of the resistance/nodulation/division efflux pump family. Proc Natl Acad Sci U S A 1998; 95 (4): 1829-1833.

(234) Shet V, Gouliouris T, Brown NM, Turton JF, Zhang J, Woodford N. IMP metallo-β-lactamase-producing clinical isolates of *Enterobacter cloacae* in the UK. J Antimicrob Chemother 2011; 66 (6): 1408-1409.

(235) Sigal N, Lewinson O, Wolf SG, Bibi E. *E. coli* multidrug transporter MdfA is a monomer. Biochemistry 2007; 46 (17): 5200-5208.

(236) Sloan J, McMurry LM, Lyras D, Levy SB, Rood JI. The *Clostridium perfringens* Tet P determinant comprises two overlapping genes: *tetA*(P), which mediates active tetracycline efflux, and *tetB*(P), which is related to the ribosomal protection family of tetracycline-resistance determinants. Mol Microbiol 1994; 11 (2): 403-415.

(237) Speer BS, Bedzyk L, Salyers AA. Evidence that a novel tetracycline resistance gene found on two *Bacteroides* transposons encodes an NADP-requiring oxidoreductase. J Bacteriol 1991; 173 (1): 176-183.

(238) Speer BS, Salyers AA. Characterization of a novel tetracycline resistance that functions only in aerobically grown *Escherichia coli*. J Bacteriol 1988; 170 (4): 1423-1429.

(239) Speer BS, Salyers AA. Novel aerobic tetracycline resistance gene that chemically modifies tetracycline. J Bacteriol 1989; 171 (1): 148-153.

(240) Stanton TB, Humphrey SB. Isolation of tetracycline-resistant *Megasphaera elsdenii* strains with novel mosaic gene combinations of *tet*(O) and *tet*(W) from swine. Appl Environ Microbiol 2003; 69 (7): 3874-3882.

(241) Sum PE, Petersen P. Synthesis and structure-activity relationship of novel glycylcycline derivatives leading to the discovery of GAR-936. Bioorg Med Chem Lett 1999; 9 (10): 1459-1462.

(242) Symmons MF, Bokma E, Koronakis E, Hughes C, Koronakis V. The assembled structure of a complete tripartite bacterial multidrug efflux pump. Proc Natl Acad Sci U S A 2009; 106 (17): 7173-7178.

(243) Takatsuka Y, Nikaido H. Covalently linked trimer of the AcrB multidrug efflux pump provides support for the functional rotating mechanism. J Bacteriol 2009; 191 (6): 1729-1737.

(244) Tauch A, Puhler A, Kalinowski J, Thierbach G. TetZ, a new tetracycline resistance determinant discovered in gram-positive bacteria, shows high homology to gram-negative regulated efflux systems. Plasmid 2000; 44 (3): 285-291.

(245) Tavio MM, Aquili VD, Poveda JB, Antunes NT, Sanchez-Cespedes J, Vila J. Quorum-sensing regulator *sdiA* and *marA* overexpression is involved in in vitro-selected multidrug resistance of *Escherichia coli*. J Antimicrob Chemother 2010; 65 (6): 1178-1186.

(246) Taylor DE, Chau A. Tetracycline resistance mediated by ribosomal protection. Antimicrob Agents Chemother 1996; 40 (1): 1-5.

(247) Teo JW, Tan TM, Poh CL. Genetic determinants of tetracycline resistance in *Vibrio harveyi*. Antimicrob Agents Chemother 2002; 46 (4): 1038-1045.

(248) Testa RT, Petersen PJ, Jacobus NV, Sum PE, Lee VJ, Tally FP. *In vitro* and *in vivo* antibacterial activities of the glycylcyclines, a new class of semisynthetic tetracyclines. Antimicrob Agents Chemother 1993; 37 (11): 2270-2277.

(249) Thaker M, Spanogiannopoulos P, Wright GD. The tetracycline resistome. Cell Mol Life Sci 2010; 67 (3): 419-431.

(250) Thamlikitkul V, Tiengrim S. Effect of different Mueller-Hinton agars on tigecycline disc diffusion susceptibility for *Acinetobacter* spp. J Antimicrob Chemother 2008; 62 (4): 847-848.

(251) Thanassi DG, Suh GS, Nikaido H. Role of outer membrane barrier in efflux-mediated tetracycline resistance of *Escherichia coli*. J Bacteriol 1995; 177 (4): 998-1007.

(252) Tornroth-Horsefield S, Gourdon P, Horsefield R, Brive L, Yamamoto N, Mori H et al. Crystal structure of AcrB in complex with a single transmembrane subunit reveals another twist. Structure 2007; 15 (12): 1663-1673.

(253) Towner KJ. *Acinetobacter*: an old friend, but a new enemy. J Hosp Infect 2009; 73 (4): 355-363.

(254) Truong-Bolduc QC, Dunman PM, Strahilevitz J, Projan SJ, Hooper DC. MgrA is a multiple regulator of two new efflux pumps in *Staphylococcus aureus*. J Bacteriol 2005; 187 (7): 2395-2405.

(255) Tsakris A, Voulgari E, Poulou A, Kimouli M, Pournaras S, Ranellou K et al. *In vivo* acquisition of a plasmid-mediated bla(KPC-2) gene among clonal isolates of Serratia marcescens. J Clin Microbiol 2010; 48 (7): 2546-2549.

(256) Tuckman M, Petersen PJ, Projan SJ. Mutations in the interdomain loop region of the *tetA*(A) tetracycline resistance gene increase efflux of minocycline and glycylcyclines. Microb Drug Resist 2000; 6 (4): 277-282.

(257) Turton JF, Baddal B, Perry C. Use of the accessory genome for characterization and typing of *Acinetobacter baumannii*. J Clin Microbiol 2011; 49 (4): 1260-1266.

(258) Turton JF, Kaufmann ME, Glover J, Coelho JM, Warner M, Pike R et al. Detection and typing of integrons in epidemic strains of *Acinetobacter baumannii* found in the United Kingdom. J Clin Microbiol 2005; 43 (7): 3074-3082.

(259) Turton JF, Kaufmann ME, Warner M, Coelho J, Dijkshoorn L, van der RT et al. A prevalent, multiresistant clone of *Acinetobacter baumannii* in Southeast England. J Hosp Infect 2004; 58 (3): 170-179.

(260) Turton JF, Ward ME, Woodford N, Kaufmann ME, Pike R, Livermore DM et al. The role of ISAba1 in expression of OXA carbapenemase genes in *Acinetobacter baumannii*. FEMS Microbiol Lett 2006; 258 (1): 72-77.

(261) Turton JF, Woodford N, Glover J, Yarde S, Kaufmann ME, Pitt TL. Identification of *Acinetobacter baumannii* by detection of the $bla_{\text{OXA-51-like}}$ carbapenemase gene intrinsic to this species. J Clin Microbiol 2006; 44 (8): 2974-2976.

(262) US Food and Drug Administration. FDA Drug Safety Communication: Increased risk of death with Tygacil (tigecycline) compared to other antibiotics used to treat similar infections. US Department of Health and Human Services . 1-9-2010. 20-6-2011.

(263) Vaccaro L, Koronakis V, Sansom MS. Flexibility in a drug transport accessory protein: molecular dynamics simulations of MexA. Biophys J 2006; 91 (2): 558-564.

(264) Vaccaro L, Scott KA, Sansom MS. Gating at both ends and breathing in the middle: conformational dynamics of TolC. Biophys J 2008; 95 (12): 5681-5691.

(265) van Dessel H, Dijkshoorn L, van der RT, Bakker N, Paauw A, van den BP et al. Identification of a new geographically widespread multiresistant *Acinetobacter baumannii* clone from European hospitals. Res Microbiol 2004; 155 (2): 105-112.

(266) Vatopoulos AC, Tsakris A, Tzouvelekis LS, Legakis NJ, Pitt TL, Miller GH et al. Diversity of aminoglycoside resistance in *Enterobacter cloacae* in Greece. Eur J Clin Microbiol Infect Dis 1992; 11 (2): 131-138.

(267) Visalli MA, Murphy E, Projan SJ, Bradford PA. AcrAB multidrug efflux pump is associated with reduced levels of susceptibility to tigecycline (GAR-936) in *Proteus mirabilis*. Antimicrob Agents Chemother 2003; 47 (2): 665-669.

(268) Volkers G, Palm GJ, Weiss MS, Wright GD, Hinrichs W. Structural basis for a new tetracycline resistance mechanism relying on the TetX monooxygenase. FEBS Lett 2011; 585 (7): 1061-1066.

(269) Wang H, Dzink-Fox JL, Chen M, Levy SB. Genetic characterization of highly fluoroquinolone-resistant clinical *Escherichia coli* strains from China:

role of *acrR* mutations. Antimicrob Agents Chemother 2001; 45 (5): 1515-1521.

(270) Wang H, Guo P, Sun H, Wang H, Yang Q, Chen M et al. Molecular epidemiology of clinical isolates of carbapenem-resistant *Acinetobacter* spp. from Chinese hospitals. Antimicrob Agents Chemother 2007; 51 (11): 4022-4028.

(271) Wang YF, Dowzicky MJ. *In vitro* activity of tigecycline and comparators on *Acinetobacter* spp. isolates collected from patients with bacteremia and MIC change during the Tigecycline Evaluation and Surveillance Trial, 2004 to 2008. Diagn Microbiol Infect Dis 2010; 68 (1): 73-79.

(272) Warner DM, Shafer WM, Jerse AE. Clinically relevant mutations that cause derepression of the *Neisseria gonorrhoeae* MtrC-MtrD-MtrE Efflux pump system confer different levels of antimicrobial resistance and in vivo fitness. Mol Microbiol 2008; 70 (2): 462-478.

(273) Waters SH, Rogowsky P, Grinsted J, Altenbuchner J, Schmitt R. The tetracycline resistance determinants of RP1 and Tn1721: nucleotide sequence analysis. Nucleic Acids Res 1983; 11 (17): 6089-6105.

(274) Webber MA, Bailey AM, Blair JM, Morgan E, Stevens MP, Hinton JC et al. The global consequence of disruption of the AcrAB-TolC efflux pump in *Salmonella enterica* includes reduced expression of SPI-1 and other attributes required to infect the host. J Bacteriol 2009; 191 (13): 4276-4285.

(275) Werner G, Gfrorer S, Fleige C, Witte W, Klare I. Tigecycline-resistant *Enterococcus faecalis* strain isolated from a German intensive care unit patient. J Antimicrob Chemother 2008; 61 (5): 1182-1183.

(276) Wong EW, Yusof MY, Mansor MB, Anbazhagan D, Ong SY, Sekaran SD. Disruption of *adeB* gene has a greater effect on resistance to meropenems than *adeA* gene in *Acinetobacter* spp. isolated from University Malaya Medical Centre. Singapore Med J 2009; 50 (8): 822-826.

(277) Woodford N, Ellington MJ, Coelho JM, Turton JF, Ward ME, Brown S et al. Multiplex PCR for genes encoding prevalent OXA carbapenemases in *Acinetobacter* spp. Int J Antimicrob Agents 2006; 27 (4): 351-353.

(278) Wroblewska MM, Towner KJ, Marchel H, Luczak M. Emergence and spread of carbapenem-resistant strains of *Acinetobacter baumannii* in a tertiary-care hospital in Poland. Clin Microbiol Infect 2007; 13 (5): 490-496.

(279) Xu Y, Song S, Moeller A, Kim N, Piao S, Sim SH et al. Functional implications of an intermeshing cogwheel-like interaction between TolC and MacA in the action of macrolide-specific efflux pump MacAB-TolC. J Biol Chem 2011; 286 (15): 13541-13549.

(280) Yang S, Lopez CR, Zechiedrich EL. Quorum sensing and multidrug transporters in *Escherichia coli*. Proc Natl Acad Sci U S A 2006; 103 (7): 2386-2391.

(281) Yang W, Moore IF, Koteva KP, Bareich DC, Hughes DW, Wright GD. TetX is a flavin-dependent monooxygenase conferring resistance to tetracycline antibiotics. J Biol Chem 2004; 279 (50): 52346-52352.

(282) Yu EW, Aires JR, McDermott G, Nikaido H. A periplasmic drug-binding site of the AcrB multidrug efflux pump: a crystallographic and site-directed *mutagenesis study. J Bacteriol 2005; 187 (19): 6804-6815.*

(283) Yu EW, McDermott G, Zgurskaya HI, Nikaido H, Koshland DE, Jr. Structural basis of multiple drug-binding capacity of the AcrB multidrug efflux pump. Science 2003; 300 (5621): 976-980.

(284) Zarrilli R, Casillo R, Di Popolo A, Tripodi MF, Bagattini M, Cuccurullo S et al. Molecular epidemiology of a clonal outbreak of multidrug-resistant *Acinetobacter baumannii* in a university hospital in Italy. Clin Microbiol Infect 2007; 13 (5): 481-489.

(285) Zgurskaya HI, Nikaido H. Bypassing the periplasm: reconstitution of the AcrAB multidrug efflux pump of *Escherichia coli*. Proc Natl Acad Sci U S A 1999; 96 (13): 7190-7195.